TN 295
.U4

No. 8906

THE LIBRARY OF CONGRESS

THE LIBRARY OF CONGRESS

IC 8906

Bureau of Mines Information Circular/1982

Mineralogical and Elemental Description of Pacific Manganese Nodules

By Benjamin W. Haynes, Stephen L. Law,
and David C. Barron

UNITED STATES DEPARTMENT OF THE INTERIOR

Information Circular 8906

Mineralogical and Elemental Description of Pacific Manganese Nodules

By Benjamin W. Haynes, Stephen L. Law,
and David C. Barron

UNITED STATES DEPARTMENT OF THE INTERIOR
James G. Watt, Secretary

BUREAU OF MINES
Robert C. Horton, Director

TN295
.U4
no.8906

As the Nation's principal conservation agency, the Department of the Interior has responsibility for most of our nationally owned public lands and natural resources. This includes fostering the wisest use of our land and water resources, protecting our fish and wildlife, preserving the environmental and cultural values of our national parks and historical places, and providing for the enjoyment of life through outdoor recreation. The Department assesses our energy and mineral resources and works to assure that their development is in the best interests of all our people. The Department also has a major responsibility for American Indian reservation communities and for people who live in Island Territories under U.S. administration.

RECEIVED APR 8 1983

This publication has been cataloged as follows:

Haynes, Benjamin W

Mineralogical and elemental description of Pacific manganese nodules.

(Information circular / Bureau of Mines ; 8906)

Supt. of Docs. no.: I 28.27:8906.

I. Manganese nodules–Pacific Ocean. I. Law, Stephen L. II. Barron, D. C. (David C.). III. Title. IV. Series: Information circular (United States. Bureau of Mines) ; 8906.

~~TN295.U4~~ [QE390.2.M35] 622s [549'.23] 82-600495

For sale by the Superintendent of Documents, U.S. Government Printing Office
Washington, D.C. 20402

CONTENTS

	Page
Abstract	1
Introduction	2
Acknowledgments	3
Manganese nodules	3
Morphology	3
Mineralogy	10
Manganese minerals	11
Todorokite or 10 Å manganite	11
Birnessite or 7 Å manganite	12
Vernadite or δ-MnO_2	12
Other manganese minerals	13
Manganese mineral-element associations	13
Iron oxide minerals	13
Feroxyhyte	14
Goethite	14
Lepidocrocite	14
Other iron oxide minerals	14
Iron oxide mineral-element association	14
Accessory minerals	14
Sheet silicates and zeolites	14
Clastic silicates and volcanics	15
Biogenics	15
Sea salt residue	15
Accessory mineral-element associations	17
Moisture content	17
Elemental composition	17
Major and minor elements of potential economic interest	17
Manganese	17
Iron	18
Nickel	18
Copper	18
Cobalt	23
Zinc	23
Vanadium	23
Molybdenum	23
General observations	28
Other major and minor elements	28
Aluminum	28
Calcium	30
Magnesium	30
Potassium	30
Silicon	30
Sodium	30
Strontium	31
Titanium	37
Zirconium	37
General observations	37
Elements of environmental interest	37
Arsenic	37
Barium	40
Cadmium	40
Chromium	40
Lead	40
Mercury	45
Selenium	45
Silver	45
General observations	45
Rare-earth elements	46
Precious-metal-group elements	49
Radioactive elements	49
Other trace elements	50
Anion-forming elements	51
Summary tables	52
Cross section analysis	52
References	57
Appendix.—Glossary of mineralogical terms	60

ILLUSTRATIONS

1. Map of the Pacific Ocean showing CC Zone and MPS areas	2
2. Northern Pacific spheroidal nodules with smooth surface texture	4
3. Study collection of manganese nodules from R/V Prospector	5
4. Discoidal nodules from box cores	6
5. Ellipsoidal nodule with large botryoidal surface protrusions and coarse granular surface texture	7
6. Flat-faced or angular nodules with relatively smooth surface texture	7
7. Cross section of ellipsoidal Pacific nodule	8
8. Cross section of north Pacific nodule	9
9. Contrasting surface textures, smooth and granular, on opposing sides of three nodules	10
10. Irregular layering with maximum thickness toward bottom of north Pacific nodule	10
11. Electron microscope observation of todorokite	12
12. Proposed atomic arrangement for one common todorokite structure	13
13. Scanning electron photomicrograph showing crystals of the zeolite phillipsite in an oxide cavity of a manganese nodule	16
14. Manganese frequency distribution by environment for Pacific manganese nodules	19
15. Iron frequency distribution by environment for Pacific manganese nodules	20
16. Nickel frequency distribution by environment for Pacific manganese nodules	21
17. Copper frequency distribution by environment for Pacific manganese nodules	22
18. Cobalt frequency distribution by environment for Pacific manganese nodules	24
19. Zinc frequency distribution by environment for Pacific manganese nodules	25
20. Vanadium frequency distribution by environment for Pacific manganese nodules	26
21. Molybdenum frequency distribution by environment for Pacific manganese nodules	27
22. Aluminum frequency distribution by environment for Pacific manganese nodules	29
23. Calcium frequency distribution by environment for Pacific manganese nodules	31
24. Magnesium frequency distribution by environment for Pacific manganese nodules	32
25. Potassium frequency distribution by environment for Pacific manganese nodules	33
26. Silicon frequency distribution by environment for Pacific manganese nodules	34
27. Sodium frequency distribution by environment for Pacific manganese nodules	35

Page

28. Strontium frequency distribution by environment for Pacific manganese nodules 36
29. Titanium frequency distribution by environment for Pacific manganese nodules 38
30. Zirconium frequency distribution by environment for Pacific manganese nodules 39
31. Arsenic frequency distribution for Pacific manganese nodules 40
32. Barium frequency distribution by environment for Pacific manganese nodules 41
33. Cadmium frequency distribution by environment for Pacific manganese nodules 42
34. Chromium frequency distribution by environment for Pacific manganese nodules 43
35. Lead frequency distribution by environment for Pacific manganese nodules 44
36. Mercury frequency distribution for Pacific manganese nodules 45
37. Selenium frequency distribution for Pacific manganese nodules 45
38. Silver frequency distribution for Pacific manganese nodules 45
39. Lanthanum frequency distribution for Pacific manganese nodules 46
40. Cerium frequency distribution for Pacific manganese nodules 46
41. Neodymium frequency distribution for Pacific manganese nodules 46
42. Samarium frequency distribution for Pacific manganese nodules 46
43. Europium frequency distribution for Pacific manganese nodules 47
44. Gadolinium frequency distribution for Pacific manganese nodules 47
45. Terbium frequency distribution for Pacific manganese nodules 47
46. Holmium frequency distribution for Pacific manganese nodules 47
47. Thulium frequency distribution for Pacific manganese nodules 48
48. Ytterbium frequency distribution for Pacific manganese nodules 48
49. Lutetium frequency distribution for Pacific manganese nodules 48
50. Hafnium frequency distribution for Pacific manganese nodules 48
51. Thorium frequency distribution for Pacific manganese nodules 49
52. Uranium frequency distribution for Pacific manganese nodules 49
53. Antimony frequency distribution for Pacific manganese nodules 50
54. Boron frequency distribution for Pacific manganese nodules 50
55. Niobium frequency distribution for Pacific manganese nodules 50
56. Rubidium frequency distribution for Pacific manganese nodules 51
57. Scandium frequency distribution for Pacific manganese nodules 51
58. Thallium frequency distribution for Pacific manganese nodules 51
59. Tin frequency distribution for Pacific manganese nodules 51
60. Yttrium frequency distribution for Pacific manganese nodules 51
61. Unpolished cross section of nodule DH 9-9 55
62. Spatial distribution of nickel and copper concentrations with respect to discrete sample locations on nodule DH 9-9 cross section 56
63. Spatial distribution of cobalt and zinc concentrations with respect to discrete sample locations on nodule DH 9-9 cross section 56
64. Spatial distribution of iron and lead concentrations with respect to discrete sample locations on nodule DH 9-9 cross section 56
65. Spatial distribution of barium and cerium concentrations with respect to discrete sample locations on nodule DH 9-9 cross section 56

TABLES

1. Morphological characteristics of Pacific manganese nodules 4
2. Manganese minerals in Pacific manganese nodules 11
3. Iron oxide minerals in Pacific manganese nodules 13
4. Accessory minerals in Pacific manganese nodules 15
5. Distribution of elements of potential economic interest in Pacific manganese nodules, by area 18
6. Distribution of elements of potential economic interest in Pacific manganese nodules, composite 18
7. Distribution of other major and minor elements in Pacific manganese nodules, by area 28
8. Distribution of other major and minor elements in Pacific manganese nodules, composite 28
9. Distribution of elements of environmental interest in Pacific manganese nodules, by area 37
10. Distribution of elements of environmental interest in Pacific manganese nodules, composite 40
11. Rare-earth elements in Pacific manganese nodules 47
12. Precious-metal-group elements in Pacific manganese nodules 49
13. Radioactive elements in Pacific manganese nodules 49
14. Other trace elements in Pacific manganese nodules 50
15. Anion-forming elements in Pacific manganese nodules 52
16. Summary of major, minor, and some trace elements in Pacific manganese nodules, by area 52
17. Summary of elements in Pacific manganese nodules 53
18. Elements for which no data were found for Pacific manganese nodules 53
19. Interelement correlation coefficients for Pacific manganese nodules, by area 53
20. Nodule cross section sample locations and analysis 55

LIST OF UNIT OF MEASURE ABBREVIATIONS USED IN THIS REPORT

Å	angstrom	ng/g	nanograms per gram
atm	atmosphere	pct	percent
cm	centimeter	pg/g	picograms per gram
° C	degrees Celsius	ppm	parts per million
m	meter	wt-pct	weight-percent
mm	millimeter	yr	year
μm	micrometer		

MINERALOGICAL AND ELEMENTAL DESCRIPTION OF PACIFIC MANGANESE NODULES

By Benjamin W. Haynes,[1] Stephen L. Law,[2] and David C. Barron[3]

ABSTRACT

This Bureau of Mines publication comprises a compilation of the state of the science in Pacific Ocean manganese nodule mineralogy and elemental composition. The report is divided into three sections: morphology, mineralogy and elemental composition.

The nodule morphology section defines what is considered a nodule for the study, and details the external characteristics and internal structure. Nodule mineralogy is discussed in three sections: manganese minerals, iron oxide minerals, and accessory minerals. The major manganese minerals discussed are todorokite, birnessite, and vernadite. The iron oxide minerals are less well known and include feroxyhyte, goethite, and lepidocrocite. Accessory minerals present include quartz, clays, and other silicates and nonsilicates. A discussion on moisture content is also included.

The elemental composition section presents data on 74 elements occurring as cations or anions. Summary data, histograms, and interelement correlation coefficients are presented. The elements are grouped as follows: major and minor elements of potential economic interest (8), other major and minor elements (9), elements of environmental interest (8), rare-earth elements (15), precious-metal-group elements (6), radioactive elements (3), other trace elements (17), and anion-forming elements (8). Cross sectional determinations of Ni, Cu, Zn, Co, Pb, Fe, Ce, and Ba are given for a single nodule to show the general tendency of different growth patterns within a nodule because of different element associations and composition.

[1] Supervisory research chemist, Avondale Research Center, Bureau of Mines, Avondale, Md.
[2] Research supervisor, Avondale Research Center, Bureau of Mines, Avondale, Md.
[3] Chemist, Avondale Research Center, Bureau of Mines, Avondale, Md.

INTRODUCTION

This report is one in a series of reports to be issued by the Bureau of Mines to document the results of a project entitled "Analysis and Characterization of Manganese Nodule Processing Rejects." Deep seabed mining for manganese nodules, including the processing of nodules to recover value metals, raises a variety of environmental, social, and economic considerations. To address the waste management aspects of the recovery of value metals from nodules, the National Oceanic and Atmospheric Administration (NOAA) of the Department of Commerce, the Environmental Protection Agency, and the Department of the Interior's Bureau of Mines and Fish and Wildlife Service, after consultation with affected and concerned interests, have agreed to embark on a multiyear cooperative research program that has the following overall objective:

> "To provide information needed by Federal and State agencies in preparation for receipt of industry's commercial waste management plans."

The NOAA-funded research being conducted by the Bureau of Mines has the objective of obtaining a "first-order chemical and physical characterization of rejects from the types of manganese nodule processing techniques representative of those being developed by industry." To better understand the nature of the waste rejects coming from nodule processing, data were first obtained on the mineralogical and chemical composition of manganese nodules from throughout the Pacific Ocean, as outlined in this report. After characterization of the nodule feed material, the major proposed processing schemes are being operated on a bench scale to generate rejects for study. These laboratory-generated rejects will be compared with industry pilot plant-generated rejects as they become available from the various deep ocean mining consortia.

The data from this research will be published for use by (a) industry and environmental scientists in subsequent research to assess the potential effects of waste management alternatives; and (b) regulatory agencies in the determination of standards and test requirements to be met. This is expected to facilitate the development of a basic framework that accommodates the desire to assure protection of the environment and the development of a new minerals processing industry.

In order to assess the potential effects of disposing of reject waste materials from manganese nodule processing, the elemental composition, the compounds present, the interelement correlations, and the mineralogical structure of manganese nodules must be determined. Because nodules from the Pacific Ocean have higher Cu, Co, and Ni contents than nodules from other areas, this report will focus on the Pacific Ocean manganese nodules with an emphasis on the area between the Clarion and Clipperton Fracture Zones (CC Zone) in the equatorial northeast Pacific (fig. 1). Major consortia involved at this time in deep ocean mining and processing of nodules have extensively surveyed the CC Zone area in the Pacific Ocean. Under the Deep Seabed Hard Minerals Resources Act of 1980 (PL 96-283), NOAA has been designated as the lead agency in developing terms, conditions, and restrictions for the proposed mining of nodules and the disposal of waste generated.

This report, focusing on the elemental and mineralogical composition of Pacific Ocean manganese nodules, is divided into the following three sections:

1. A description of manganese nodules as they occur in the Pacific Ocean.
2. Mineralogical composition and element-mineral associations.
3. Elemental composition and interelement correlations.

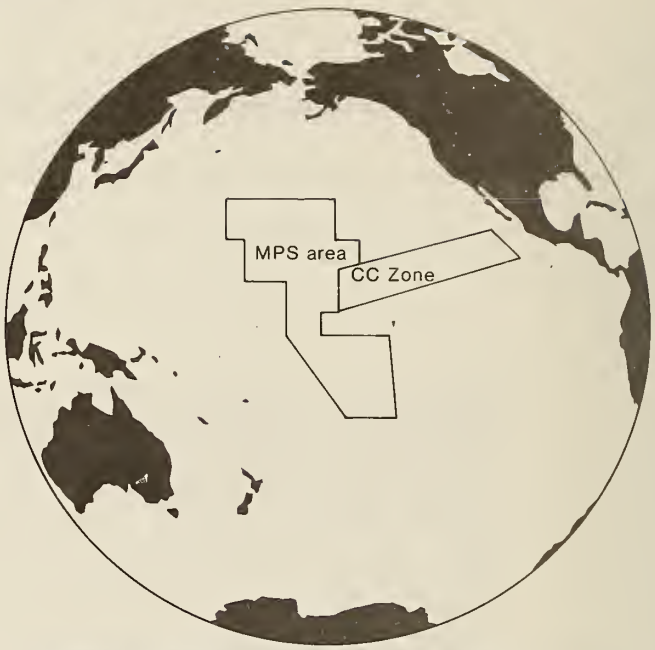

Figure 1.—Map of the Pacific Ocean showing CC Zone and MPS areas.

The elemental composition is presented for major and some minor and trace elements by areas of the Pacific in the form of histograms. These areas are as follows:

1. The Clarion-Clipperton Fracture Zone area.
2. The mid-Pacific seamounts area (MPS), <3,000-m depth.
3. Other abyssal plains area (>3,000-m depth and exclusive of CC Zone).
4. Other seamounts, ridges, and continental margins area (<3,000-m depth).

The elements for which data were insufficient to be presented by area, are presented as a composite of the Pacific Ocean nodule population. The majority of data for all elements, however, is from the CC Zone owing to commercial interest, abundance, and grade of deposits found there. No data are presented for Indian and Atlantic Ocean nodules. Figure 1 shows the CC Zone and MPS areas of study used in this report. The other two areas comprise the remainder of the Pacific Ocean.

The mineralogical composition of nodules is presented for the entire Pacific Ocean with some emphasis placed on major mineral differences with respect to environment (depth, sediment type, etc.). The interelement correlations are presented for the major, some minor, and some trace elements where a significant positive or negative correlation was determined. The element-mineral associations are presented for those elements where the evidence is supportive.

Information and data contained in this report were obtained through many sources. The majority of the elemental and mineralogical information came from the following sources: The Sediment Data Bank, operated by Science Applications, Inc., (SAI) in LaJolla, Calif.; the Bureau of Mines nodule data base at the Denver (Colo.) Research Center; Bureau of Mines in-house research; published literature; other governmental agencies; private industry and consulting firms; and personal contacts with experts in the field of nodule

chemistry and mineralogy (*1-2, 9-10, 12-13, 25-26, 31, 38-39, 41-45, 47-50, 60, 63, 67-68, 72, 74, 79-89, 91, 93, 95-97, 102, 107, 109-110, 112-114, 118, 121-128, 130-132*).[4] Special mention should be made of the extensive reliance upon the books, *Marine Manganese Deposits,* edited by G. P. Glasby (*59*); *Manganese Nodules,* by R. K. Sorem and R. H. Fewkes (*117*); and *Marine Minerals* (*17*), edited by R. G. Burns, for information on the description and mineralogy of Pacific manganese nodules.

ACKNOWLEDGMENTS

This work was performed under interagency agreement NA80AAGO 3026 with the Department of Commerce, National Oceanic and Atmospheric Administration (NOAA). The overall research direction and monitoring responsibilities of Amor L. Lane, M. Karl Jugel, and Robert F. Dill, Office of Oceanic Minerals and Energy, NOAA, and of Thomas A. Henrie, Chief Scientist, Bureau of Mines, are gratefully acknowledged.

The authors wish to thank Virginia M. Burns and Roger G. Burns, Massachusetts Institute of Technology, Cambridge, Mass., for their many helpful discussions, comments, and reviews as well as their assistance in providing information on newly published articles and also for their assistance in providing scanning electron microscope photomicrographs of nodules. The authors also thank Ronald K. Sorem, Washington State University, Pullman, Wash., for assistance in providing nodule photographs, Ronald H. Fewkes, consultant, Pullman Wash., for manuscript review, Jane B. Frazer, Chevron Research Co., Richmond, Calif., for providing the required information from the Sediment Data Bank, and Allan R. Foster, NORTECH, Kirkland, Wash., and Mike Williamson, consultant, Kirkland, Wash., in providing the cross-sectional analysis.

MANGANESE NODULES

Ferromanganese oxides are deposited in a variety of forms in marine environments. In reporting on samples collected by the H.M.S. Challenger expedition (1872-76), Murray and Renard (*101*) noted hydrates of manganese as "colouring matters, or as thin or thick coatings on shells, corals, shark's teeth, bones, and fragments of rock." There is no universally accepted delineation between objects that are stained or very thinly encrusted with manganese and objects that may be called manganese nodules (*59*). However, for purposes of chemical comparison of nodules from throughout the Pacific Ocean, a "manganese nodule" will be arbitrarily defined as having a ferromanganese oxide encrustation at least four times greater in bulk than the nucleus object. Otherwise, a nucleus, or multinucleated objects, greater than 20 pct of the total weight will have too significant an influence upon the observed chemistry of the specimen for valid comparisons with manganese nodules having small nuclei. For example, the Drake Passage series of nodules described by Sorem and Fewkes (*117*) contain rock fragment cores comprising 50 pct or greater of the nodule and are therefore not included in the study. Also, it is doubtful that thinly encrusted objects will ever be considered commercially attractive in the same sense as implied in the term "manganese nodule." Of course, if the nucleus of a nodule is a fragment of another nodule, it will be classified as a manganese nodule regardless of nucleus size.

Manganese micronodules are a special case of the nodule category not included in this study. Micronodules are individual grains generally less than 1 mm in diameter and usually lack a discernible nucleus. Also not included as manganese nodules are the large, slablike concretions such as the manganese pavement from the San Pablo Seamount described by Aumento (*6*).

The existence of varying populations of nodules at different localities in the Pacific Ocean can be attributed to several factors including type of nucleation substrate available, bathymetric position, bottom current activity, sediment type, benthic organism activity, and the chemical environment (*59*). Details of nodule genesis are still poorly understood, though the layering nature and chemical associations characteristic of manganese nodules have been known for many years.

That nodule formation requires some special conditions is illustrated by the discontinuous distribution of nodule fields and the fact that some fields are rich in Mn, Cu, and Ni whereas others, with essentially the same underlying sediments, are high in Fe and low in Mn, Cu, and Ni. Nodules apparently accrete from both sides, with nickel and copper accreting primarily from the sediment side. Raab and Meylan (*59,* pp. 109-146) were unable to verify that chemical gradients found in nodules could be ascribed to the upward migration of trace metals owing to diffusion, and their theory on accretion only on the sediment side is no longer accepted by most researchers. Intraplate igneous activity resulting in the extraction and transport of metals from the sediment to the mud-water interface is postulated by Raab and Meylan (*59,* pp. 109-146) as the source of metals for the concentric layering of nodules. Once the warm, metal-rich brine layer is dissipated, the newly formed nodules are exposed to normal seawater leaching of metals until the next intraplate intrusive event.

The key to a more complete understanding of manganese nodule origin lies in the domain of researchers studying the microfeatures and chemical associations in nodules from many areas and is beyond the scope of this report.

MORPHOLOGY

Table 1 provides an abbreviated summary of the nature and variability of the morphological characteristics of Pacific manganese nodules. The term morphology is used here in its broadest sense to include not only external shape but also the internal structure of the nodule contributing to the total nodule properties.

Figures 2 through 6 show examples of five external

[4] Italicized numbers in parentheses refer to items in the list of references preceding the appendix.

Table 1.—Morphological characteristics of Pacific manganese nodules

Characteristic	Nature and extent of variability
Size	Generally 0.5 to 20 cm. Concretions larger than about 20 cm in diameter generally assume the form of slabs.
External shape	Numerous terms used. Most frequent are— Spheroidal (peas to cannonballs). Ellipsoidal (potatoes). Discoidal or tabular (includes slabs). Botryoidal, polylobate, or coalespheroidal (grape cluster). Flat faced or polygonal (or irregular shape, owing to angular nucleus or fracturing).
Surface texture	Surfaces are usually mammillated, with texture occurring in two general classifications— Smooth: Smooth to the touch and to the eye, though close examination may reveal densely packed minute botryoids. Granular: Feels gritty and may leave tiny oxide particles on the hand upon handling. Close examination may show tiny, closely spaced dendritic oxide forms that may be so abundant in some nodules that the surface botryoids are almost completely obscured.
Color	Refers to nodule exterior, free of clay. Generally dark reddish brown to black, with variations of black as the most common color.
Crustal zone	The outermost layer or set of layers that appear to represent continuous accretion up to the time of collection. Varies from well-defined, uniform to asymmetric, to very thin or absent.
Nucleus	Can be any solid object. Often influences external shape of nodule. Examples— Rock: Igneous, metamorphic, sedimentary. Nodule fragment. Slab of clay. Biological fragment: Tooth, vertebra, bone, fossil, sponges, etc. Volcanic glasses—like pumice, glassy lapilli—almost always profoundly altered. No apparent foreign nucleus: May have formed around a nodule fragment with indeterminate laminations, or original nucleus was altered and replaced.
Internal fractures	Generally filled with clay and readily visible in cut nodules. Occasional clay-free fractures lined with overgrowth of ferromanganese oxides. Two types— Radial or random: An extension feature having greatest separation toward center of nodule and tapering toward edges. Often do not emerge at surfaces but some open toward the sediment side. Show characteristics of shrinkage cracks. Concentric: A fracture along nodule zoning but almost never continuous around entire nodule, frequently terminated by radial fractures.
Breaks	Breakup generally attributed to benthic organisms or bottom currents acting on a fracture-weakened nodule. Terms include— Spalling: Peeling of layers, observed occasionally only in larger nodules (7-cm diam. or larger). Cross section: Transects the nodule layers more or less at right angles; a more common break. α-breaks: Fresh breaks essentially complete before physical recovery from the ocean floor, with the final break occurring during handling in a crust holding the nodule together; more common in larger nodules. β-breaks: Old fracture surfaces with entire fracture covered by a crust of manganese material; more common in smaller nodules (<7-cm diam.).
Interior zoning	Some zonal pattern in nodule cross section, produced by variation in mineral content of the growth layers, is generally present in all nodules. Three types— Continuous, varied bands: Thicker in one half of the nodule, tapering to a thin portion starting near the equator and becoming very thin at the side opposite the thick portion. Textures and composition of the two portions of the band usually differ. Continuous, uniform bands: Often close to the core, suggesting a uniform growth environment. Discontinuous bands: Bands that are completely terminated, usually by sudden tapering near the nodule equator.

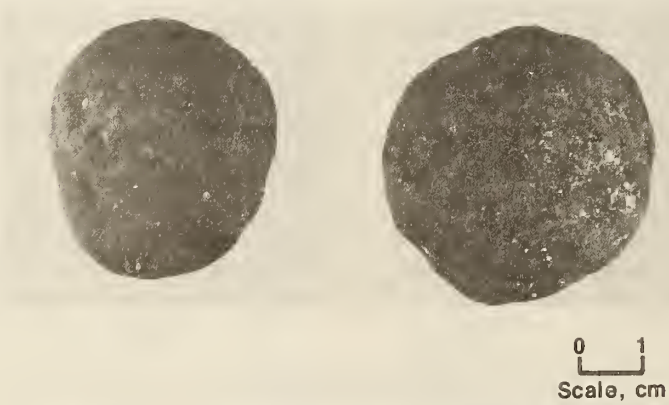

Figure 2.—Northern Pacific spheroidal nodules with smooth surface texture. Latitude 32° 43′ N, longitude 158° 15.8′ W; depth dredged, 1,120 to 1,400 m. Photograph courtesy of reference 117, p. 37.

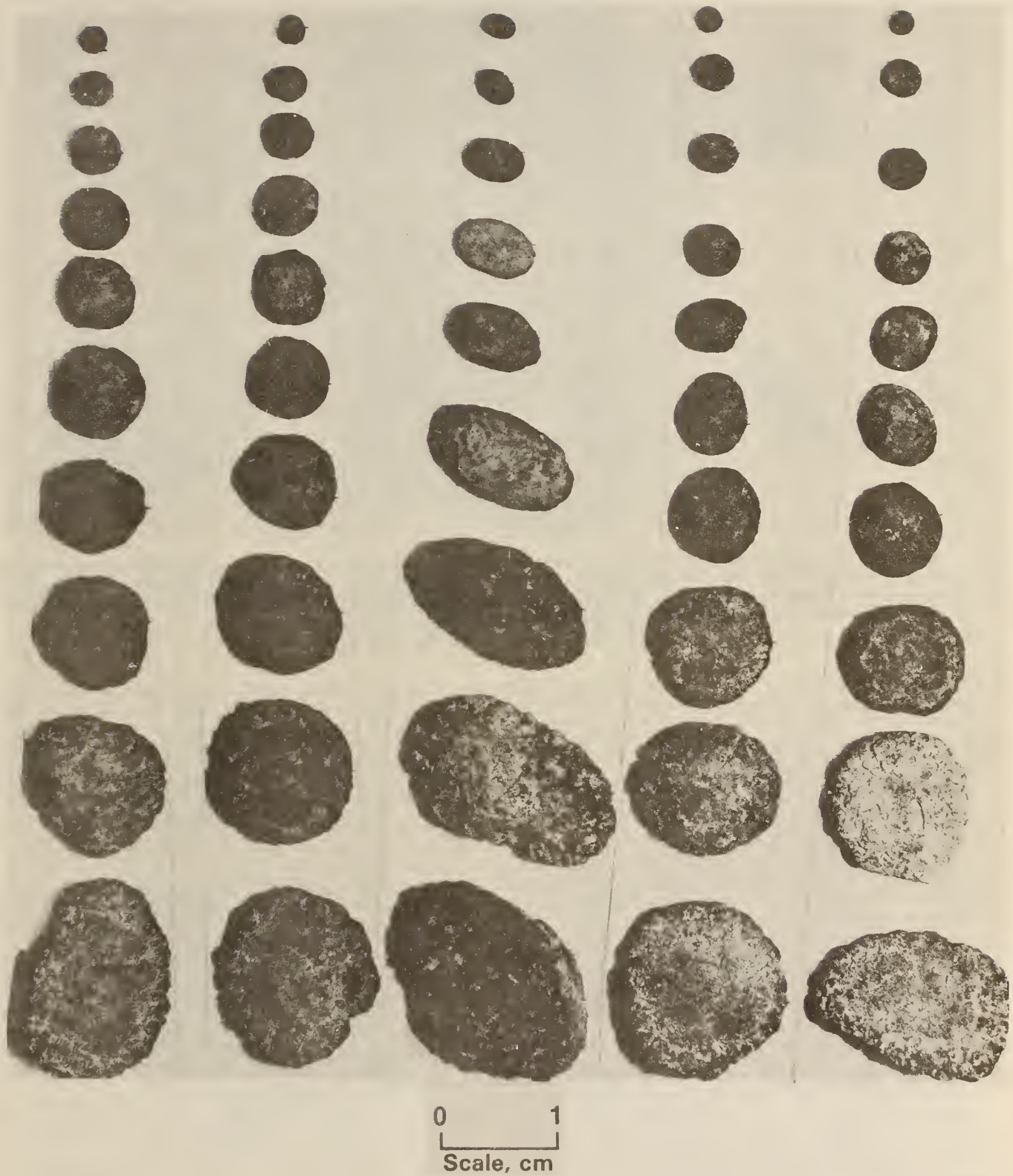

Figure 3.—Study collection of manganese nodules from R/V Prospector at Washington State University. Nodules in the two vertical rows at right are *spheroidal-ellipsoidal* in morphology; center row nodules are *elongate-ellipsoidal;* and nodules in the two vertical rows at left are *discoidal.* Nodules are representative of types in 1-ton dredge haul near DOMES RP8-OC-76 site C area. Photograph courtesy of reference 10, p. 493.

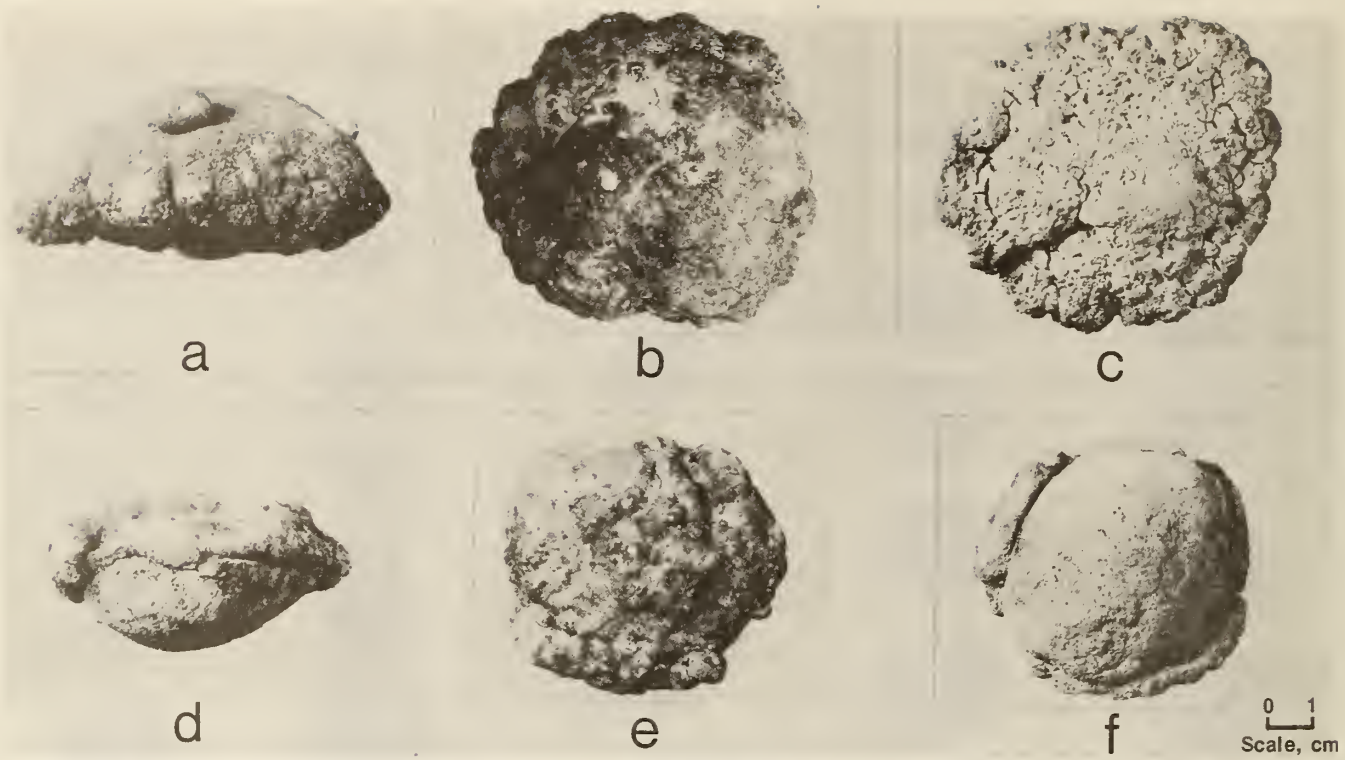

Figure 4.—Discoidal nodules from box cores. Side views (a, d); top views (b, e); bottom views (c, f). Both nodules are from DOMES RP8-OC-76, leg 9. Top nodule is from 15°11.73′ N. latitude, 126°03.89′ W. longitude at a depth of 4,524 m. Bottom nodule is from 15°13.04′ N. latitude, 125°55.94′ W. longitude at a depth of 4,465 m. Photograph courtesy of reference 117, p. 39.

shapes, listed in table 1, generally exhibited by Pacific manganese nodules—spheroidal, ellipsoidal, discoidal, botryoidal, and flat faced. The shape of a nodule, especially the smaller flat faced nodules, may be influenced by the shape of the nucleus. Table 1 lists the various solid objects that may form the nucleus, and figures 7 and 8 show examples of nuclei. These photographs were taken in reflected light with vertical illumination so that oxides appear bright and clay materials appear dark.

Figure 9 shows the two general surface textures, smooth or granular, in this case occurring on opposite sides of the same nodules. A different surface texture for the top and bottom of a nodule is not uncommon, especially for the larger asymmetric nodules.

Nodule size is an important factor because of the relationship between mineralogy and the nodule contact with ocean floor sediments. Accretion of crystalline manganese oxides seems to be enhanced on the portion of the nodule resting in water-saturated, fine-grained silicate sediments. Small nodules (<3-cm diam.), virtually enclosed in soupy sediment, tend to accrete crystalline oxides on all sides and maintain a spheroidal or ellipsoidal shape, or maintain the shape of the nucleus. At a size of about 3 cm or greater, nodules usually tend to develop a pronounced asymmetry of shape because of nonuniform growth rates. The most common pattern is a gradual increase in the horizontal dimensions so that a spheroidal nodule becomes ellipsoidal, and an ellipsoidal nodule approaches a discoidal shape. When the top of the larger nodule comes in contact with relatively sediment-free water, thin iron-rich amorphous oxide layers are slowly added. The bottom and sides of the large nodule, however, remain in contact with watery sediment and continue adding layers of crystalline manganese oxides in which fine silicate grains from the substrate are entrapped.

The accentuated asymmetrical shape of many nodules is due to the more rapid deposition of manganese-rich oxides compared with the amorphous iron-oxide layer growth, and growth of the manganese-rich layers is further enhanced by the incorporation of sediment. The cross-sectional zonal patterns, shown in figure 10 and summarized in table 1, show the two principal types of growth passing gradationally from one to the other near the equator of the nodule. The photograph in figure 10 was taken in reflected light with vertical illumination so that oxides appear bright and clay materials appear dark.

The upper surface and the bottom surface of a nodule are usually chemically different from each other and from the nodule interior. The top is generally high in Fe, Co, and Pb and low in Cu, Ni, Mo, Zn, and Mn; the bottom shows the reverse general pattern. The equatorial area of the surface shows intermediate concentrations of the metals. The core of a nodule is often deficient in Fe, Co, and Pb content relative to the crustal surface. However, the zoning within a nodule generally exhibits the same antithetic relationship between manganese content and iron content, and provides further evidence for the different growth process for the top and bottom portions of nodules. This gradational variation in the character of a layer is called a facies change. The texture of the layer refers to the relationships of the intergrown oxides and nonoxides. The variations in texture are often accompanied by variations in thickness of layers.

With aging, only limited changes seem to occur in the older layers of a nodule. These include the development of shrinkage cracks, both radial and concentric, followed by deposition of oxide veinlets and clay fillings from solutions circulating along the cracks and through pore spaces. The nodule cracking and subsequent physical disturbance may result in breakage of the nodule. As noted in table 1, older fracture surfaces with the entire fracture covered by an oxide

Figure 5.—Ellipsoidal nodule with large botryoidal surface protrusions and coarse granular surface texture. Southern Pacific Ocean, latitude 15° S., longitude 90° W. Photograph courtesy of reference 117, p. 41.

Figure 6.—Flat-faced or angular nodules with relatively smooth surface texture. Minute botryoids cover left nodule. Botryoids are much larger on the right nodule. Pacific Ocean locations: left, latitude 15° S., longitude 145° W.; right, latitude 10° S., longitude 150° W. Photograph courtesy of reference 117, p. 41.

Figure 7.—Cross section of an ellipsoidal Pacific nodule, latitude 9°59.3′ N., longitude 152°56.7′ W., from a depth of about 5,000 m, showing a multiple nuclei core: two subround clay fragments, one shark tooth, and one bone fragment. The original nodule enclosed these fragments, was broken, and a fragment formed the core of the final nodule. Photograph courtesy of reference 117, p. 253.

Figure 8.—Nodule cross section of a north Pacific specimen, latitude 11°21.4′ N., longitude 153°37.5′ W., from a depth of 5,190 m, showing the angular fragment of another nodule as the nucleus. Photograph courtesy of reference 117, p. 251.

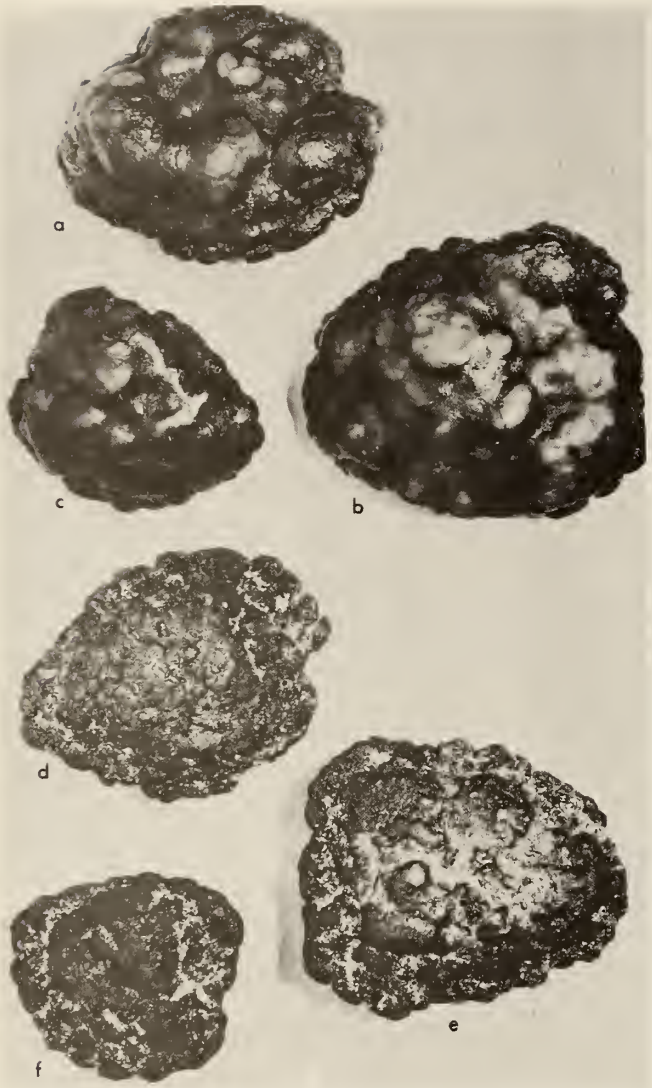

Figure 9.—Contrasting surface textures, smooth and granular, on opposing sides of three nodules (a-d, b-c and c-f) from latitude 10° N., longitude 140° W., at a depth of about 4,500 m. The large nodule is approximately 9 cm long. Photograph courtesy of reference 117, p. 43.

Figure 10.—Irregular layering with the maximum thickness toward the bottom of a north Pacific nodule from latitude 14°35′ N., longitude 124°26′ W., at a depth of about 4,353 m. Photograph courtesy of reference 117, p. 523.

crust are referred to as β-breaks. Fractures that occur at the time of nodule removal from the ocean floor environment are called α-breaks.

Recrystallization and/or replacement of oxides and nonoxides may be observed to some extent in older nodules, and alteration or even complete replacement of the original nucleus may occur. Basically, however, the mineralogy and most of the textural features in nodule interiors are virtually identical to the outermost layers, indicating that most nodules change little upon aging.

MINERALOGY

Manganese nodules consist of a complex mixture of materials, including organic and colloidal matter and nucleus fragments as well as crystallites of various minerals of detrital and authigenic origins. The phases in nodules are fine grained, often metastable, poorly crystallized, and so intimately intergrown that it is often quite difficult to characterize the minute mineral crystallites or to extract a homogeneous, single-phase mineral sample for study. The minerals are usually characterized by numerous structural defects, essential vacancies that may not be ordered, domain intergrowths, extensive solid solution, and cation exchange properties that lead to nonstoichiometry and detract from long-range ordering of the crystals. Distinguishing between authigenic and detrital minerals, particularly the silica, clay, and iron oxyhydroxide phases, is also a challenge, as these phases either formed in situ or were transported to the nodule as suspensions in seawater.

The major interest in manganese nodules centers on the

oxide minerals of manganese and iron. However, mention will also be made of authigenic and detrital accessory phases. For the purposes of this study, a mineral is defined as an inorganic solid with a crystalline particle size exceeding 30 to 40 Å, having a limited chemical composition range and a systematic three-dimensional atomic order. The isotropic oxides in manganese nodules are amorphous to X-ray diffraction and cannot be classified usefully by optical means. Particle sizes less than 30 to 40 Å are also amorphous even to electron microscopy. These amorphous materials in manganese nodules and other materials lacking an internal structure of atoms are not included as minerals, but are classed as mineraloids.

Prior to discussion of the manganese, iron, and accessory mineral phases, it is important to note that much of the work involving the minerals present in manganese nodules is based on laboratory studies using special sampling techniques, especially in the case of the iron phase. Standard X-ray diffraction techniques cannot generally determine more than one or two of the manganese and accessory phase minerals. The best results to date have been obtained by scanning and transmission microscope studies. Recent work by Turner (*124-126*) and Siegel (*113*) has determined the existence and structure of todorokite in manganese nodules. Chukhrov (*34-36*) has done research on the iron phases in nodules, but identification is difficult because of the need to preserve the nodule mineralogy once the nodule is removed from the ocean and the potential for dehydration and oxidation of both the manganese and iron phase minerals.

MANGANESE MINERALS

Manganese forms a large number of oxide minerals, but only the low-temperature oxides that can be formed in water are relevant to the mineralogy of nodules. The tetravalent manganese predominates in nodules, but the presence of Mn^{2+} and Mn^{3+} ions in some phases has been inferred from crystallographic and thermodynamic data. Table 2 lists the oxide phases of manganese relevant to manganese nodule mineralogy as provided by Burns and Burns (*59,* pp. 185-248). Available crystallographic data, crystal structures, chemical composition, and references to occurrence in nodules are also provided. The mineral listing in table 2 follows an approximate order of increasing complexity of crystal structure and decreasing oxidation state of the manganese.

Todorokite, birnessite, and vernadite are the predominant manganese oxide minerals, occurring as cryptocrystalline phases in manganese nodules. The todorokite and birnessite appear to contain variable linkages of edge-shared [MnO_6] octahedra and are characterized by numerous structural defects, cation vacancies in the chains or layers of linked octahedra, domain intergrowths of mixed periodicities, cation exchange properties, and extensive substitution of Ni^{2+}, Cu^{2+}, Zn^{2+}, Mg^{2+}, or other divalent ions for Mn^{2+}. The formation of vernadite, sometimes catalyzed by microorganisms, results in a poorly crystalline to amorphous phase with high surface area and cation adsorption properties, concentrating cobalt by substitution of Co^{3+} for Mn^{4+} (*13, 100*). Postdepositional recrystallization of vernadite to todorokite may occur inside manganese nodules.

Todorokite or 10-Å Manganite

The manganese oxide mineral characterized by X-ray diffraction lines at 9.5 to 9.8 Å and 4.8 to 4.9 Å is one of the most common phases observed in manganese nodules. This phase, a hydrated Mn-Mg-Ca-Na-Ni-Cu oxide often with significant concentrations of nickel and copper, has been identified as either todorokite or 10-Å manganite. A synthetic structural analog of todorokite also gives a ~10-Å diffraction peak, but to avoid confusion with the mineral manganite (γ-$Mn^{III}OOH$), this synthetic 10-Å manganite phase, called buserite in honor of W. Buser (*73*), is generally considered not to occur in nodules.

The chemical formula for todorokite is $(Mn^{2+},Ca,Mg)Mn_3^{4+}O_7 \cdot H_2O$ (*46*). The marine form of todorokite found in manganese nodules as adopted by Burns and Burns (*17*) is $(Ca,Na,K)(Mg, Mn^{2+})Mn_5^{4+}O_{12} \cdot H_2O$. Most todorokites consist of fibrous aggregates of small acicular crystals. The crystals consist of narrow laths or blades elongated along the b axis (fig. 11) and frequently show two perfect cleavages parallel to the (001) and (100) planes. These fibers are commonly twinned at 120° angles. Chukhrov (*31-33*) has indicated that as many as five todorokite polymorphs might exist, all having similar b (2.84 Å) and c (9.59 Å) unit cell parameters, but with the a parameters as multiples of 4.88 Å.

Todorokite, both terrestrial and marine, has a tunnel structure with single, double, and triple chains of edge-shared [MnO_6] octahedra (*31-33, 124-126*) along the b axis. Essential Mn^{2+} and other divalent cations of comparable ionic radii (e.g., Mg^{2+}, Co^{2+}, Ni^{2+}, Cu^{2+}, Zn^{2+}) may be located in

Table 2.—Manganese minerals in Pacific manganese nodules

Mineral	Approximate formula	Crystal system and space group	Cell parameters, Å				References
			a	b	c	z	
Pyrolusite (β-MnO_2)	MnO_2	Tetragonal, $P4_2/mnm$	4.39	4.39	2.87	2	8
Ramsdellite	MnO_2	Orthorhombic, Pbnm	4.53	9.27	2.87	4	70
Nsutite (γ–MnO_2)	$(Mn^{2+},Mn^{3+},Mn^{4+})(O,OH)_2$	Hexagonal, NA	9.65	NAp	4.43	NA	52, 56, 90, 111
Hollandite (α–MnO_2)	$(Ba,K)_{1-2}Mn_8O_{16} \cdot xH_2O$	Tetragonal, I4/m	9.96	9.96	2.86	NA	15
		Monoclinic, $P2_1/n$	10.03	5.76	9.90	NA	
Cryptomelane	$K_{1-2}Mn_8O_{16} \cdot xH_2O$	Tetragonal, I4/m	9.84	9.84	2.86	NA	52, 56, 103
		Monoclinic, I2/m	9.79	2.88	9.94	NA	
Romanechite (psilomelane)	$(Ba,K,Mn^{2+},Co)_2\ Mn_5O_{10} \cdot xH_2O$	Monoclinic, A2/m	9.56	2.88	13.85	2	4, 8, 70, 98
		Orthorhombic, $P2_12_12$	8.254	13.40	2.864	NA	
Todorokite	$(Ca,Na,K,Ba,Ag,)\ (Mg,Mn^{2+},Zn)$ $Mn_5O_{12} \cdot xH_2O$.	Monoclinic, NA	9.75	2.85	9.59	NA	3, 66, 70, 72, 90, 108, 116, 119-120, 126
Buserite	NaMn oxide hydrate	Hexagonal, NA	8.41	NAp	10.01	NA	7, 21, 53-58, 106
Chalcophanite	$Zn_2Mn_6O_{14} \cdot 6H_2O$	Triclinic, $P\bar{1}$	7.54	7.54	8.22	NA	34
Synthetic birnessite	$Na_4Mn_{14}O_{27} \cdot 9H_2O$	Orthorhombic, NA	8.54	15.39	14.26	NA	56, 129
Do.	$Mn_7O_{13} \cdot 5H_2O$	Hexagonal, NA	2.84	NAp	7.27	NA	57
Birnessite	$(Na,Ca,K)\ (Mg,Mn)\ Mn_6O_{14} \cdot 5H_2O$	Hexagonal, NA	2.85	NAp	7.08–7.31	NA	7, 18, 21, 29-30, 37, 40, 58, 64, 70, 90, 108, 116, 119-120
Vernadite[1] (δ–MnO_2)	$MnO_2 \cdot m(R_2O,RO,R_2O_3) \cdot nH_2O$	Hexagonal, NA	2.86	NAp	4.7	NA	7, 18, 22, 29-30, 106, 108
Rancieite	$(Ca,Mn)Mn_4O_9 \cdot 3H_2O$	Hexagonal	2.84	NAp	7.07	NA	16, 116
Groutite	α–MnOOH	Orthorhombic, Pbnm	4.56	10.70	2.85	NA	63, 103
Manganite	γ–MnOOH	Monoclinic, $B2_1/d$	8.88	5.25	5.71	8	70

NA Not available. NAp Not applicable. [1]R = Na, Ca, Co, Fe, Mn.

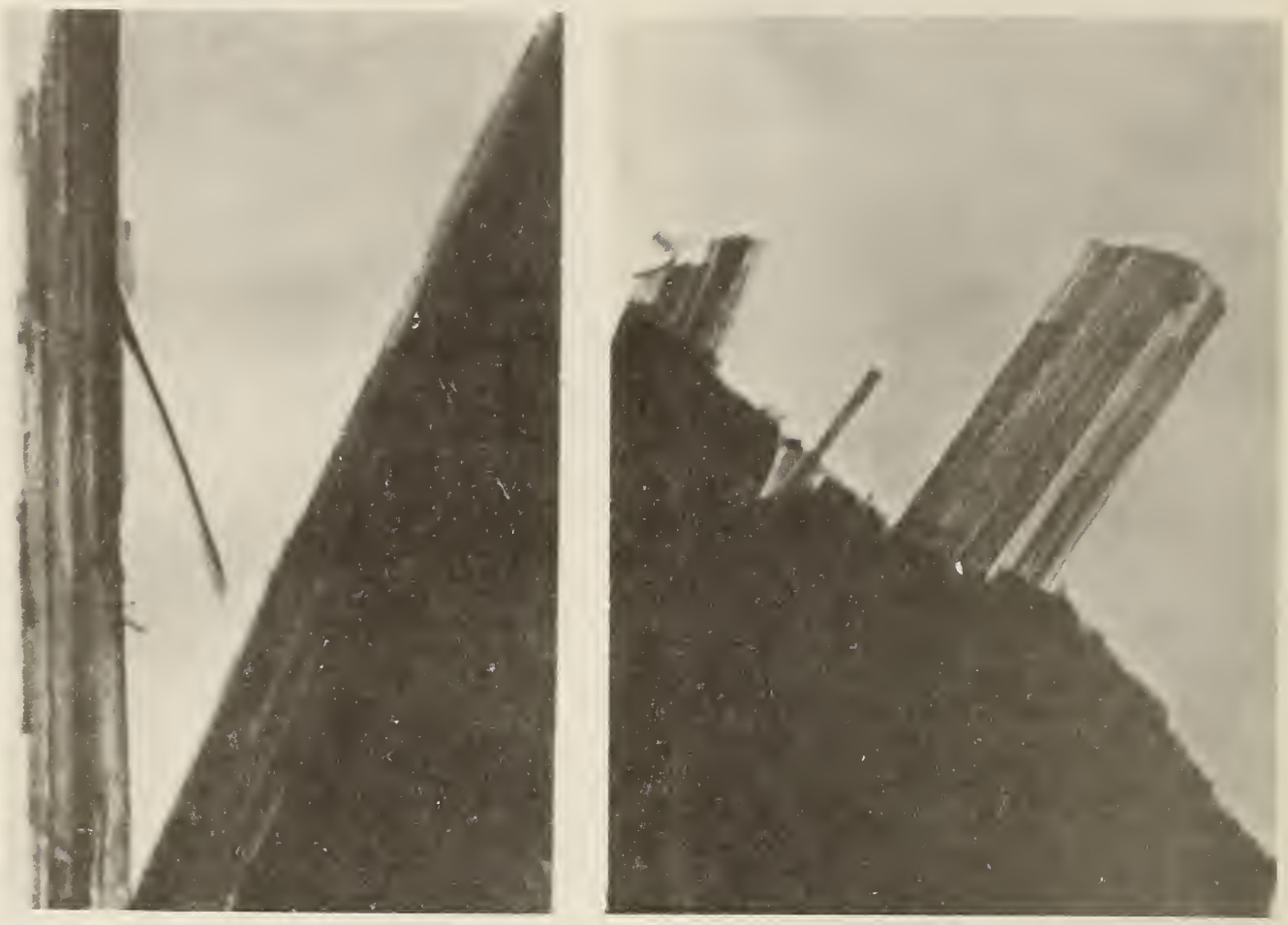

Figure 11.—Electron microscope observation of todorokite. Photograph courtesy of reference 17.

specific positions in the chains of edge-shared $[MnO_6]$ octahedra. The larger Ca^{2+}, Na^{+}, and related group I and II cations, together with water molecules, may occupy the large tunnel structure of todorokite. Some tunnel structures are disrupted by faults along the chain length with the faults going from triple to quadruple chains (*126*). Marine todorokites have been observed to contain quadruple, quintuple, and larger chains. Figure 12 shows the proposed atomic arrangement of one common structure for todorokite (*126*).

Birnessite or 7-Å Manganite

Birnessite in manganese nodules is characterized by X-ray diffraction lines at 7.0 to 7.3 Å and 3.5 to 3.6 Å. Both sets of lines must be present to establish the presence of birnessite, because hollandite-cryptomelane, zeolites such as phillipsite, and clay-mica groups also have d-spacings around 7 Å. The chemical formula for birnessite is $Na_4Mn_{14}O_{22}{\cdot}9H_2O$ (*46*); however, Burns and Burns (*17*) use $(Na,Ca,K)(Mg,Mn)Mn_6O_{14}{\cdot}5H_2O$ as the marine form. The platy habit of birnessite observed by scanning electron microscopy is distinctive.

The birnessite structure is postulated to contain layers of edge-shared $[MnO_6]$ octahedra separated by about 7.2 Å along the c axis, which enclose sheets of H_2O molecules. In synthetic sodium birnessite, one out of six octahedral sites in the layer of linked $[MnO_6]$ is unoccupied. The vacant Mn^{4+} sites are distributed according to different patterns for adjacent $[MnO_6]$ octahedral layers, resulting in a two-layer orthorhombic cell with periodicity c = 14.26 Å. The Mn^{2+} and Mn^{3+} ions are arranged above and below the vacancies, and are bonded with oxygens in both the $[MnO_6]$ layer and the sheet of H_2O molecules. The structure of sodium-free birnessite has disordered vacancies in the $[MnO_6]$ layers, leading to a hexagonal cell with periodicity c = 7.27 Å. Divalent cations of Cu, Ni, Co, Zn, etc. are located directly above and below vacancies in the edge-shared $[MnO_6]$ octahedral sheets, bound in the birnessite structure rather than randomly adsorbed on external surfaces of the microcrystallites.

Vernadite or δ-MnO_2

The phase in manganese nodules giving only two diffuse X-ray diffraction lines at 2.40 to 2.45 Å and 1.40 to 1.42 Å is designated as vernadite, a poorly crystalline δ-MnO_2 or supergene hydrated manganese (IV) oxide. The chemical composition of vernadite is variable, as reflected in its proposed formula: $MnO_2{\cdot}m(R_2O, RO, R_2O_3){\cdot}nH_2O$, where R = Na, Ca, Co, Fe, Mn (*17*). Fleischer (*46*) lists vernadite as $(Mn^{4+},Fe^{3+},Ca,Na)(O,OH)_2{\cdot}nH_2O$. The iron observed to be present may be an intimately associated or epitaxial intergrowth of feroxyhyte, δ′-FeOOH, rather than a part of the vernadite structure.

The vernadite is distinguished from a structurally dis-

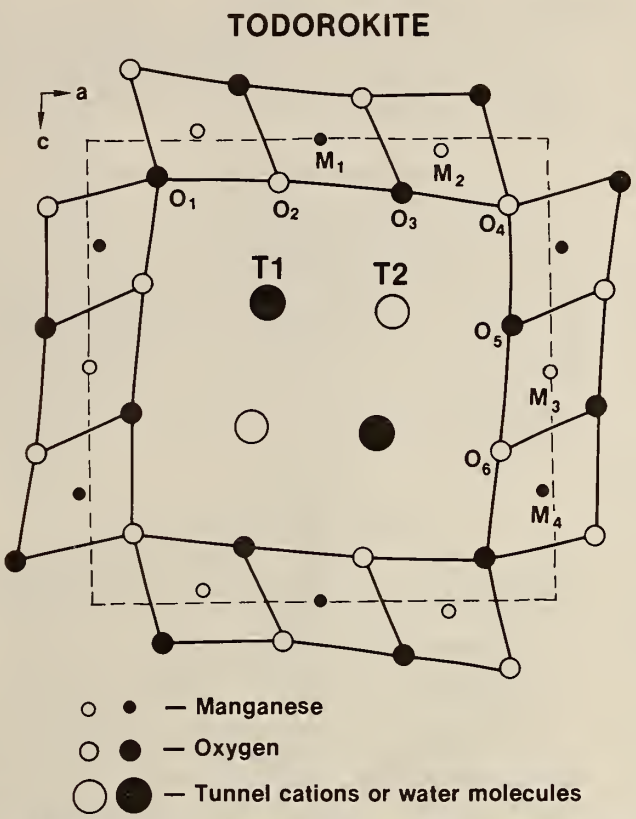

Figure 12.—Proposed atomic arrangement for one common todorokite structure.

ordered birnessite by its distinctive high specific surface area and its significant concentrations of Co, Ca, and Pb. The leaflets of vernadite are tens of angstroms smaller than flakes of birnessite, and are often curved and folded to resemble fibers.

The vernadite structure is represented as a two-layer hexagonal packing of oxygen atoms and water molecules in which the octahedra are completely filled, but less than half with the tetravalent manganese. The extent of filling by Mn^{4+} is apparently determined by the contents of water and cations other than Mn^{4+}. By inclining leaflets of vernadite with respect to the electron beam, reflections with d spacing equal to 2.18 to 2.20 Å, corresponding to the (101) plane, lead to an approximate c parameter of 4.7 Å. This is the approximate width of two layers of close-packed oxygens.

The poor crystallinity and high specific surface areas of vernadite result in this phase having high cation adsorption properties, particularly for cobalt. The substitution of low-spin Co^{3+} (ionic radius 0.53 Å) for Mn^{4+} (0.54 Å) in the $[MnO_6]$ octahedra of vernadite has been confirmed by photoelectron spectroscopy (*100*).

Other Manganese Minerals

Other manganese minerals that have been reported in manganese nodules are listed in table 2. These include pyrolusite or β-MnO_2, ramsdellite, nsutite or γ-MnO_2, hollandite or α-MnO_2, cryptomelane, romanechite or psilomelane, chalcophanite, rancieite, groutite, and manganite. However, they do not appear to be common, and some identifications are not fully accepted. A good discussion of these minerals and others is found in the review by Burns and Burns (*15, 17*).

Manganese Mineral-Element Association

Several elements are associated solely with the manganese mineral phase of the nodule. Other elements have been shown to exist with the manganese mineral phase and with the iron or accessory mineral phases. Those elements associated almost entirely with the manganese mineral phase are Cu, Mo, Ni, and Zn. Other elements associated with the manganese phase, but which may be found in other phases also, are Ba, Cd, Ca, Mg, Sb, Sr, and V.

IRON OXIDE MINERALS

The oxide, oxide hydroxide (or oxyhydroxide), and hydrated oxide phases of iron relevant to manganese nodule mineralogy are listed in table 3. Included in table 3 are the crystallographic data and some of the literature references to the occurrence of each iron oxide mineral in manganese nodules. As stated earlier, the information to date is based on limited studies, and identification of these iron minerals is difficult because they are extremely fine grained. By analogy with the manganese oxides, the structures of many of the iron oxides consist of close-packed oxygens containing Fe^{3+} and/or Fe^{2+} ions in various octahedral interstices forming different assemblages of edge-shared $[FeO_6]$ octahedra. Certain iron (III) oxide hydroxides are isostructural with manganese (IV) oxides, with $[FeO_6]$ and $[MnO_6]$ octahedra edge-shared in different arrangements. The larger ionic radius of Fe^{3+} compared with Mn^{4+} results in larger spacings for the $(10\bar{1}0)$ and $(11\bar{2}0)$ planes of the hexagonal close-packed systems (approximately 2.50 to 2.56 Å and 1.48 to 1.54 Å, respectively), and Fe-Fe interatomic distances across edge-shared $[Fe(O,OH)_6]$ octahedra range from 2.95 to 3.05 Å. The most commonly observed iron-bearing minerals in manganese nodules, to be discussed in more detail, are goethite, lepidocrocite, and feroxyhyte. Other iron minerals observed include akaganeite, ferrihydrite, hematite, magnetite, and maghemite.

Table 3. — Iron oxide minerals in Pacific manganese nodules

Mineral	Approximate formula	Crystal system and space group	Cell parameters, Å				References
			a	b	c	z	
Goethite (α–FeOOH)	FeOOH	Orthorhombic, Pbnm	4.65	10.02	3.04	4	22, 27, 51, 62, 78
Akaganeite (β–FeOOH)	$(OH,Cl,H_2O)_{1-2}$ $Fe_8(O,OH)_{16}$	Tetragonal, I4/m	10.48	10.48	3.028	1	61
Lepidocrocite (γ–FeOOH)	FeOOH	Orthorhombic, Amam	3.88	12.54	3.07	4	27, 35, 51, 62, 78
Hydrated oxyhydroxide polymer (synthetic).	$FeO_{(3-x)/2}(OH)_x$	Hexagonal, NA	5.88	NAp	9.4	NA	71, 75-77
	$Fe_5HO_8{\cdot}4H_2O$	Hexagonal, NA	5.08	NAp	9.4	NA	28, 129
Ferrihydrite	$5Fe_2O_3{\cdot}9H_2O$	Hexagonal, NA	5.08	NAp	9.4	NA	23
Feroxyhyte (δ'–FeOOH)	FeOOH	Hexagonal, NA	2.93	NAp	4.60	1	36
Hematite (α–Fe_2O_3)	Fe_2O_3	Hexagonal, R3c	5.04	NAp	13.77	6	69
Maghemite (γ–Fe_2O_3)	Fe_2O_3	Cubic, $P2_13$	8.32	8.32	8.32	8	27, 62, 129
		Tetragonal, $P4_12_12$	8.338	8.338	25.014	NA	
Magnetite (spinel)	Fe_3O_4	Cubic, Fd3m	8.39	8.39	8.39	8	27

NA Not available. NAp Not applicable.

Feroxyhyte

Feroxyhyte is considered to be a polymorph with akaganeite, goethite, and lepidocrocite and has a formula of δ′-FeOOH (*36*). The structure is thought to be a hexagonal close packing of oxygen and differs only from δ-FeOOH by the arrangement of the iron atoms. Feroxyhyte is found as yellow-brown plates in admixtures of clay minerals and goethite. Its strongest diffraction lines are 2.54 and 2.23 Å, with other lines at 1.69 and 1.47 Å (*36*).

As a magnetically disordered form of δ-FeOOH, no reflection characterizing an ordered distribution of Fe^{3+} in the octahedral sites is observed in electron diffraction patterns from feroxyhyte. Feroxyhyte is unstable in air and transforms to goethite (*99*).

Goethite

Goethite (α-FeOOH) is the polymorph to which most other FeOOH phases revert upon aging. It is isostructural with the manganese minerals ramsdellite and groutite, consisting of double chains of $[Fe(O,OH)_6]$ octahedra linked together by sharing opposite edges. An octahedron from one chain shares an edge with two octahedra from another chain, and the double chains are further crosslinked to adjacent double chains through double sharing of oxygen, producing an orthorhombic symmetry. The goethite in this structure occurs in a habit of acicular needles, 0.1 to 1.0 μm in length. The iron atoms occupy only octahedral positions in this yellow-brown colored mineral (*99*).

Goethite is an antiferromagnetic mineral, that is, goethite remains magnetized even when a magnetic field is removed. The magnetization is not reversible. High Cl^- concentrations in seawater should inhibit the formation of goethite. Thus, the widely reported occurrence of goethite in nodules may result from the fact that it is the end product of both hydrolysis and oxidation action in the other FeOOH phases (*99*).

Lepidocrocite

The abundance of reported lepidocrocite (γ-FeOOH) appears to indicate a relatively rapid oxidation of Fe(II) solutions, though it may occasionally form from Fe(III). Lepidocrocite has a cubic close-packed oxygen lattice structure with no structural analogs among the manganese oxides or hydroxide phases. The iron atoms occupy only octahedral positions in the stacking of oxygen-hydroxyl planes along the [051] direction. This orange-colored mineral forms lath-shaped crystals ranging from 0.5 to 1.0 μm long (*99*).

Lepidocrocite is neither ferrimagnetic nor antiferromagnetic (see appendix) at ordinary temperatures, and so it carries no magnetic remnants. It is transformed to maghemite at 250° to 300° C.

Other Iron Oxide Minerals

Akaganeite (β-FeOOH) is the form of iron that precipitates from Cl-rich solutions such as seawater. The failure to identify akaganeite more frequently in nodules may be the result of rapid conversion to the more stable goethite under seawater conditions, though akaganeite has been shown to be stable for up to 2 yr at pressures up to 1,000 atm (*99*). Also, the cryptocrystallinity of akaganeite may have resulted in the mineral being amorphous to X-ray diffraction, or phases identified as phillipsite may have actually been mixtures of goethite and akaganeite (*99*).

Magnetite (Fe_3O_4) and maghemite (γ-Fe_2O_3) result from relatively slow oxidation of Fe(II) solutions, and can form authigenically in the ferromanganese nodules. Hematite can crystallize from the seawater dissolution of fine-grained goethite or by dehydration of the goethite, but environmental conditions may result in the formation of both minerals by separate pathways. Hematite, once formed, does not appear to rehydrate to form goethite. Hematite is also formed by the aggregation of small ferrihydrite particles followed by nucleation and crystallization of hematite. Ferrihydrite also serves as a source of dissolved iron for the crystallization of goethite.

Iron Oxide Mineral-Element Association

Several elements are associated solely with the iron oxide phase of the nodule. Other elements have been shown to exist in iron oxide mineral phases and with manganese or accessory mineral phases. Those elements associated almost entirely with the iron oxide phase are Pb and Ti with Co occurring in both the iron and manganese phase depending on the oxidation-reduction potential of the seafloor (generally related to depth). Other elements associated with the iron phase, but which may also be found in other phases, are Ce, Co, Sr, V, and Zr.

ACCESSORY MINERALS

The accessory minerals found in Pacific manganese nodules can be divided into the following three general categories:

1. Sheet silicates and zeolite minerals.
2. Clastic silicate and volcanic minerals.
3. Biogenic minerals.

These minerals are poorly defined in manganese nodules because most exist as fine-grained crystallites similar to the manganese- and iron-phase minerals. Some of these accessory minerals were identified in the residues of acid leached nodules. This acid leaching tends to concentrate, and potentially recrystallize and/or flocculate these minerals together with the iron-phase minerals while dissolving the manganese-phase minerals. Because of their low concentrations in nodules, the accessory minerals are often not detected by X-ray diffraction methods on bulk samples. Some minerals have been identified by selective area electron diffraction.

Although most published studies on manganese nodules do not address the accessory minerals, some of these minerals may be necessary for the nucleation and growth of the iron and manganese oxides. Quite often, the core or nucleus of nodules consists of volcanic rock fragments, glass, shark teeth, fish bones, or siliceous and calcareous remains of marine organisms. Table 4 lists the various accessory minerals, their formulas, cell parameters, crystal system, and references where they were reported.

Sheet Silicates and Zeolites

Several sheet silicates and zeolites have been reported in manganese nodules. The clay found in nodules are those associated with the sediments where the nodules were formed (*19-20*), and are fine-grained hydrous aluminum silicates probably formed by submarine alteration of the primary minerals in basalts. The sheet silicates reported in nodules are chlorite, illite, kaolinite, montmorillonite, nontronite, pyrophyllite, and talc. The common clay present is generally montmorillonite. These minerals in nodules occur probably from inclusion of the sediments during nodule growth.

The zeolites found in nodules are authigenic and are found in cracks and cavities in the interior of nodules. The zeolites are hydrous silicates with a very open framework and large interconnecting spaces or channels that are filled with sodium, calcium, and variable amounts of water. The zeolites reported in nodules are analcite, clinoptilolite, epistilbite, erionite, mordenite, and phillipsite. The most commonly reported zeolite is phillipsite whereas the remaining zeolites

Table 4. — Accessory minerals in Pacific manganese nodules

Mineral group and mineral	Formula	Crystal system and space group	Cell parameters, Å a	b	c	z	References
SILICATES							
Tectosilicates:							
Zeolites:							
Analcite	$NaAlSi_2O_6 \cdot H_2O$	Isometric, Ia3d	13.72	13.72	13.72	16	70
Clinoptilolite	$(Na,K,Ca)_{2-3}Al_3(Al,Si)_2Si_{13}O_{36} \cdot 12H_2O$	Monoclinic, I2/m	15.85	17.89	7.41	4	94
Epistilbite	$CaAl_2Si_6O_{16} \cdot 5H_2O$	Monoclinic, NA	8.92	17.73	10.21	3	94
Erionite	$(Ca,Na,K,Mg)_5Al_9Si_{27}O_{72} \cdot 27H_2O$	Hexagonal, $P6_3/mmc$	13.26	NAp	15.12	NA	94
Mordenite	$(Ca,Na_2,K_2)_4Al_8Si_{40}O_{96} \cdot 28H_2O$	Orthorhombic, Cmcm	18.13	20.49	7.52	4	3, 94
Phillipsite	$KCa(Al_3Si_5O_{16}) \cdot 6H_2O$	Orthorhombic, B2mb	9.96	14.25	14.25	4	3-4, 11, 65, 104-106, 115
Do.	$K_{2.8}Na_{1.6}Al_{4.4}Si_{11.6}O_{32} \cdot 10H_2O$	Monoclinic, $P2_1$ or $P2_1/m$	10.02	14.28	8.64	2	
K-feldspar (orthoclase)	$KAlSi_3O_8$	Monoclinic, C2/m	8.56	12.96	7.21	4	11, 22, 115
Labradorite (feldspar)	$Ab_{50}An_{50} \rightleftharpoons Ab_{30}An_{70}$	Triclinic, NA	8.17	12.85	7.13	NA	11
Plagioclase (feldspar)	$(Na,Ca)Al(Si,Al)Si_2O_8$	Triclinic, NA	8.14	12.84	7.16	8	94, 115
Sanidine (feldspar)	$KAlSi_3O_8$	Monoclinic, C2/m	8.56	13.03	7.17	4	94
Quartz	SiO_2	Hexagonal, $P3_221$–$P3_121$	4.91	NAp	5.41	3	5, 11, 22, 24, 62, 70, 104-106, 115, 121
Phyllosilicates:							
Chlorite	$(Mg,Fe)_3(Si,Al)_4O_{10}(OH)_2 \cdot (Mg,Fe)_3(OH)_6$	Monoclinic, C2/m	5.2	9.2	28.6	4	4, 11, 24
Illite	General term for mica-like clays	NAp	NAp	NAp	NAp	NAp	94, 115, 121
Kaolinite	$Al_2Si_2O_5(OH)_4$	Triclinic, Pl	5.14	8.93	7.37	2	106, 115
Montmorillonite	$(Al,Mg)_8(Si_4O_{10})_3(OH)_{10} \cdot 12H_2O$	Monoclinic, C2/m	5.23	8.93–9.00	29.8	NA	3-4, 6, 11, 58, 65, 94, 105, 129
Nontronite	$Fe_2(Al,Si)_4O_{10}(OH)_2Na_{0.3}(H_2O)_4$	Monoclinic, NA	5.23	9.10–9.12	NA	NA	5, 11, 93, 106
Pyrophyllite	$Al_2Si_4O_{10}(OH)_2$	Monoclinic, C2/c	5.16	8.88	18.64	2	94
Talc	$Mg_3Si_4O_{10}(OH)_2$	Monoclinic, C2/c	5.27	9.12	18.85	4	94
Biotite (mica)	$K(Mg,Fe)_3(AlSi_3O_{10})(OH)_2$	Monoclinic, C2/m	5.31	9.23	10.18	2	93
Prehnite	$Ca_2Al(AlSi_3O_{10})(OH)_2$	Orthorhombic, P2c/m	4.65	5.48	18.49	2	94
Stilpnomelane	$K(Fe,Mg,Al)_3Si_4O_{10}(OH)_2 \cdot xH_2O$	Monoclinic, NA	5.40	9.42	12.14	1	106
Inosilicates (double chain):							
Hornblende (amphibole)	$(Ca,Na)_{2-3}(Mg,Fe,Al)_5Si_6(SiAl)_2O_{22}(OH)_2$	Monoclinic, C2/m	9.87	18.01	5.33	2	5, 93
Inosilicates (single chain):							
Augite (pyroxene)	$(Ca,Na)(Mg,Fe,Al)(Si,Al)_2O_6$	Monoclinic, C2/c	9.73	8.91	5.25	4	5, 11, 70, 93-94, 106
Nesosilicates: Olivine	$(Mg,Fe)_2SiO_4$	Orthorhombic, Pmcn	4.76–4.82	10.20–10.48	5.98–6.11	4	11, 94
Other silicates:							
Opal (amorphous)	$SiO_2 \cdot nH_2O$	NAp	NAp	NAp	NAp	NAp	5, 93
Titanite (sphene)	$CaTiO(SiO_5)$	Monoclinic, C2/c	6.56	8.72	7.44	4	14
NONSILICATES							
Volcanics:							
Anatase	TiO_2	Tetragonal, $I4_1/amd$	3.78	3.78	9.51	4	5, 70, 93
Barite	$BaSO_4$	Orthorhombic, Pnma	8.87	5.45	7.14	4	5, 70, 93
Ilmenite	$FeTiO_3$	Hexagonal, R3	5.09	NAp	14.06	6	94
Magnetite (spinel)	$(Fe,Mg)Fe_2O_4$	Isometric, Fd3m	8.40	8.40	8.40	8	94
Rutile	TiO_2	Tetragonal, $P4_2/mnm$	4.59	4.59	2.96	2	5, 70, 93
Biogenics:							
Apatite	$Ca_5(PO_4)_3(F,Cl,OH)$	Hexagonal, $P6_3/m$	9.39	NAp	6.89	2	4-5, 9, 90
Aragonite	$CaCO_3$	Orthorhombic, Pmcn	4.95	7.96	5.73	4	92
Calcite	$CaCO_3$	Hexagonal, R3c	4.99	NAp	17.06	6	72, 90

NA Not available. NAp Not applicable.

are rare with some question of their proper identification. Phillipsite, because of its delicate euhedral crystal habit and its occurrence in the leached interior cavities of nodules appears to have formed authigenically (fig. 13). Phillipsite crystals in some nodules appear to have grown together with some of the manganese oxide phase minerals, particularly todorokite (*19-20*).

Clastic Silicates and Volcanics

Many silicate minerals and some volcanic minerals have been observed in manganese nodules. They consist of individual grains of clastic sediments of various minerals that may form the core or become incorporated into the nodule during nodule growth. The clastic silicate (detrital) minerals observed in nodules are given in table 4. The more common minerals present are quartz and various feldspars. One mineral, opal, is believed to have formed authigenically. The volcanic minerals reportedly observed in manganese nodules are barite, magnetite (spinel), and the titanium-containing minerals, anatase, ilmenite, rutile, and sphene.

Biogenics

The biogenic minerals found in manganese nodules come from the debris of dead organisms, such as bones and teeth of fish, sharks, and whales, and the siliceous remains of the zooplankton radiolaria. The larger debris such as bones and teeth are generally associated with the cores of nodules whereas the radiolaria remains are observed throughout the nodules. These radiolaria remains are probably incorporated from the sediment as the nodule grows. The debris in the interior of the nodule may undergo dissolution and may be associated with the formation of phillipsite and todorokite. The minerals of biogenic origin are apatites, primarily from bones and teeth; aragonite and calcite, from the shells of various animals; and opal, which may also be derived from radiolaria.

Sea Salt Residue

Minerals in dried nodules that are the result of seawater evaporation are sylvite, halite, and other common evaporites

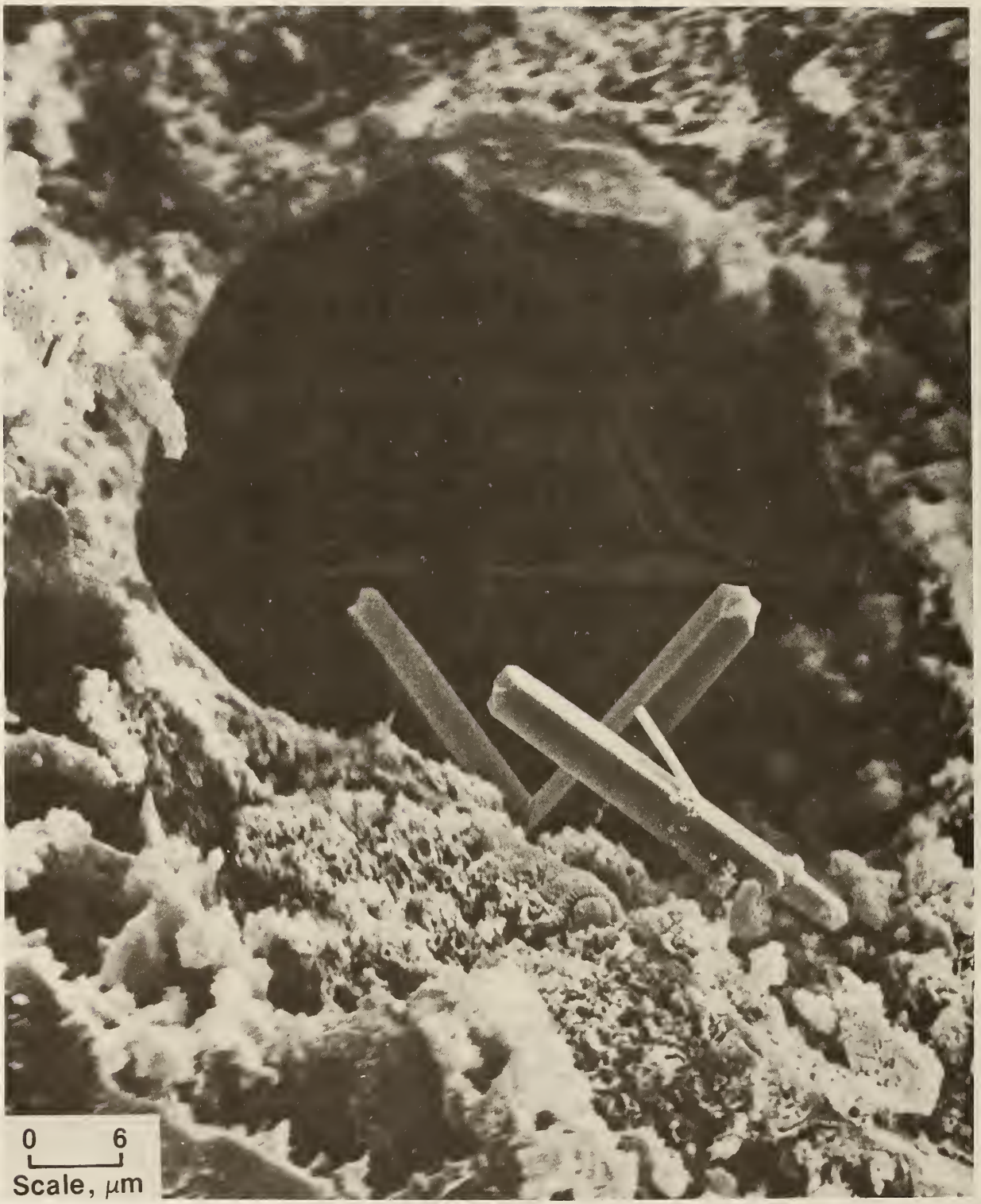

Figure 13.—Scanning electron photomicrograph showing crystals of the zeolite phillipsite in an oxide cavity of a manganese nodule. Photograph courtesy of reference 117, p. 60.

present in dissolved form in seawater. These residues are also the primary source of the anions—borate, bromide, chloride, fluoride, and iodide—in manganese nodules.

Accessory Mineral-Element Association

Several elements are associated solely with the accessory minerals of the nodule. Other elements have been shown to exist in accessory minerals and with the iron oxide or manganese phases. Those elements associated almost entirely with the accessory minerals are Al, Cr, K, P, and Si. Other elements associated with the accessory minerals and possibly other phases are Ba, Mg, Na, and Zr.

MOISTURE CONTENT

Water in manganese nodules comprises about 45 to 50 wt-pct of the nodule when removed from the sea. Drying in air removes approximately half of the water. Drying at 110° C reduces the moisture content of nodules to approximately 5 to 10 wt-pct. Thermal gravimetric analysis in the temperature range of 110° to 1,200° C indicates that the 5 to 10 wt-pct water is bound in the crystal structure.

ELEMENTAL COMPOSITION

The elemental characterization of Pacific manganese nodules is a topic addressed by many authors. Major element composition of these nodules is well established, whereas data on many minor and most trace elements are limited. This section summarizes available data on most of the naturally occurring elements, and where data are sufficient, gives ranges, means, medians, and number of samples. In the case of the major, most minor, and some trace elements, the data are divided into four distinct areas of the Pacific Ocean floor.

1. The Clarion-Clipperton Fracture Zone area (CC-Zone area).
2. The mid-Pacific seamounts area (MPS area), <3,000-m depth.
3. Other abyssal plains area >3,000-m depth, and exclusive of CC-Zone area.
4. Other seamounts, ridges, and continental margins area (<3,000-m depth).

For these elements, histograms and comparison tables are presented for the different areas to show variations of these elements by area. Where a paucity of data exists for the remaining elements, histograms, and tables are presented for the composition based on the total Pacific Ocean. In some cases, data are so limited (<40 sample analyses) that no histogram is presented. Nodules from the Drake Passage area of the Pacific and most of the ocean area directly south of Australia have also been omitted. The Drake Passage nodules are omitted because of their tendency to contain large rock fragments as nuclei, thereby making their bulk chemical analysis atypical of the other Pacific nodules. The area south of Australia is the southeast portion of the Indian Ocean and therefore is not considered part of the Pacific Ocean.

The data for the elements are broken down into eight groups based on either their chemistry or special interest. The groups of elements are presented in the following order:

1. Major and minor elements of potential economic interest (Mn, Fe, Ni, Cu, Co, Zn, V, Mo).
2. Other major and minor elements (Al, Ca, Mg, K, Si, Na, Sr, Ti, Zr).
3. Elements of environmental interest (As, Ba, Cd, Cr, Pb, Hg, Se, Ag).
4. Rare-earth elements (lanthanides) (La, Ce, Pr, Nd, Sm, Eu, Gd, Tb, Dy, Ho, Er, Tm, Yb, Lu, Hf).
5. Precious-metal-group elements (Au, Ir, Pd, Pt, Re, Ru).
6. Radioactive elements (Ra, Th, U).
7. Other trace elements (Sb, Be, Bi, B, Cs, Ga, Ge, Li, Nb(Cb), Rb, Sc, Ta, Te, Tl, Sn, W, Y).
8. Anion-forming elements (Br, C, Cl, F, I, N, P, S).

Within the first three groups, each element is discussed briefly; the chemical form of occurrence in nodules is given if known, and for 21 elements listed within the first three groupings (exclusive of Ag, As, Hg, and Se), interelement correlations are presented by area where data are sufficient. The interelement correlation coefficients (presented in table 19) are results of linear regression analysis with the correlation coefficients varying from -1 to $+1$. Correlations with values >0.3 and <-0.3 were considered significant positive or negative correlations. Of the naturally occurring elements (exclusive of inert gases and hydrogen), no data were obtained for the following elements: Rh, In, Pm, Os, Po, At, Fr, Ac, and Pa. Oxygen is not discussed specifically but is the major combining form for most elements. All concentrations are reported on a dry-weight basis. The majority of the information contained in these sections was obtained from the Sediment Data Bank (*48*), as compiled by Frazer with information from Frazer (*44, 48-50*), Sorem (*118*), Fewkes (*42-43*), and Monget (*97*).

MAJOR AND MINOR ELEMENTS OF POTENTIAL ECONOMIC INTEREST

The elements in this section are those major and minor elements that are of potential economic interest. The eight elements are Mn, Fe, Ni, Cu, Co, Zn, V, and Mo. Because of the amount of data available, the concentrations of these elements are divided into the four areas of the Pacific previously mentioned. Table 5 is a breakdown, by element, for the four areas, and gives range, median range, arithmetic mean, standard deviation of the mean, and the number of samples used for the statistical base. Table 6 gives composite data for those elements from Pacific nodules. The overall mean in table 6 is calculated based on the number of data points for each element in each area and the respective concentrations.

Manganese

Manganese concentrations in Pacific nodules vary from 1 to 40 wt-pct, with a median range of 16 to 27 wt-pct, and weighted mean of 21.6 wt-pct based on 5,079 sample analyses. The median value for CC-Zone area nodules is the highest of all other areas at 26 to 27 wt-pct with a mean of 25.4 wt-pct. Nodules from the other three areas are much lower with a median range of 16 to 21 wt-pct and much higher iron values. Figure 14 provides histograms that show manganese distribution in each of the four areas.

Manganese occurs in Pacific nodules as several minerals, all oxides and hydrated oxides. These minerals are todorokite, birnessite, and vernadite (δ-MnO_2). A discussion of these and other forms of manganese is given in detail in the "Mineralogy" section.

Manganese in the CC-Zone area is positively correlated

Table 5. — Distribution of elements of potential economic interest in Pacific manganese nodules, by area, weight-percent

Area	Range	Median	Mean, $\bar{x}$	Standard deviation of mean, $\sigma\bar{x}$	Number of samples	Range	Median	Mean, $\bar{x}$	Standard deviation of mean, $\sigma\bar{x}$	Number of samples
	Manganese					Cobalt				
Clarion-Clipperton zone	1–39	26–27	25.4	4.9	2,227	<0.10–0.90	0.20–0.30	0.24	0.08	1,925
Mid-Pacific seamounts	1–40	20–21	20.8	8.1	183	<.10–2.50	.70–.80	.76	.45	182
Other abyssal plains, >3,000 m	1–40	18–19	18.5	7.2	2,354	<.10–1.40	.20–.30	.24	.17	2,219
Other seamounts, <3,000 m	1–40	16–17	17.8	8.6	315	<.05–1.40	.20–.30	.31	.27	293
	Iron					Zinc				
Clarion-Clipperton zone	1–25	6–7	6.9	2.6	2,215	<0.05–0.95	0.10–0.15	0.14	0.05	1,539
Mid-Pacific seamounts	2–25	14.5–15.5	14.7	4.1	185	<.05–.25	.05–.10	.07	.03	82
Other abyssal plains, >3,000 m	1–25	12–13	12.7	5.1	2,325	<.05–.95	.05–.10	.09	.1	1,285
Other seamounts, <3,000 m	1–25	16–17	15.6	6.4	312	<.05–.55	.05–.10	.07	.05	191
	Nickel					Vanadium				
Clarion-Clipperton zone	0.10–2.00	1.30–1.40	1.28	0.30	2,237	<0.005–0.08	0.04–0.05	0.047	0.048	70
Mid-Pacific seamounts	.10–1.50	.40–.50	.49	.24	188	<.005–.30	.07–.08	.086	.087	29
Other abyssal plains, >3,000 m	.10–2.00	.50–.60	.63	.40	2,334	<.010–.30	.04–.05	.048	.025	370
Other seamounts, <3,000 m	.10–1.30	.30–.40	.35	.24	315	<.005–.14	.06–.07	.067	.028	38
	Copper					Molybdenum				
Clarion-Clipperton zone	0.10–2.00	1.00–1.10	1.02	0.33	2,236	<0.005–0.12	0.05–0.06	0.052	0.018	265
Mid-Pacific seamounts	<.01–1.00	<.05	.10	.10	176	<.005–.11	.05–.06	.052	.022	56
Other abyssal plains, >3,000 m	<.05–2.00	.30–.40	.42	.32	2,282	<.005–.13	.03–.04	.036	.021	746
Other seamounts, <3,000 m	<.05–1.20	<.05	.11	.14	304	<.005–.15	.03–.04	.050	.067	88

Table 6. — Distribution of elements of potential economic interest in Pacific manganese nodules, composite, weight-percent

Element	Range	Range of medians	Weighted mean	Number of samples
Manganese	1–40	16–27	21.6	5,079
Iron	1–25	6–17	10.4	5,037
Nickel	.1–2.0	.3–1.4	.9	5,074
Copper	<.01–2.0	<.05–1.10	.66	4,998
Cobalt	<.05–2.5	.2–.8	.26	4,619
Zinc	<.05–.95	.05–.15	.11	3,097
Vanadium	<.005–.30	.04–.08	.05	507
Molybdenum	<.005–.15	.03–.06	.04	1,157

(table 19) with Cd, Cu, Mg, Mo, Ni, Sr, V, and Zn, and is negatively correlated with Al, Fe, K, Na, Si, and Ti. In the MPS area, manganese shows a positive correlation with Co, Mo, Ni, Pb, Sr, Zn, and Zr, and a negative correlation with Al and Ca. In the other abyssal plains area, manganese is positively correlated with Cd, Cu, Mo, Ni, and Zn, and negatively correlated with Al, Fe, K, and Si. In the other seamounts area, manganese is positively correlated with Ba, Na, and Ni, and negatively correlated with Al, Cd, and Fe. Where elements are not mentioned, no correlation (<0.3 to >–0.3) was obtained. A positive correlation of manganese with Cu, Ni, Mo, and Zn and a negative correlation of manganese with Al and Fe are observed in all areas. The difference in elemental composition between the lesser depths (MPS and other seamounts) and greater depths (CC Zone and other abyssal plains) may reflect differences in oxidation potential as well as sediment type.

Iron

Iron concentrations in Pacific nodules vary from 1 to 25 wt-pct, with a median range of 6 to 17 wt-pct and a weighted mean of 10.4 wt-pct based on 5,037 sample analyses. The median value for CC-Zone area nodules is lowest of all areas at 6 to 7 wt-pct with a mean of 6.9 wt-pct. The other three areas are much higher in iron with a median range for these areas of 12 to 17 wt-pct. Figure 15 provides histograms that show iron distribution in each of the four areas. Iron occurs in Pacific nodules as goethite and other iron oxides and hydrated oxides as discussed in the "Mineralogy" section.

Iron in CC-Zone nodules is positively correlated (table 19) with Co, Pb, Ti, and Zr, and negatively correlated with Cd, Cu, Mg, Mn, Mo, Ni, and Zn. In the MPS area, iron is positively correlated with Ti and Zr, and negatively correlated with Ba and Ca. In the other abyssal plains area, iron is positively correlated with Co, Pb, Sr, Ti, V, and Zr, and negatively correlated with Cd, Cu, K, Mn, and Ni. In the other seamounts area, iron is positively correlated with Cr, Ti, V, and Zr, and negatively correlated with Ba, Ca, and Mn.

Nickel

Nickel concentrations in Pacific nodules vary from 0.1 to 2.0 wt-pct, with a median range of 0.3 to 1.4 wt-pct and a weighted mean of 0.9 wt-pct based on 5,074 sample analyses. The median value for CC-Zone area nodules is 1.3 to 1.4 wt-pct with a mean of 1.3 wt-pct. The other three areas are much lower in nickel content with a median range of 0.3 to 0.6 wt-pct. Figure 16 provides histograms that show nickel distributions for each of the four areas.

Nickel occurs in Pacific nodules as part of the manganese mineral structure probably adding stability to the minerals. The nickel is strongly correlated with manganese in all areas of the Pacific. The ionic radius of Ni^{2+} allows for direct substitution of Ni^{2+} for Mn^{2+} in the crystal structures.

Nickel in CC-Zone area nodules is positively correlated (table 19) with Cd, Cu, Mg, Mn, Mo, Sr, V, and Zn, and negatively correlated with Fe, Si, and Ti. In the MPS area, nickel is positively correlated with Co, Cr, Mg, Mn, Mo, Na, and Zn, and negatively correlated with Al only. In the other abyssal plains area, nickel is positively correlated with Cd, Cu, Mn, Mo, and Zn, and negatively correlated with Fe and Si. In the other seamounts area, nickel is positively correlated with Cd, Co, Cu, Mg, Mn, and Zn, and no negative correlations are found.

Copper

Copper concentrations in Pacific nodules vary from <0.01 to 2.0 wt-pct with a median range of <0.05 to 1.1 wt-pct and a weighted mean of 0.66 wt-pct based on 4,998 sample analyses. The median value for CC-Zone area nodules is 1.0 to 1.1 wt-pct with a mean of 1.0 wt-pct. The other three areas are much lower in copper with a median range of <0.05 to 0.4 wt-pct. Figure 17 provides histograms that show copper distribution in each of the four areas.

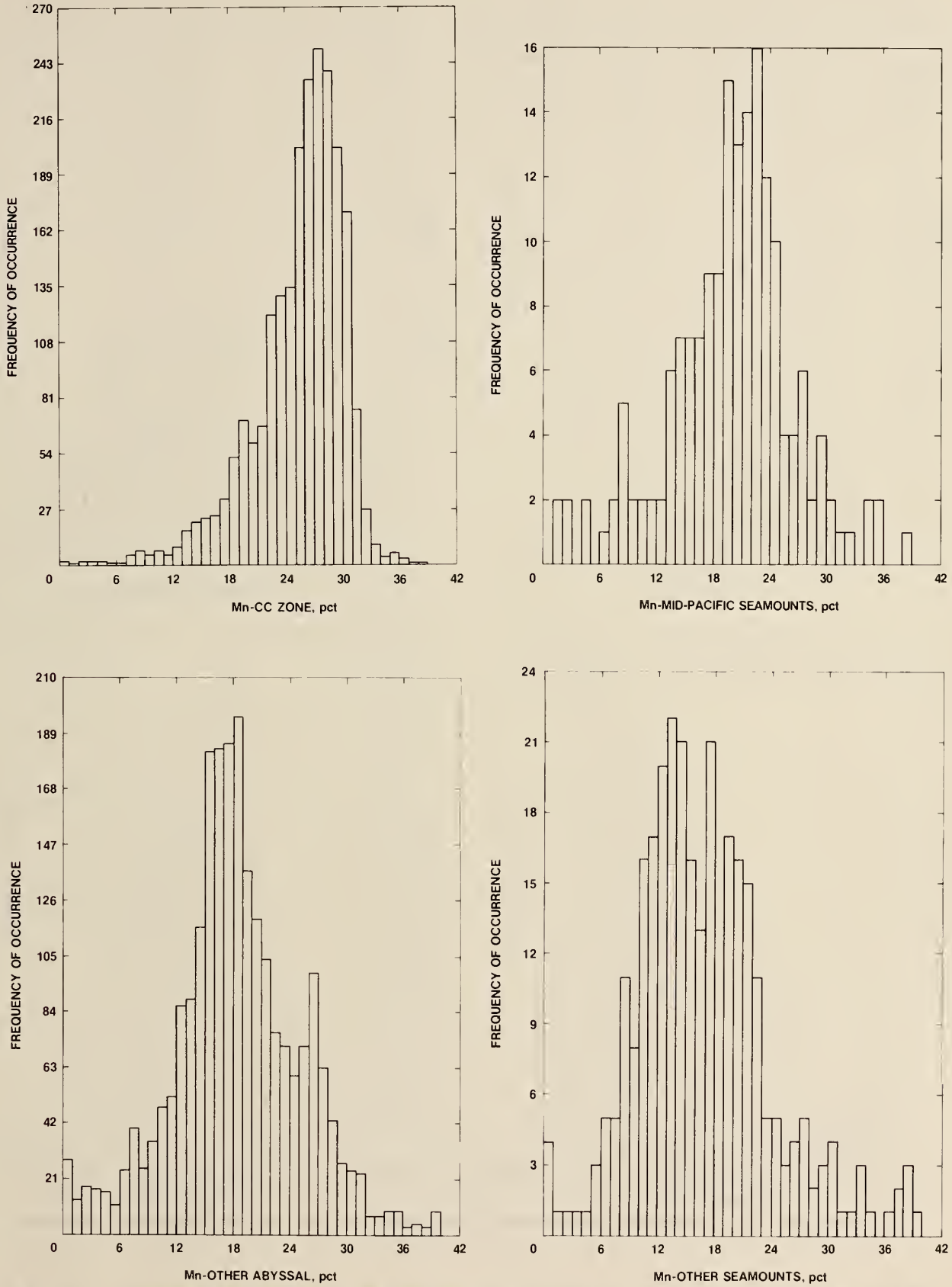

Figure 14.—Manganese frequency distribution by environment for Pacific manganese nodules.

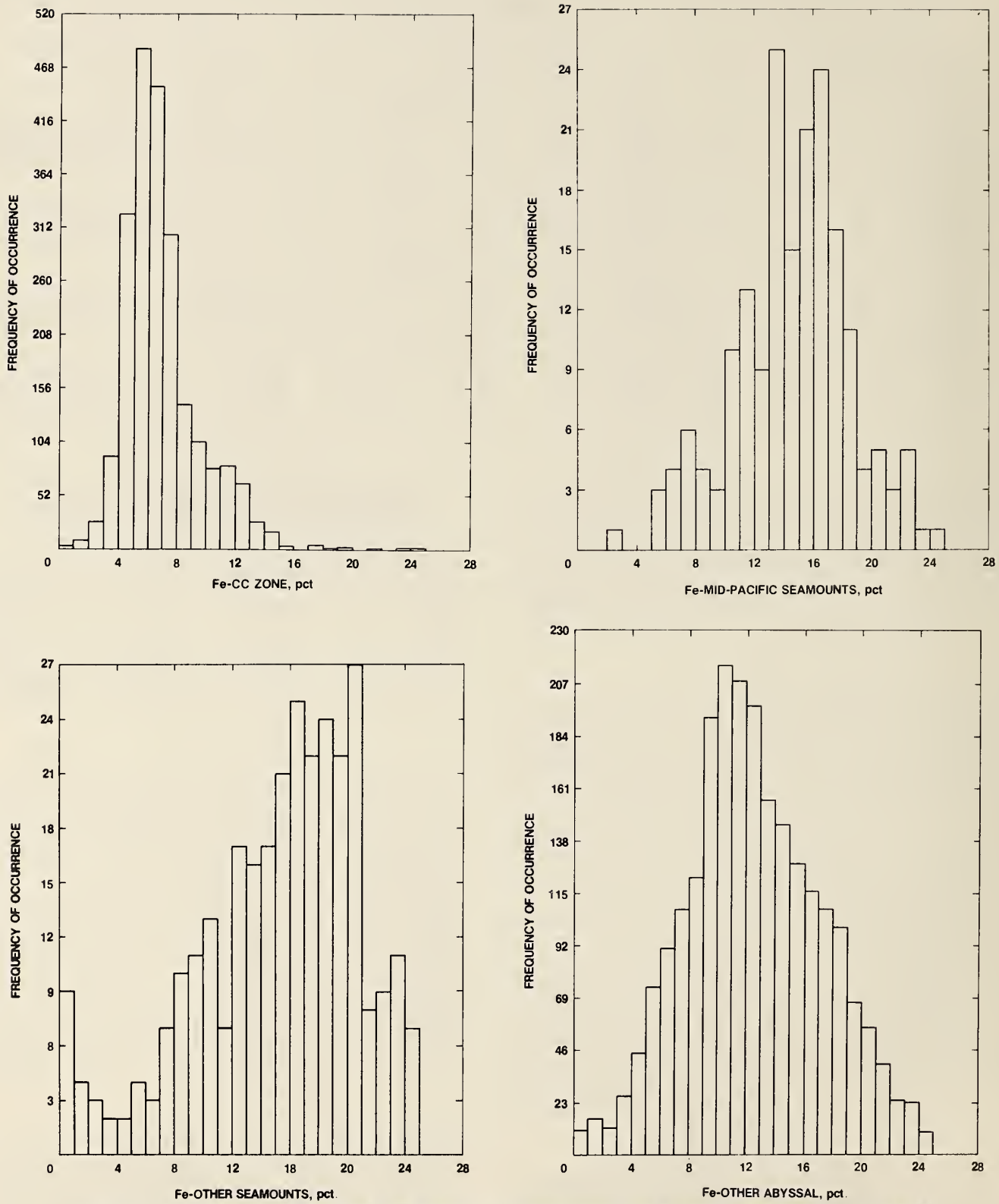

Figure 15.—Iron frequency distribution by environment for Pacific manganese nodules.

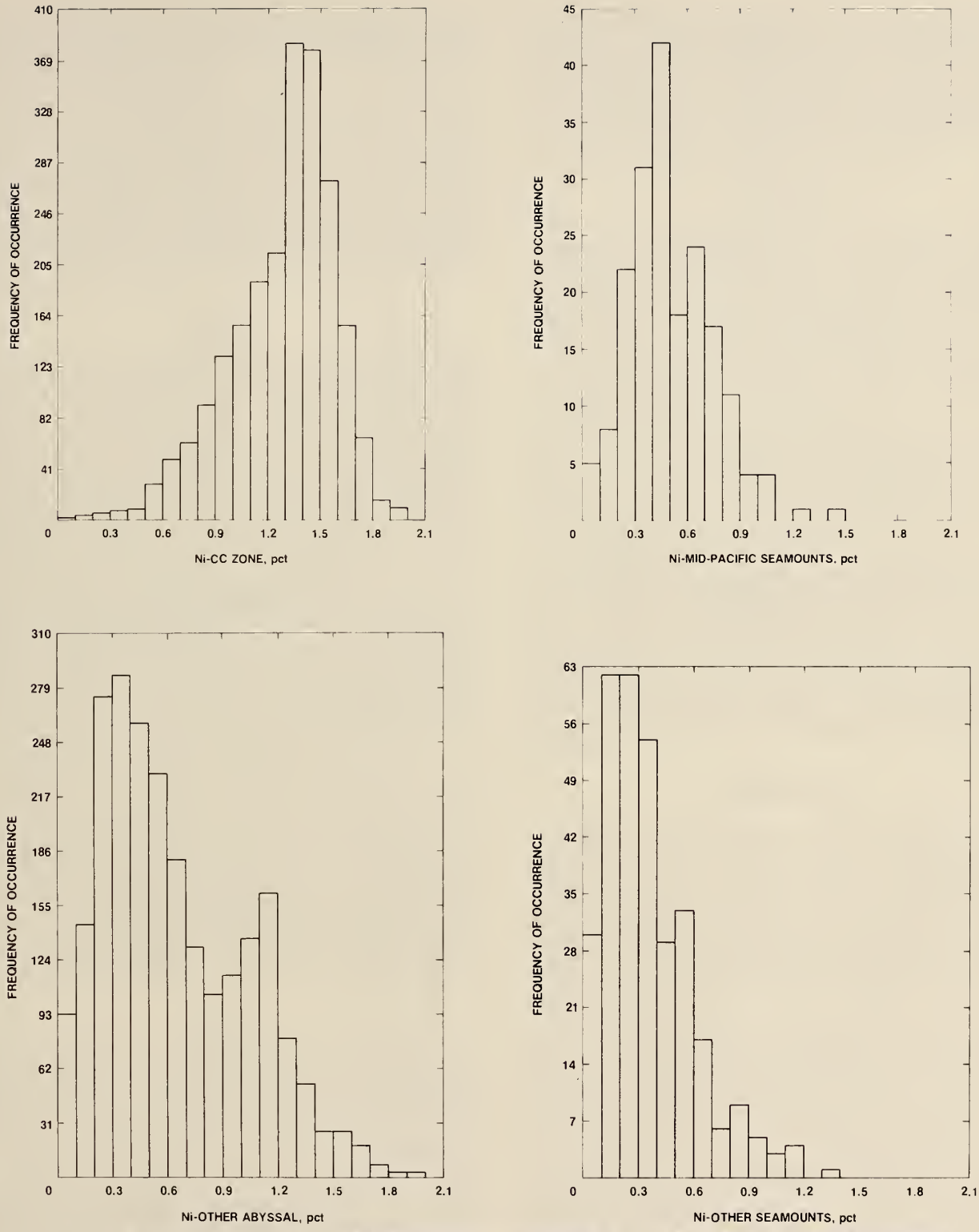

Figure 16.—Nickel frequency distribution by environment for Pacific manganese nodules.

Figure 17.—Copper frequency distribution by environment for Pacific manganese nodules.

Copper occurs in Pacific nodules in a manner similar to that of nickel, which is part of the manganese mineral structure with no copper minerals present. The ionic radius of Cu^{2+} allows direct substitution for Mn^{2+} in the manganese minerals crystal structures.

Copper in CC-Zone area nodules is positively correlated (table 19) with Al, Cd, Mg, Mn, Mo, Ni, Sr, V, and Zn, and negatively correlated with Fe, K, Na, Pb, Si, Ti, and Zr. In the MPS area, copper is positively correlated with Cr only and negatively correlated with Al and Zr. In the other abyssal plains area, copper is positively correlated with Cd, Mn, Ni, and Zn, and negatively correlated with Fe and Pb. In the other seamounts area, copper is positively correlated with Cd, Mg, Ni, V, and Zn, and shows no negative correlation with the other elements.

Cobalt

Cobalt concentrations in Pacific nodules vary from <0.05 to 2.5 wt-pct, with a median range of 0.2 to 0.8 wt-pct and a weighted mean of 0.26 wt-pct based on 4,619 sample analyses. The median value for CC-Zone area nodules is 0.2 to 0.3 wt-pct with a mean of 0.24 wt-pct. Cobalt values are lowest in the two deep-ocean areas (CC Zone and other abyssal plains) and the other seamounts area with all three having similar median ranges and means. The MPS area has the highest cobalt values, with a median range of 0.7 to 0.8 wt-pct and a mean of 0.76 wt-pct. Figure 18 provides histograms that show cobalt distribution in each of the four areas.

Cobalt occurs in Pacific nodules in both the manganese and iron phases. Its occurrence is dependent on the oxidation of cobalt to either Co^{2+} or Co^{3+}. In the MPS area, oxidation to Co^{3+} is one probable explanation of high cobalt values, whereas in the deep ocean the oxidation potential may be insufficient to oxidize Co^{2+} to Co^{3+}. Some cobalt in nodules can also be attributed to volcanic seamounts. Cobalt in the Co^{2+} state has an ionic radius similar to Mn^{2+}, whereas Co^{3+} has an ionic radius very close to that of Mn^{4+} and substitutes for Mn^{4+} in vernadite (*13*, *100*).

Cobalt in CC-Zone area nodules has a slight positive correlation (table 19) with Fe, Pb, and Ti, and a slight negative correlation with Cd. In the MPS area, cobalt is positively correlated with Ba, Mg, Mn, Ni, Pb, Sr, Ti, and Zr, and negatively correlated with Al, Ca, K, Na, and Si. In the other abyssal plains area, cobalt has a slight positive correlation with Fe and Sr, and a slight negative correlation with Al, Cd, and Si. In the other seamounts area, cobalt is positively correlated with Ti and Pb, and has a slight positive correlation with Ni. Cobalt in this area has a slight negative correlation with Cd and Si.

Zinc

Zinc concentrations in Pacific nodules vary from <0.05 to 0.95 wt-pct, with a median value of 0.05 to 0.15 wt-pct and a weighted mean of 0.11 wt-pct based on 3,097 sample analyses. The median value for CC-Zone area nodules is 0.10 to 0.15 wt-pct with a mean of 0.14 wt-pct. Zinc values are highest in CC-Zone nodules; approximately a factor of two higher than in the other three areas. The median range for the other three areas is 0.05 to 0.10 wt-pct with a mean range of 0.07 to 0.09 wt-pct; the lower values occur in the seamount areas. Figure 19 provides histograms that show zinc distribution in each of the four areas.

Zinc appears to occur in Pacific nodules as a substitute in the manganese mineral structure similar to copper and nickel. No zinc minerals have been identified in Pacific nodules. The zinc ionic radius is similar to Mn^{2+} and would allow a direct substitution.

Zinc in CC-Zone area nodules is positively correlated (table 19) with Cu, Mn, and Ni, and negatively correlated with Fe and Zr, with only a slight negative correlation with Pb and Ti. In the MPS area, zinc is positively correlated with Ba, Mn, Na, Ni, and V, and negatively correlated with Mg, Ti, and Zr. In the other abyssal plains area, zinc is positively correlated with Cu, Mn, and Ni, and negatively correlated with Al. In the other seamounts area, zinc is positively correlated with Cd, Cu, and Ni, and negatively correlated with Na.

Vanadium

Vanadium concentrations in Pacific nodules vary from <0.005 to 0.300 wt-pct, with a median value of 0.040 to 0.080 wt-pct and a weighted mean of 0.050 wt-pct based on 507 sample analyses. The median value for CC-Zone area nodules is 0.04 to 0.05 wt-pct with a mean of 0.047 wt-pct. The CC-Zone area and other abyssal plains area have somewhat lower median and mean values than the two seamount areas by about a factor of 1.5 to 2.0. Figure 20 provides histograms that show vanadium distribution for each of the four areas.

Vanadium appears to be another of the many elements that occur with manganese and may possibly substitute for Mn^{4+} or fill the large tunnels in the manganese mineral structure as oxides. Correlation coefficient data (table 19) indicate a tendency for vanadium to occur with Mn, Cu, and Ni, all of which have been shown to substitute for manganese in the manganese mineral structure.

Vanadium in CC-Zone area nodules correlates with Ca, Cu, Mn, and Ni, and negatively with Al and Na. In the MPS area, vanadium correlates positively with K, Na, and Zn, and negatively with Mo, Pb, and Ti. In the other abyssal plains area, vanadium correlates positively with Fe and Mo and negatively with Si. In the other seamounts area, vanadium correlates positively with Al, Cu, Fe, K, and Ti, and negatively with Ba and Ca. Vanadium data for the seamounts areas are very limited; therefore, correlation coefficients may not accurately reflect the actual correlation of vanadium to other elements.

Molybdenum

Molybdenum concentrations in Pacific nodules vary from <0.005 to 0.150 wt-pct, with a median value of 0.03 to 0.06 wt-pct and a weighted mean of 0.04 wt-pct based on 1,157 sample analyses. The median value for CC-Zone area nodules is 0.05 to 0.06 wt-pct with a mean value of 0.05 wt-pct. Molybdenum concentrations appear to be somewhat uniform throughout all four areas with only a slightly lower mean for the other abyssal plains area. Figure 21 provides histograms that show molybdenum distribution for each of the four areas.

Molybdenum appears to occur in a manner similar to that of Cu and Ni; that is, as a substitute in the manganese mineral structure. No molybdenum minerals have been identified in Pacific nodules. The ionic radius of molybdenum in oxidation states 4 and 6 is similar to Mn^{4+}, and therefore it may be a substitute for Mn^{4+} or it may be contained in the smaller tunnel structure of the manganese minerals.

Molybdenum in CC-Zone area nodules is positively correlated (table 19) with Cd, Cu, Mn, and Ni, and negatively correlated with Fe. In the MPS area, molybdenum is positively correlated with Mn, Na, and Ni, and negatively correlated with Al and V. In the other abyssal plains area, molybdenum is positively correlated with Cd, Mn, Ni, and V, and negatively correlated with Al and Si. In the other seamounts area, molybdenum is positively correlated with Na and Pb and has no negative correlation. Molybdenum data in the two seamounts areas are limited; therefore, correlation coefficients may not accurately reflect the actual correlation of molybdenum to other elements.

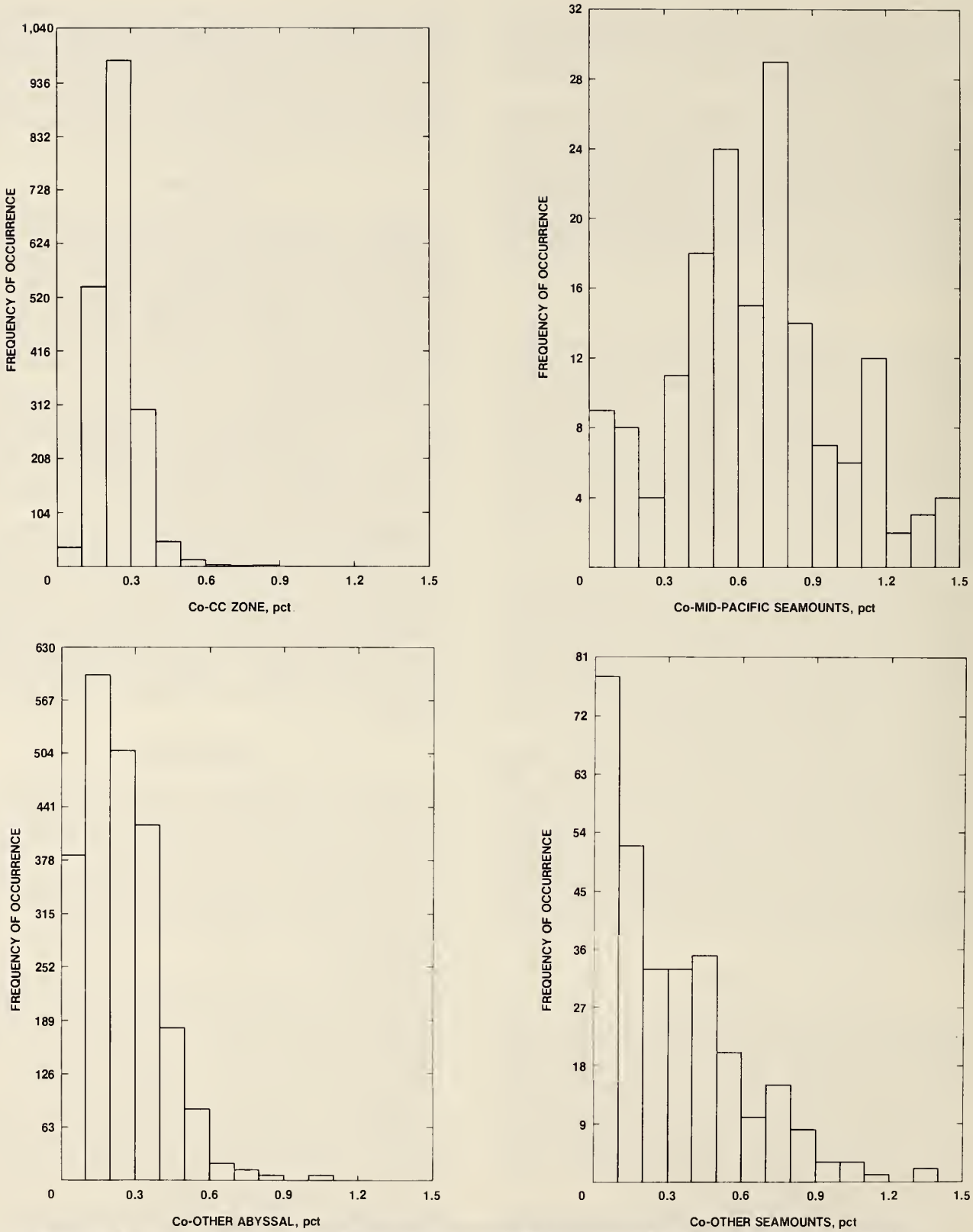

Figure 18.—Cobalt frequency distribution by environment for Pacific manganese nodules.

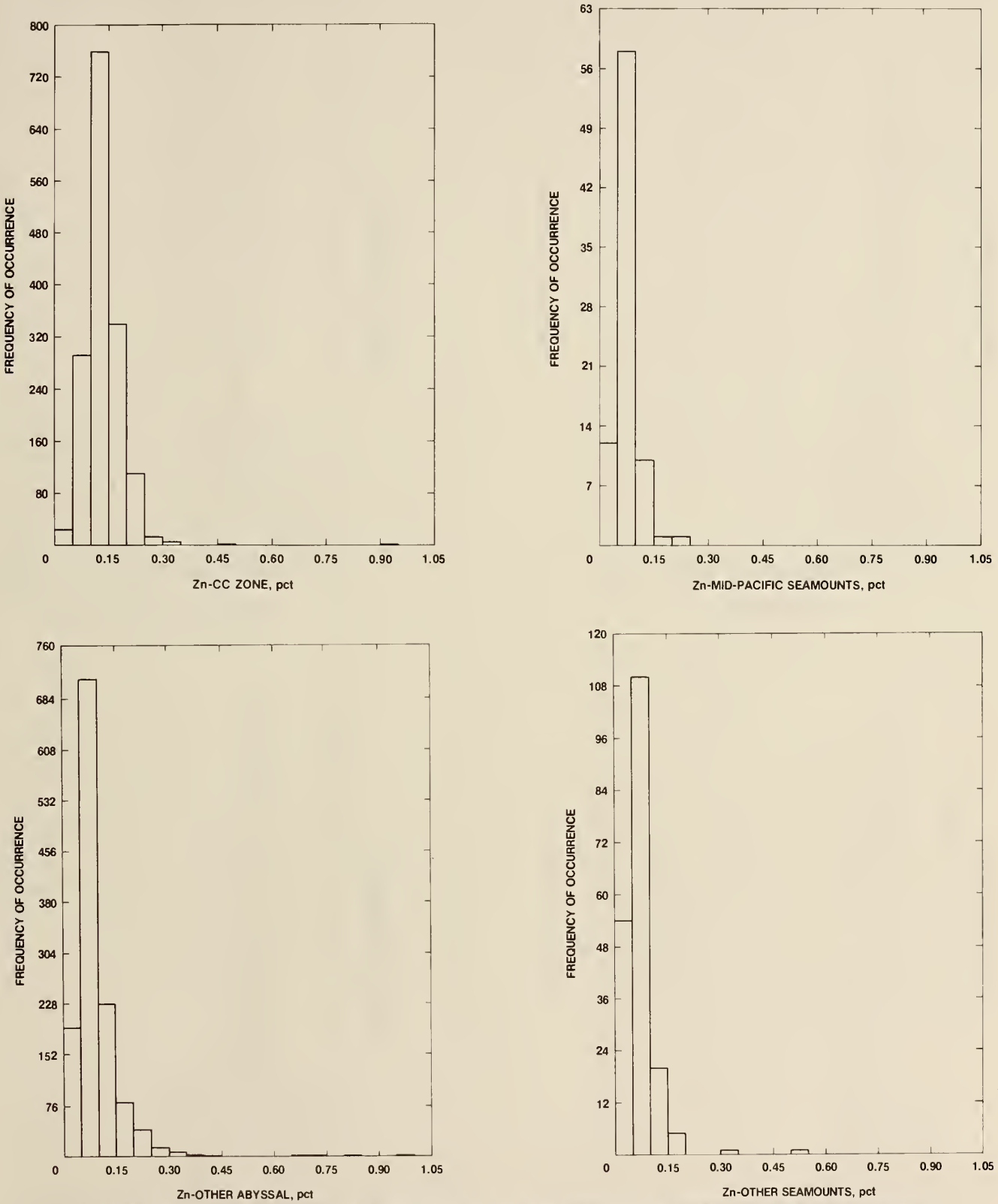

Figure 19.—Zinc frequency distribution by environment for Pacific manganese nodules.

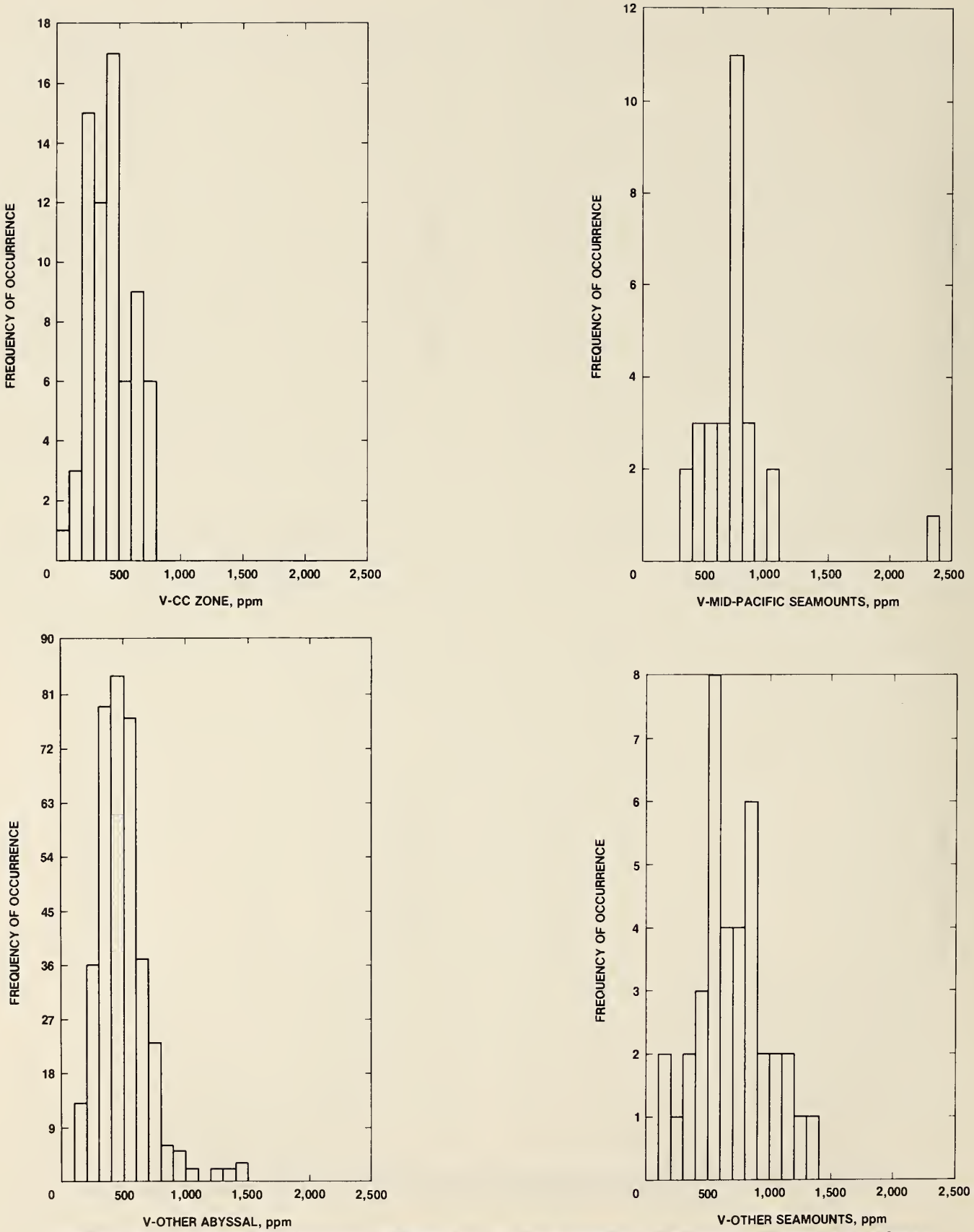

Figure 20.—Vanadium frequency distribution by environment for Pacific manganese nodules.

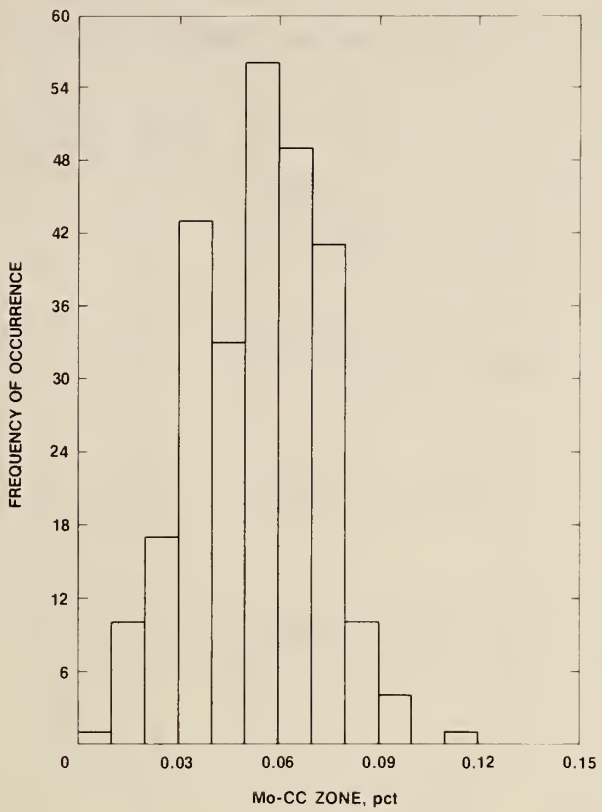

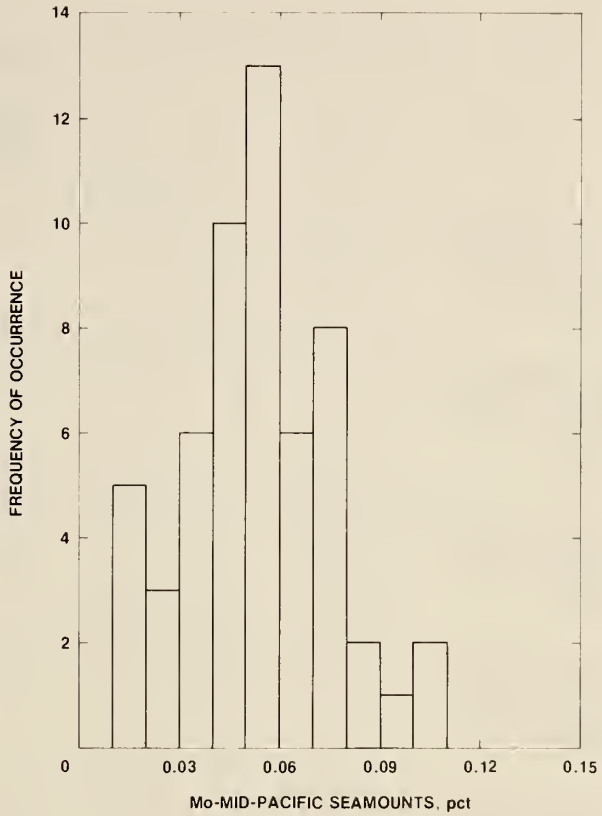

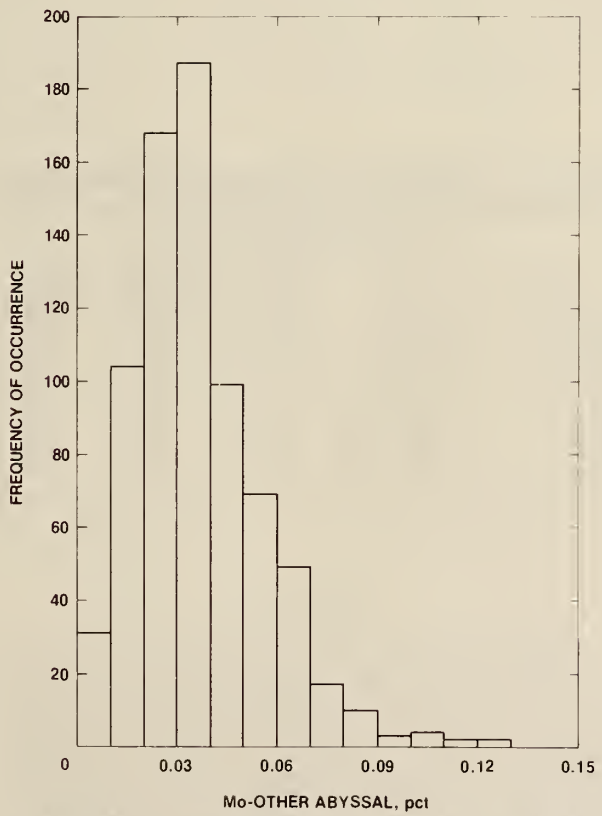

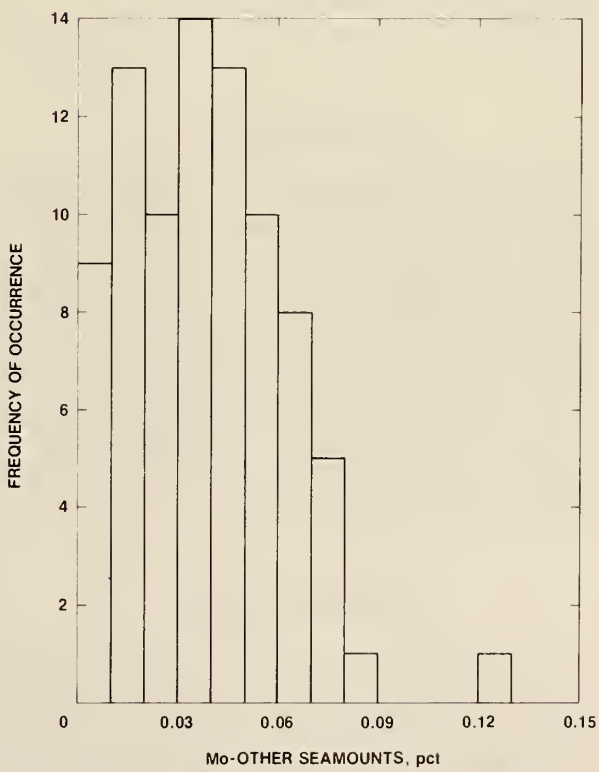

Figure 21.—Molybdenum frequency distribution by environment for Pacific manganese nodules.

Table 7. — Distribution of other major and minor elements in Pacific manganese nodules, by area, weight-percent

Area	Range	Median	Mean, $\bar{x}$	Standard deviation of mean, $\sigma\bar{x}$	Number of samples	Range	Median	Mean, $\bar{x}$	Standard deviation of mean, $\sigma\bar{x}$	Number of samples
	Aluminum					Sodium				
Clarion-Clipperton zone	0.50– 8.00	2.50– 3.00	2.90	1.04	234	0.50 –6.75	2.00–2.25	2.79	1.72	106
Mid-Pacific seamounts	<.25– 6.00	.25– .75	1.20	.94	48	.50 –5.50	1.45–1.55	2.13	1.04	28
Other abyssal plains, >3,000 m	<.50–10.0	2.50– 3.00	3.05	1.48	570	<.25 –5.75	1.75–2.00	2.07	.78	297
Other seamounts, <3,000 m	<.50– 7.00	1.00– 1.50	1.70	1.11	79	.25 –3.75	1.25–1.50	1.64	.76	37
	Calcium					Strontium				
Clarion-Clipperton zone	<0.5 –18.0	1.5 – 2.0	1.7	0.8	872	<0.005–0.16	0.04–0.05	0.045	0.03	78
Mid-Pacific seamounts	<.5 –25.0	2.0 – 2.5	4.2	3.9	91	<.005– .30	.14– .15	.13	.07	27
Other abyssal plains, >3,000 m	<.5 –13.0	1.5 – 2.0	1.8	1.2	914	<.005– .18	.07– .08	.08	.03	320
Other seamounts, <3,000 m	<.5 –25.0	2.0 – 3.0	4.5	5.3	200	<.005– .28	.13– .14	.135	.06	68
	Magnesium					Titanium				
Clarion-Clipperton zone	<0.25– 3.00	1.50– 1.75	1.65	0.43	209	0.10 –2.20	0.40–0.50	0.53	0.29	265
Mid-Pacific seamounts	.50– 3.50	.75– 1.25	1.41	.52	35	.20 –2.20	1.10–1.20	1.12	.40	102
Other abyssal plains, >3,000 m	<.25– 5.00	1.25– 1.50	1.43	.69	361	<.05 –2.50	.60– .70	.78	.75	854
Other seamounts, <3,000 m	<.25– 4.25	1.50– 1.75	1.79	.84	64	<.05 –1.60	.40– .50	.47	.35	89
	Potassium					Zirconium				
Clarion-Clipperton zone	0.20– 3.00	0.80– 0.90	1.01	0.53	123	0.010–0.09	0.03–0.04	0.035	0.01	33
Mid-Pacific seamounts	.10– .90	.30– .40	.41	.16	35	<.005– .11	.07– .075	.06	.03	18
Other abyssal plains, >3,000 m	.10– 3.00	.70– .80	.93	.60	335	<.005– .20	.05– .06	.06	.04	226
Other seamounts, <3,000 m	.10– 1.60	.30– .40	.54	.47	66	<.005– .20	.04– .05	.05	.04	27
	Silicon									
Clarion-Clipperton zone	1.0 –25.0	6.0 – 6.5	7.6	2.91	339					
Mid-Pacific seamounts	<.50–15.0	2.0 – 3.0	3.6	3.03	45					
Other abyssal plains, >3,000 m	<.50–25.0	7.0 – 8.0	8.8	5.10	460					
Other seamounts, <3,000 m	<.50–23.0	3.0 – 4.0	4.8	4.45	91					

General Observations

CC-Zone area nodules contain the highest levels of Mn, Ni, Cu, and Zn and the lowest amounts of Fe and Co. Vanadium is slightly lower in the CC-Zone area than in other areas and molybdenum appears to be uniformly concentrated in all areas. The seamounts areas contain the highest levels of Fe and Co with a slight elevation of V, and they contain the lowest levels of Ni and Cu. The different environments encountered in the seamounts areas versus the abyssal areas may show the effect of oxidation and sediment types on the formation of Pacific nodules. Cobalt occurs with both the Fe and Mn phases, with higher Co and Fe values being observed in nodules formed in the more elevated sea floor areas (MPS and other seamounts areas). The majority of data in this section came from the work of Frazer (*44, 48-50*), Sorem (*118*), and Fewkes (*42-43*).

OTHER MAJOR AND MINOR ELEMENTS

The major and minor elements discussed in this section are not of any present economic or environmental interest as applied to manganese nodule processing. The nine elements, Al, Ca, Mg, K, Si, Na, Sr, Ti, and Zr, are presented in the same manner as those of economic interest, with data divided into the four geographic areas as shown in table 7. Possible mineral forms and compounds are presented as well as positive and negative interelement correlations (table 19). Table 8 gives composite data for these elements from Pacific nodules.

Table 8. — Distribution of other major and minor elements in Pacific manganese nodules, composite, weight-percent

Element	Range	Range of medians	Weighted mean	Number of samples
Aluminum	<0.25 –10.0	0.25–3.0	2.80	931
Calcium	< .05 –25.0	1.50–3.0	2.12	2,077
Magnesium	< .25 – 5.0	.75–1.75	1.53	669
Potassium	.10 – 3.0	.30– .90	.87	559
Silicon	<.50 –25.0	2.0 –8.0	7.72	935
Sodium	<.25 – 6.75	1.25–2.25	2.20	468
Strontium	<.005– .300	.04– .15	.083	493
Titanium	<.05 – 2.50	.40–1.20	.73	1,310
Zirconium	<.005– .20	.03– .075	.058	304

Aluminum

Aluminum concentrations in Pacific nodules vary from <0.25 to 10.0 wt-pct, with a median value of 0.25 to 3.00 wt-pct and a weighted mean of 2.80 wt-pct based on 931 sample analyses. The median value for CC-Zone area nodules is 2.5 to 3.0 wt-pct with a mean of 2.9 wt-pct. Nodules from the two abyssal plains areas contain about twice the amount of aluminum found in nodules from the two seamounts areas. The two seamount areas have a median range of 0.25 to 1.5 wt-pct, with means around 1.2 wt-pct for MPS area and 1.7 wt-pct for the other seamounts area. Figure 22 provides histograms that show aluminum distribution in each of the four areas.

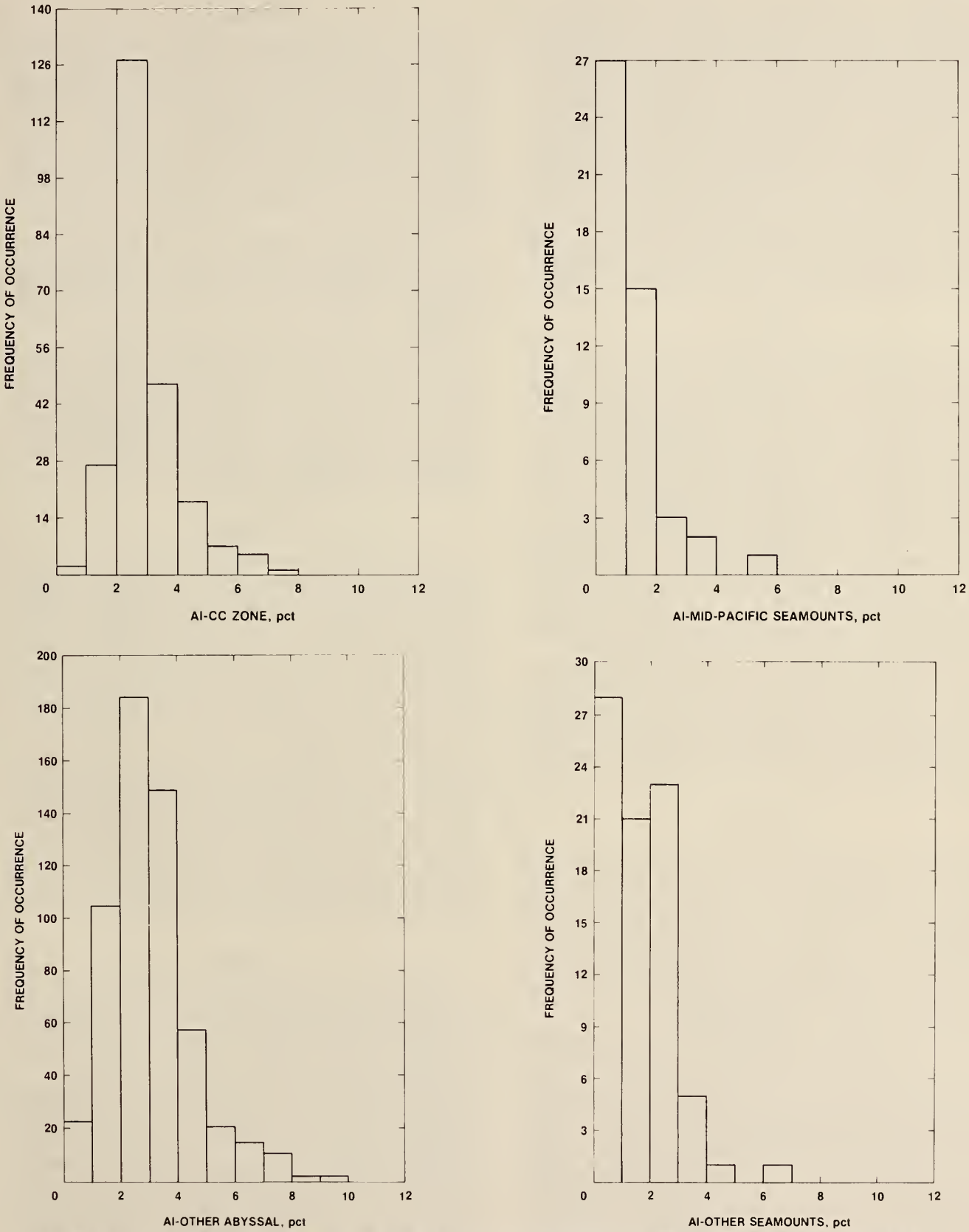

Figure 22.—Aluminum frequency distribution by environment for Pacific manganese nodules.

Aluminum occurs primarily as an aluminum silicate in clay inclusions in Pacific nodules in the form of alkali and plagioclase feldspars. This is reflected in the correlation data (table 19) by positively correlating with K, Si, and, in some cases, Na. No correlation with Ca is observed except for a slight negative correlation in the other seamounts area. The most likely form is plagioclase, other feldspars, and clays.

Aluminum in CC-Zone area nodules correlates positively with Ba, Cu, K, Na, and Si and negatively with Cd, Mg, Mn, Sr, and V. In the MPS area, aluminum is positively correlated with Cr, Mg, Ti, and Zr, and negatively correlated with Co, Cu, Mn, Mo, Na, and Ni. In the other abyssal plains area, aluminum is positively correlated with K and Si, and negatively correlated with Cd, Co, Mn, Mo, and Zn. In the other seamounts area, aluminum is positively correlated with Si, V, and Zr, and a slight negative correlation is observed with Ca, Cr, Mn, and Sr.

Calcium

Calcium concentrations in Pacific nodules vary from <0.5 to 25.0 wt-pct, with a median value of 1.5 to 3.0 wt-pct and a weighted mean of 2.1 wt-pct based on 2,077 sample analyses. The median value for CC-Zone area nodules is 1.5 to 2.0 wt-pct with a mean of 1.7 wt-pct. Nodules from the two abyssal plains areas contain about one-half the calcium levels of nodules from the two seamounts areas. These two areas have a median range of 2.0 to 3.0 wt-pct with means between 4.2 and 4.5 wt-pct. Figure 23 provides histograms that show calcium distribution in each of the four areas.

Calcium occurs in Pacific nodules in several possible forms. It can occur in some cases as calcite, apatite and/or in feldspars, and it correlates negatively in some areas with Fe and Mn. Calcium also is known to substitute in the manganese mineral structure to some degree. The multiform occurrence may be why the correlation coefficients (table 19) are not conclusive evidence for calcium association.

Calcium in CC-Zone area nodules correlates positively with Cd, Sr, and V, and negatively with Ba. In the MPS area, calcium correlates positively with Sr and negatively with Cr, Co, Fe, and Mn. In the other abyssal plains area, calcium correlates positively with Mg and has no negative correlation. In the other seamounts area, calcium correlates positively with Cd and Sr, and negatively with Al, Fe, K, Na, Si, Ti, and V.

Magnesium

Magnesium concentrations in Pacific nodules vary from <0.25 to 5.0 wt-pct, with a median value of 0.75 to 1.75 wt-pct and a weighted mean of 1.53 wt-pct based on 669 sample analyses. The median value for CC-Zone area nodules is 1.5 to 1.75 wt-pct with a mean of 1.65 wt-pct. Magnesium concentrations are uniform in all four areas with only insignificant differences in median ranges and means. Figure 24 provides histograms that show magnesium distribution in each of the four areas.

Magnesium occurs in Pacific nodules in several forms. Some of the magnesium content of nodules is a result of dissolved seawater salts. Magnesium also appears to occur in the manganese mineral structure based on its positive correlation (table 19) with Mn, Ni, and Cu in most areas. Its ionic radius is such that it could substitute in the same sites as Cu and Ni in the manganese crystal structure.

Magnesium in CC-Zone area nodules correlates positively with Cu, Mn, Ni, and Sr, and negatively with Al, Fe, K, Na, and Ti. In the MPS area, magnesium is positively correlated with Al, Co, Cr, Ni, Pb, and Sr, and negatively correlated with Zn and Zr. In the other abyssal plains area, magnesium is positively correlated with Cd and Ca (slightly) and shows no negative correlation. In the other seamounts area, magnesium is positively correlated with Ba, Cu, and Ni, and negatively correlated with Na and Sr.

Potassium

Potassium concentrations in Pacific nodules vary from 0.10 to 3.0 wt-pct, with a median value of 0.30 to 0.90 wt-pct and a weighted mean of 0.87 wt-pct based on 559 sample analyses. The median value for CC-Zone area nodules is 0.80 to 0.90 wt-pct with a mean of 1.01 wt-pct. The two abyssal plains areas contain about two times the amount of potassium found in the two seamounts areas. The median value for the seamounts areas is 0.30 to 0.40 wt-pct with means of 0.41 and 0.54 wt-pct. Figure 25 provides histograms that show potassium distribution in each of the four areas.

The occurrence of potassium in Pacific nodules is in two forms: as dissolved sea salts that crystallize when the samples dry, probably as KCl (sylvite), and as plagioclase feldspars. Evidence for the latter is seen in the high correlation coefficients (table 19) for potassium with Al, Si, and Na.

Potassium in CC-Zone area nodules is positively correlated with Al, Na, and Si, and negatively correlated with Cu, Mg, Mn, and Sr. In the MPS area, potassium is positively correlated with Na, Si, and V, and negatively correlated with Co and Pb. In the other abyssal plains area, potassium is positively correlated with Al and Si and negatively correlated with Cd, Fe, Mn, and Sr. In the other seamounts area, potassium is positively correlated with Cr and V and negatively correlated with Ca and Sr.

Silicon

Silicon concentrations in Pacific nodules vary from <0.50 to 25 wt-pct, with a median value of 2.0 to 8.0 wt-pct and a weighted mean of 7.7 wt-pct based on 935 sample analyses. The median value for CC-Zone area nodules is 6.0 to 6.5 wt-pct with a mean of 7.6 wt-pct. Silicon content in the two abyssal plains areas is a factor of two higher than for the two seamounts areas. The two seamounts areas have a median range of 2.0 to 4.0 wt-pct, with mean values of 3.6 wt-pct for the MPS area and 4.8 wt-pct for the other seamounts area. Figure 26 provides histograms that show silicon distribution in each of the four areas.

Silicon occurs in Pacific nodules in two forms. It occurs as silicates in the feldspars and clays and as silica (SiO_2). Silicon in CC-Zone area nodules correlates positively (table 19) with Al, K, and Na, and negatively with Cu, Mn, Ni, and Sr. In the MPS area, silicon correlates positively with Cr, K, Na, and Zr, and negatively with Co, Pb, and Sr. In the other abyssal plains area, silicon correlates positively with Al, Cr, and K, and negatively with Co, Mn, Mo, Ni, Sr, V, and Zr. In the other seamounts area, silicon is correlated positively with Al and negatively with Ba, Ca, Co, and Sr.

Sodium

Sodium concentrations in Pacific nodules vary from <0.25 to 6.75 wt-pct, with a median value of 1.25 to 2.25 wt-pct and a weighted mean of 2.20 wt-pct based on 468 sample analyses. The median value for CC-Zone area nodules is 2.0 to 2.25 wt-pct with a mean value of 2.8 wt-pct. Sodium content of Pacific nodules from all four areas is similar with lower sodium values occurring in the two seamounts areas based on limited data in these areas. Figure 27 provides histograms that show sodium distribution in each of the four areas.

Sodium occurs in Pacific nodules in several forms. It occurs as dissolved sea salts that crystallize upon drying. It can also occur in some feldspars in the plagioclase group. Sodium is also a constituent of the manganese mineral structure of todorokite but is generally replaced by other cations such as Cu^{2+} and Ni^{2+}, which are thought to stabilize the crystal structure of the todorokite.

Sodium in CC-Zone area nodules is correlated positively

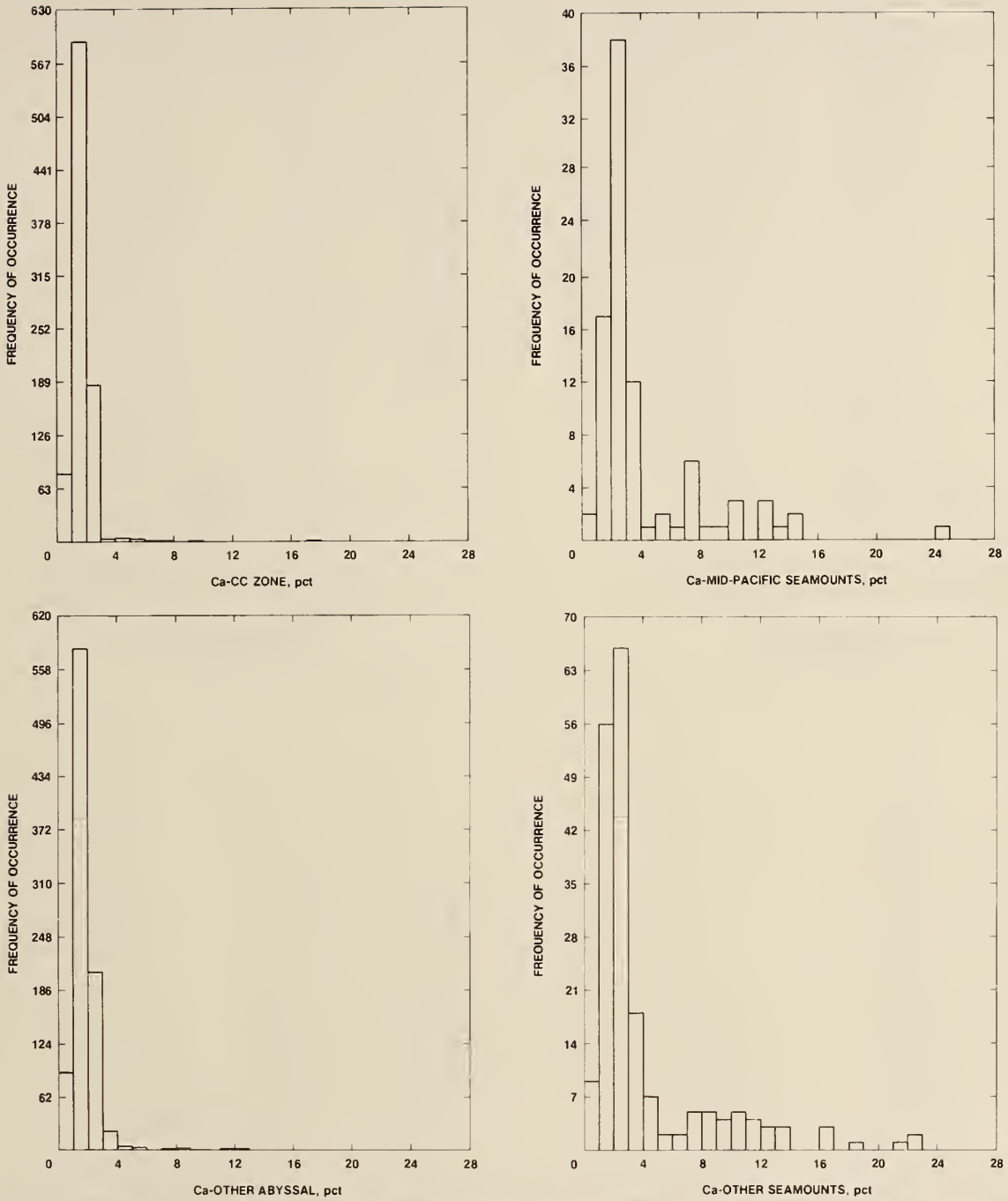

Figure 23.—Calcium frequency distribution by environment for Pacific manganese nodules.

(table 19) with Al, Ba, K, Si, and Ti, and negatively with Cd, Cu, Mg, Mn, Sr, and V. In the MPS area, sodium is correlated positively with Ba, K, Mo, Ni, Si, V, and Zn, and negatively with Al, Co, Cr, Pb, Sr, and Ti. In the other abyssal plains area, sodium is correlated positively with none of the other elements and negatively with Cd and Cr. In the other seamounts area, sodium is correlated positively with Mn and Mo and negatively with Ca, Cr, Mg, and Zn.

Strontium

Strontium concentrations in Pacific nodules vary from <0.005 to 0.300 wt-pct, with a median value of 0.04 to 0.15 wt-pct and a weighted mean value of 0.083 wt-pct based on 493 sample analyses. The median value for CC-Zone area nodules is 0.04 to 0.05 wt-pct with a mean value of 0.045 wt-pct. Strontium values are lower by a factor of two to three in the two abyssal plains areas than in the two seamounts areas. The two seamounts areas have a median range of 0.13 to 0.15 wt-pct with a mean of 0.135 wt-pct. Figure 28 provides histograms that show strontium distribution in each of the four areas.

Strontium substitutes for calcium in the manganese nodules. Strontium is positively correlated (table 19) with Ca and in some areas with Mn, Ni, and Cu. Calcium can be part of the manganese mineral structure and is replaced by

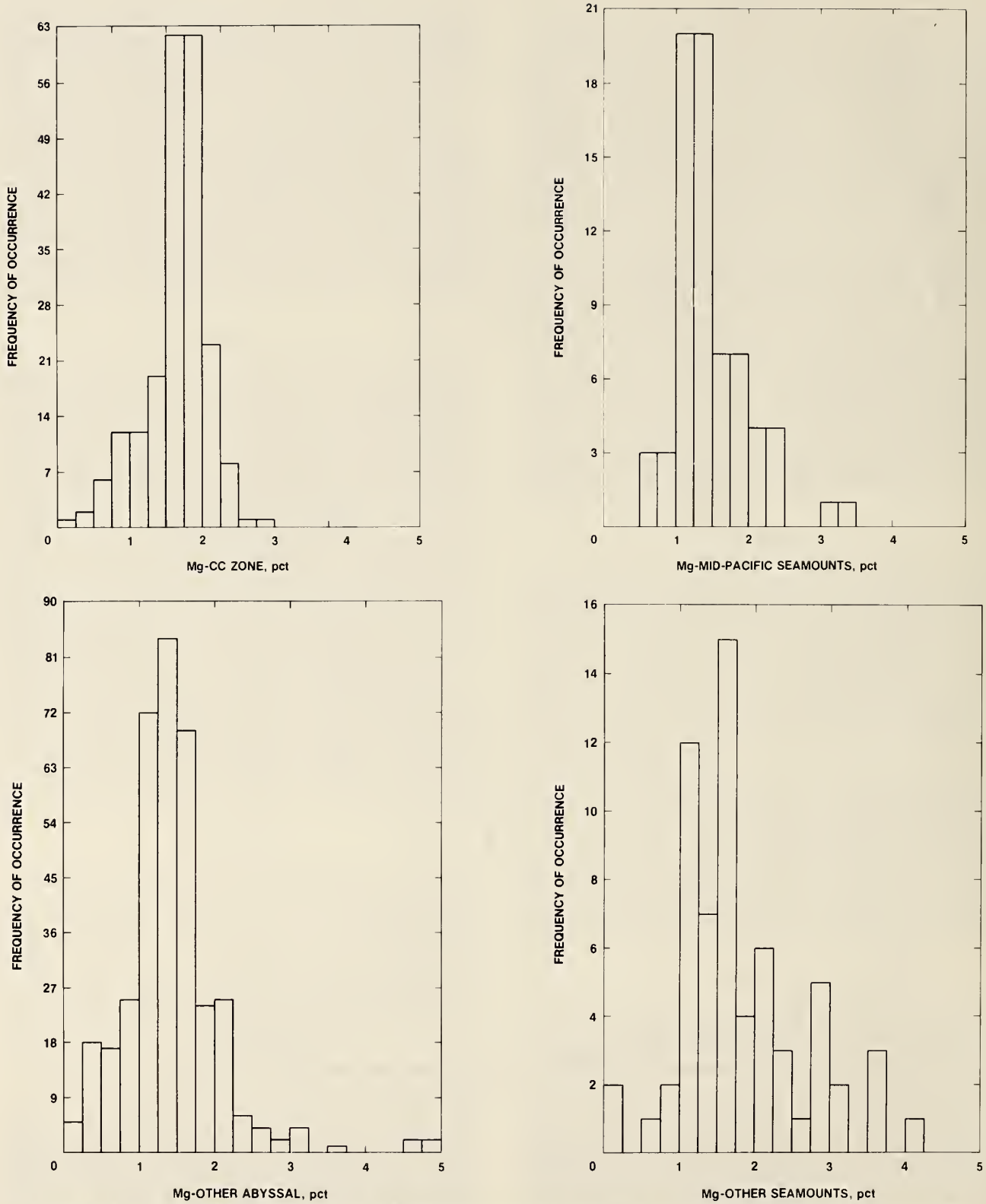

Figure 24.—Magnesium frequency distribution by environment for Pacific manganese nodules.

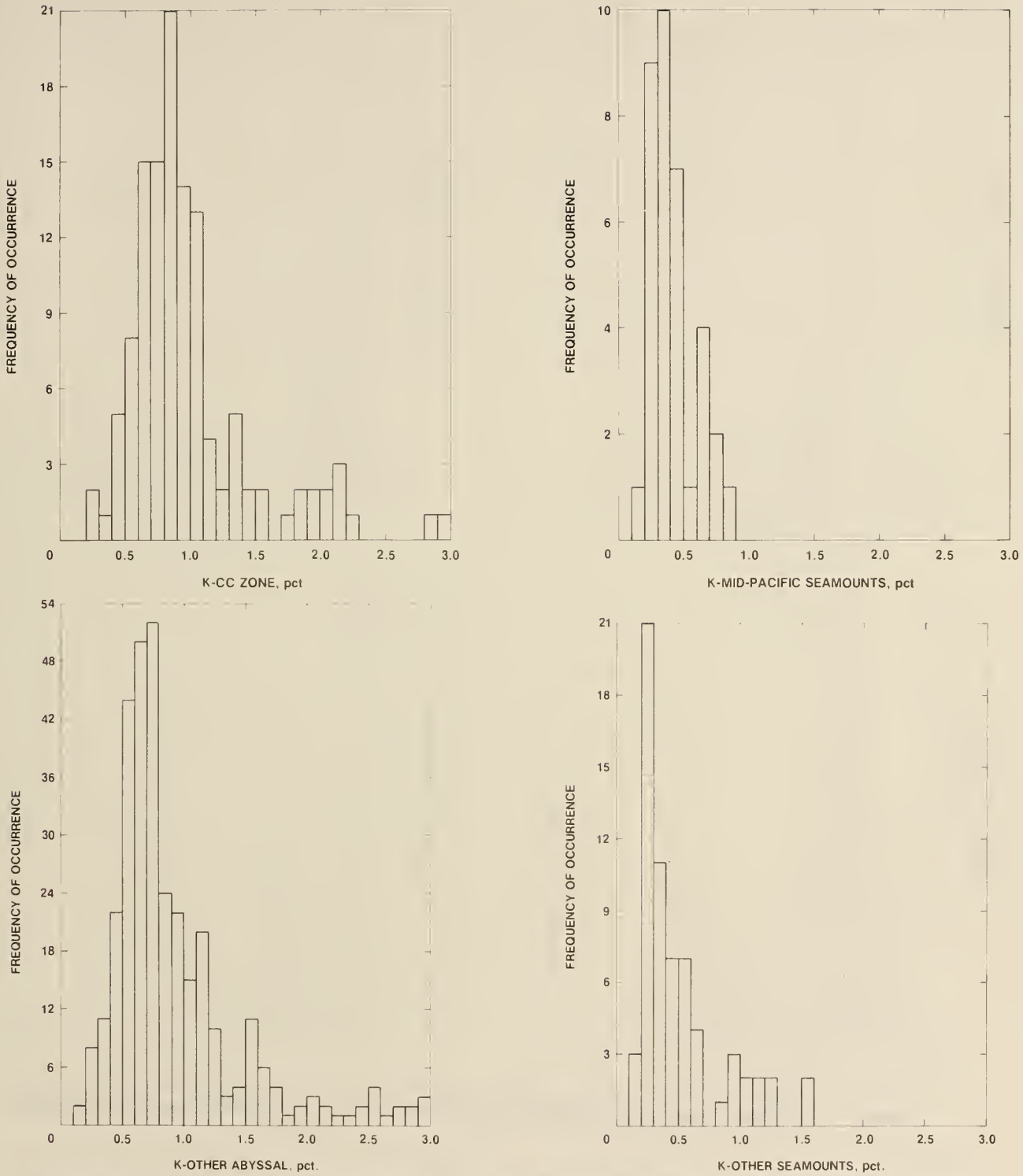

Figure 25.—Potassium frequency distribution by environment for Pacific manganese nodules.

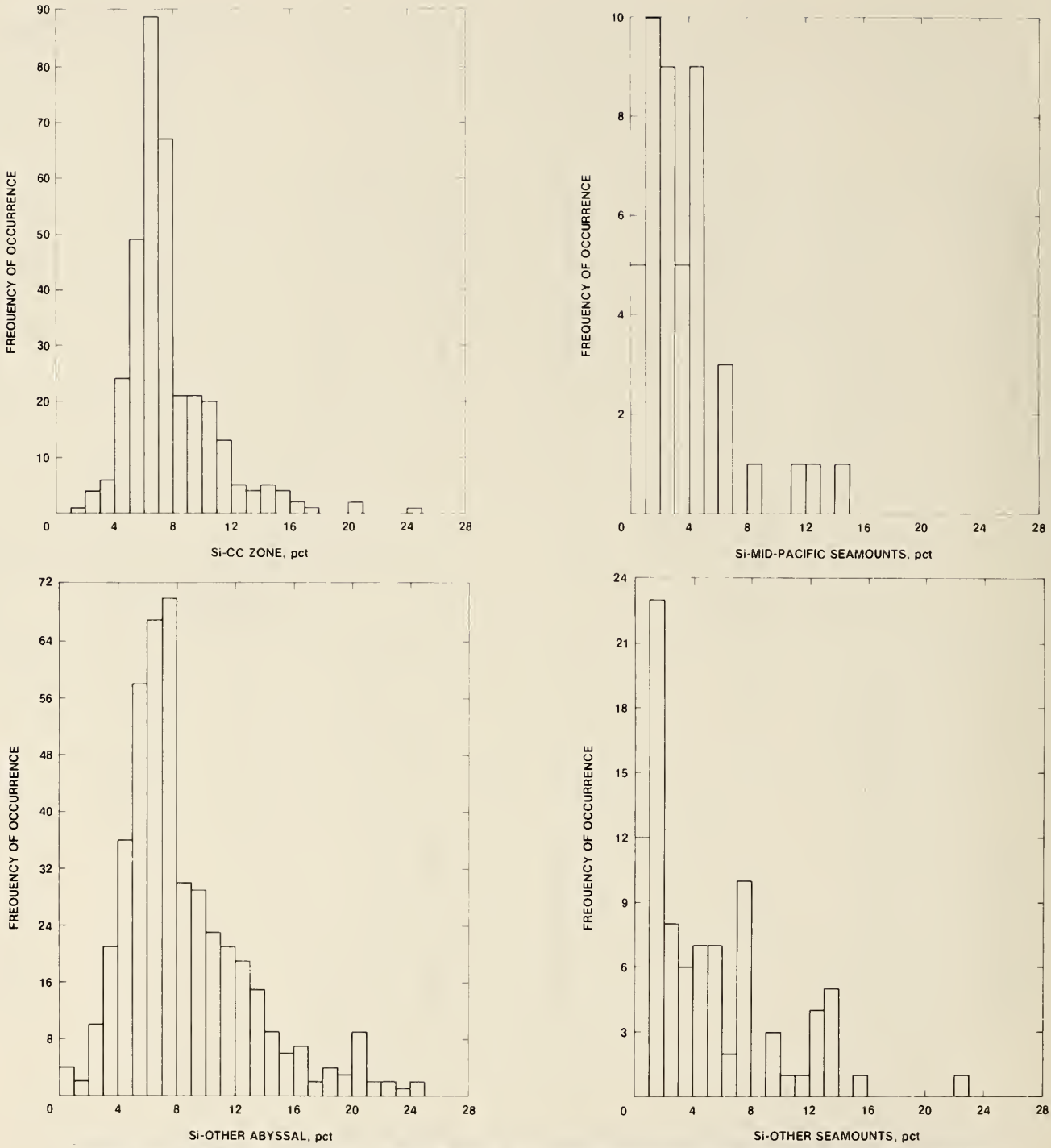

Figure 26.—Silicon frequency distribution by environment for Pacific manganese nodules.

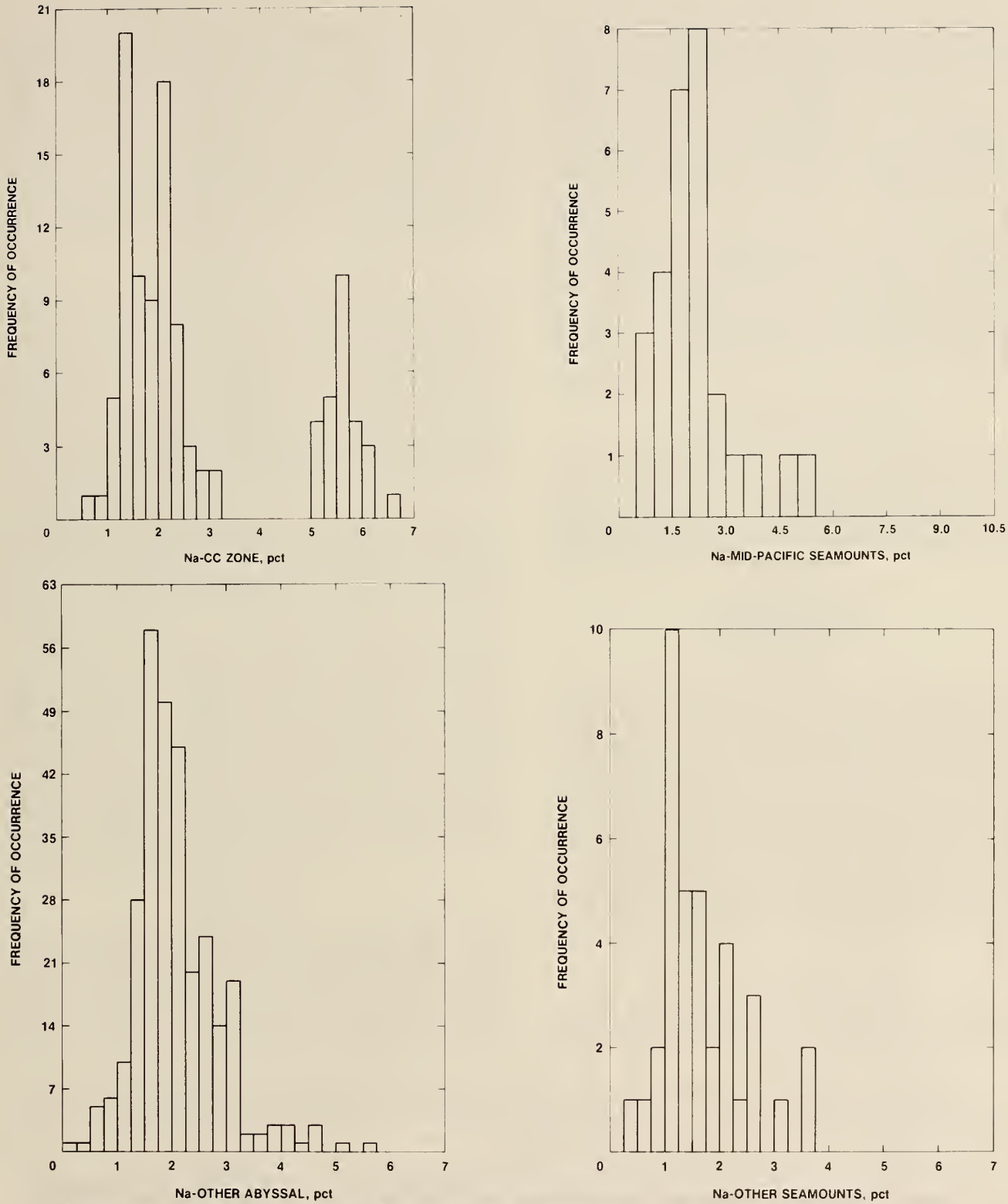

Figure 27.—Sodium frequency distribution by environment for Pacific manganese nodules.

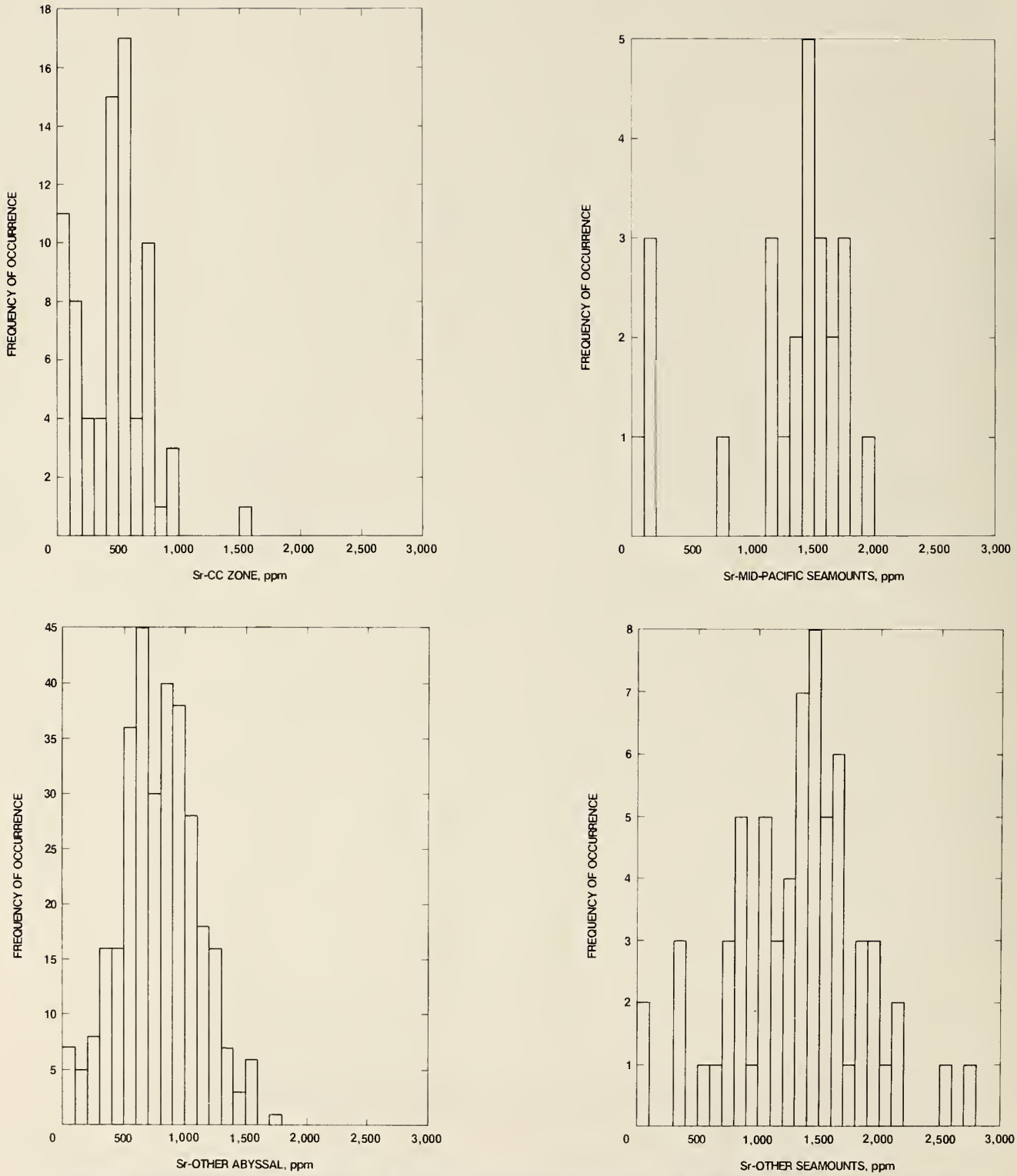

Figure 28.—Strontium frequency distribution by environment for Pacific manganese nodules.

strontium to a certain extent. Strontium does not occur in the feldspars based on the high negative correlation with Al, K, and Si.

Strontium in CC-Zone area nodules correlates positively with Ca, Cu, Mg, Mn, Ni, and Pb, and negatively with Al, K, Na, Si, and Ti. In the MPS area, strontium is positively correlated with Ca, Co, Mg, Mn, Pb, and Ti, and negatively correlated with Na, Si, and Zr. In the other abyssal plains area, strontium is correlated positively with Co, Fe, Pb, and Ti, and negatively with Cr, K, and Si. In the other seamounts area, strontium is correlated positively with Ba and Ca and negatively with Al, K, Mg, and Si.

Titanium

Titanium concentrations in Pacific nodules vary from <0.05 to 2.5 wt-pct, with a median value of 0.40 to 1.20 wt-pct and a weighted mean of 0.73 wt-pct based on 1,310 sample analyses. The median value for CC-Zone area nodules is 0.40 to 0.50 wt-pct with a mean value of 0.53 wt-pct. Titanium values are similar in the CC-Zone area, in the other abyssal plains area, and in the other seamounts area. The MPS area titanium values are about twice the concentrations seen in the other areas, with a median value of 1.10 to 1.20 wt-pct and a mean of 1.12 wt-pct. Figure 29 provides histograms that show titanium distribution in each of the four areas.

Titanium in Pacific nodules appears to be associated with the iron phases present based on the positive correlation (table 19) obtained with Fe and Co and negative correlation with Mn, Cu, and Ni. The ionic radius of Ti^{4+} is similar to that of Fe^{3+} and may allow it to substitute for Fe. Titanium has also been observed in nodules as ilmenite, rutile, and anatase.

Titanium in CC-Zone area nodules is correlated positively with Co, Fe, Na, Pb, and Zr, negatively correlated with Cu, Mg, Mn, and Ni, and slightly negative with Sr and Zn. In the MPS area, titanium correlated positively with Al, Co, Cr, Fe, Pb, Sr, and Zr, and negatively with Na, V, and Zn. In the other abyssal plains area, titanium is correlated positively with Fe and Sr and has no negative correlation. In the other seamounts area, titanium is correlated positively with Co, Fe, Pb, and V, and negatively with Ba, Ca, and Cr. The number of sample analyses in the two seamounts areas is limited; therefore, correlation coefficients may not reflect the actual correlation of titanium to other elements.

Zirconium

Zirconium concentrations in Pacific nodules vary from <0.005 to 0.20 wt-pct, with a median value of 0.03 to 0.075 wt-pct and a weighted mean of 0.058 wt-pct based on 304 sample analyses. The median value for CC-Zone area nodules is 0.03 to 0.04 wt-pct with a mean value of 0.035 wt-pct. The CC-Zone nodules have the lowest zirconium levels of the four areas; about one-half the levels of the other three areas. The median range for the other three areas is 0.40 to 0.075 wt-pct with mean values from 0.054 to 0.062 wt-pct. Figure 30 provides histograms that show zirconium distribution in each of the four areas.

Zirconium appears to occur in Pacific nodules in association with the iron phases based on its strong negative correlations (table 19) with Mn, Cu, and Ni and positive correlations with Co and Fe. The ionic radius of Zr^{4+} is similar to that of Fe^{3+} and may allow some substitution in the iron phases.

Zirconium in CC-Zone area nodules is correlated positively with Fe and Ti and negatively with Cr, Cu, and Zn. In the MPS area, zirconium is correlated positively with Al, Co, Fe, Si, and Ti, slightly positive with Mn, and negatively with Ba, Cr, Cu, Mg, Pb, Sr, and Zn. In the other abyssal plains area, zirconium is correlated positively with Fe and negatively with Cr and Si. In the other seamounts area, zirconium is correlated positively with Al and Fe and exhibits no negative correlations.

General Observations

The two abyssal plains areas have the higher levels of Al, K, Si, and Na by about a factor of two over the two seamounts areas. In contrast, the two seamounts areas have higher Ca and Sr by the same factor. Magnesium, titanium, and zirconium values are relatively uniform with the CC-Zone area having the lowest zirconium values and the MPS area having the highest titanium values.

ELEMENTS OF ENVIRONMENTAL INTEREST

Any of the following eight elements—As, Ba, Cd, Cr, Pb, Hg, Se, Ag—when leached from wastes under conditions specified by the U.S. Environmental Protection Agency, will result in the waste being classified as a hazardous material, if their concentrations are greater than 100 times the National Drinking Water Standard. Data for Ba, Cd, Cr, and Pb are presented in table 9, by area, as in the previous sections. Data for the remaining elements (As, Hg, Se, and Ag), along with the other four listed in table 9, are presented in table 10 as a composite for Pacific Ocean nodules. Correlation coefficients are given in table 19. These data are taken from the Sediment Data Bank (*44, 48-50*) as well as from Toth (*123*), Harris (*67*), and from analytical studies sponsored by the Bureau of Mines.

Arsenic

Arsenic concentrations in Pacific nodules vary from 20 to 540 ppm, with a median value of 164 ppm and a mean value

Table 9. — Distribution of elements of environmental interest in Pacific manganes nodules, by area

Area	Range	Median	Mean, $\bar{x}$	Standard deviation of mean, $\sigma\bar{x}$	Number of samples	Range	Median	Mean, $\bar{x}$	Standard deviation of mean, $\sigma\bar{x}$	Number of samples
	Barium, wt-pct					Chromium, ppm				
Clarion-Clipperton zone	<0.01 – 0.76	0.20– 0.22	0.28	ND	213	1– 150	15– 20	27	ND	107
Mid-Pacific seamounts	.04 – .68	.18– .20	.30	0.27	39	1– 40	10– 20	58	147	22
Other abyssal plains, >3,000 m	<0.005– 0.800	.14– .16	.20	.18	499	1– 150	15– 20	25	38	227
Other seamounts, <3,000 m	0.06 – 0.80	.32– .34	.37	.33	59	1– 130	30– 40	60	129	38
	Cadmium, ppm					Lead, ppm				
Clarion-Clipperton zone	1 –35	10 –15	12.3	ND	127	50–1,800	400– 500	450	190	921
Mid-Pacific seamounts	1 –25	5 –10	8.3	7.6	15	100–4,700	1,700–1,800	1,860	950	105
Other abyssal plains, >3,000 m	1 –35	5 –10	10.7	7.1	133	50–3,000	700– 800	820	710	1,185
Other seamounts, <3,000 m	1 –35	5 –10	10.2	8.2	23	50–3,000	1,000–1,100	1,030	770	206

ND Not determined.

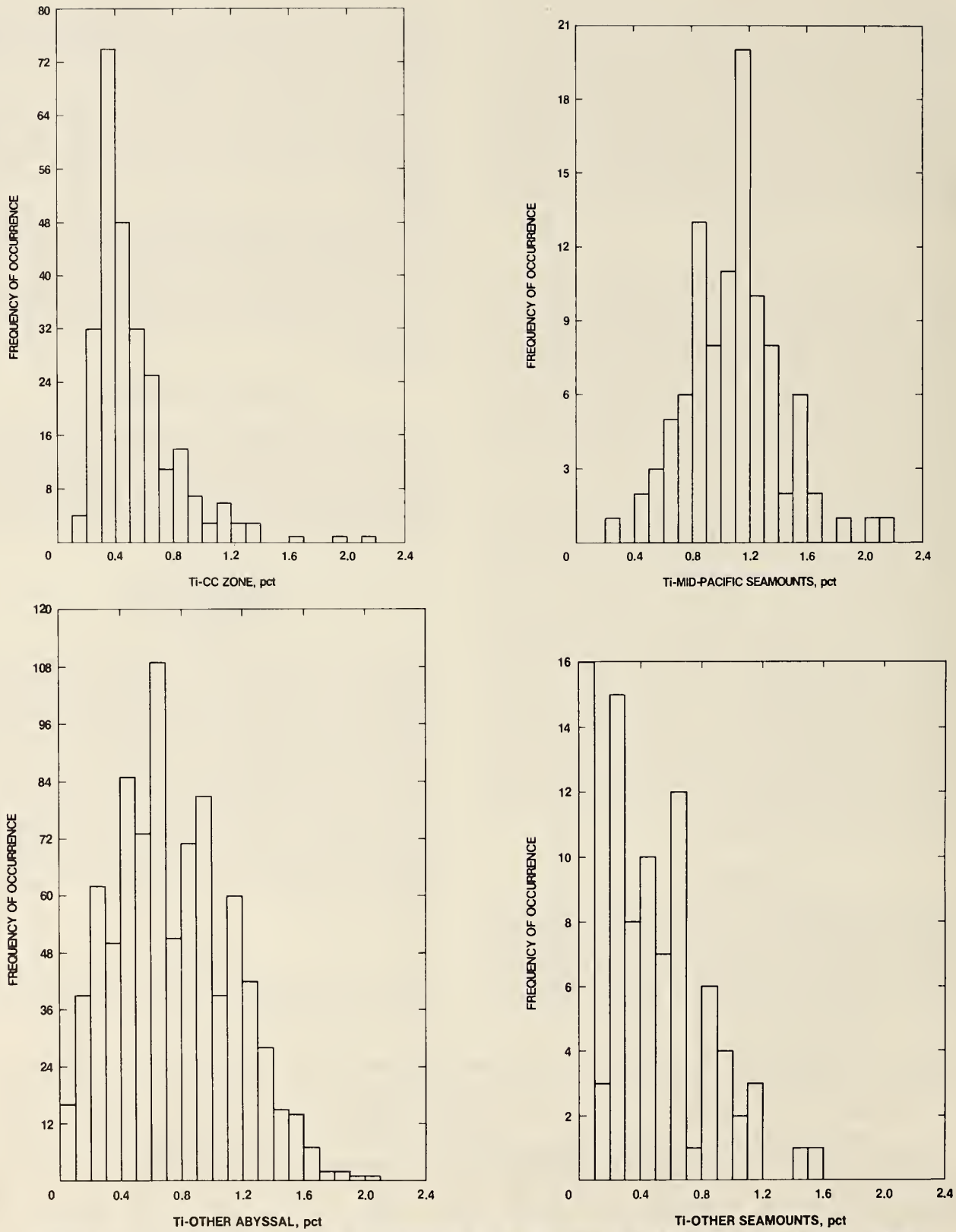

Figure 29.—Titanium frequency distribution by environment for Pacific manganese nodules.

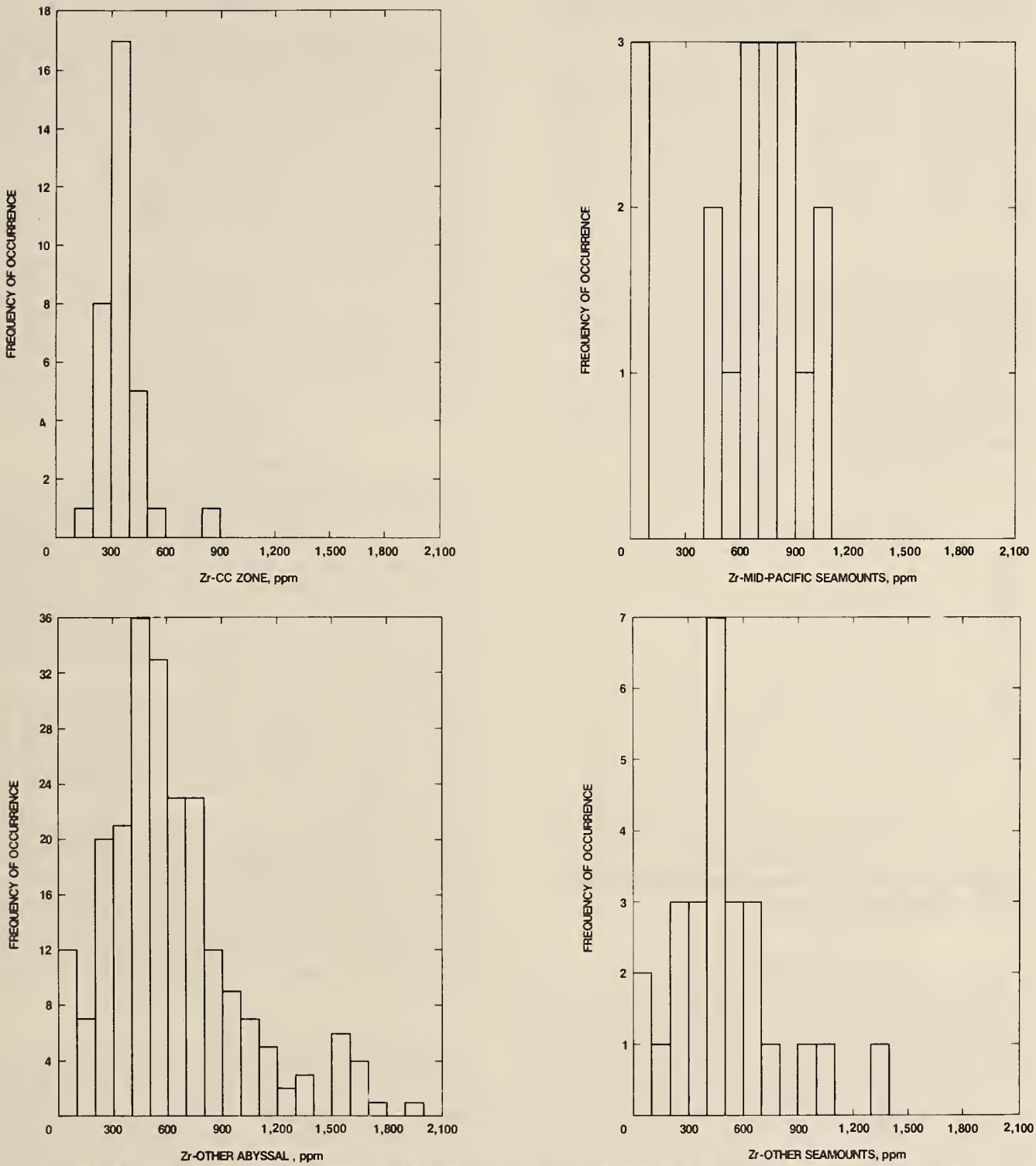

Figure 30.—Zirconium frequency distribution by environment for Pacific manganese nodules.

Table 10. — Distribution of elements of environmental interest in Pacific manganese nodules, composite

Element	Range	Range of medians	Weighted mean	Number of samples
Arsenic . . . . ppm . .	20–540	164	159	122
Barium . . wt-pct . .	<0.005–0.800	0.140–0.340	0.24	810
Cadmium . . ppm . .	1.0–35	5–15	11	298
Chromium . ppm . .	1.0–150	10–40	31	394
Lead . . . . . ppm . .	50–4,700	400–1,800	742	2,417
Mercury . . . ppm . .	0.002–0.78	0.085	0.15	68
Selenium . . ppm . .	30–77	53	52	56
Silver . . . . . ppm . .	0.001–0.68	0.039	0.10	56

of 159 ppm based on 118 sample analyses. Arsenic concentrations are generally lower in the CC-Zone area and higher in the seamounts area. The highest arsenic values appear in the other abyssal areas. Figure 31 is a histogram for Pacific nodules showing arsenic distribution.

Arsenic occurs in Pacific nodules in association with iron and may be part of the iron phase structure. Arsenic is probably oxidized to the As^{5+} state in nodules. Arsenic is correlated positively with Fe, Co, and Pb, with the strongest correlation occurring in CC-Zone area nodules.

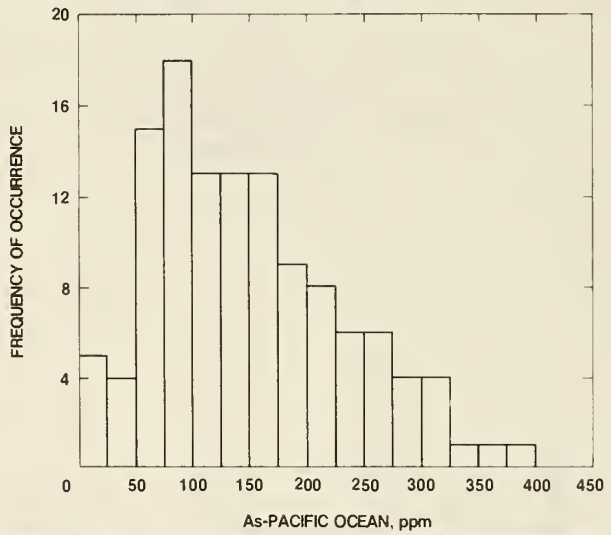

Figure 31.—Arsenic frequency distribution for Pacific manganese nodules.

Barium

Barium concentrations in Pacific nodules vary from <0.005 to 0.800 wt-pct, with a median value of 0.14 to 0.34 wt-pct and a weighted mean of 0.24 wt-pct based on 810 sample analyses. The median value for CC-Zone area nodules is 0.20 to 0.22 wt-pct with a mean value of 0.28 wt-pct. The two abyssal plains areas have lower barium values than the two seamounts areas. Figure 32 provides histograms that shows barium distribution in each of the four areas.

Barium in Pacific nodules occurs as barite and also substitutes into the structure of certain manganese minerals. Barium in CC-Zone area nodules is correlated positively (table 19) with Al and Na and negatively with Ca. Some indications are that barium is positively correlated in CC-Zone area nodules with Mn, Ni, Cu, and Zn based on a selected analysis of 22 samples in this area. In the MPS area, barium is correlated positively with Co, Na, Pb, and Zn, and negatively with Fe and Zr. In the other abyssal plains area, barium is positively correlated only with Cd. In the other seamounts area, barium is positively correlated with Cd, Mg, Mn, and Sr, and negatively with Fe, Si, Ti, and V.

Cadmium

Cadmium concentrations in Pacific nodules vary from 1 to 35 ppm, with a range of median values for the different areas of 5 to 15 ppm and a mean value of 11 ppm based on 298 sample analyses. The median value for CC-Zone area nodules is 10 to 15 ppm with a mean of 12 ppm. Cadmium is higher for CC-Zone area nodules than for other areas but only marginally. Figure 33 provides histograms that show cadmium distribution in each of the four areas.

Cadmium levels in nodules are enriched over the sediment levels in deep sea clays. Cadmium appears to be part of the manganese mineral structure and may substitute in or fill the tunnels of these structures.

Cadmium in CC-Zone area nodules is correlated positively (table 19) with Ca, Cu, Mn, Mo, and Ni, and negatively with Al, Co, Fe, Na, and Pb. In the MPS area, cadmium does not correlate with any element based on a limited number of sample analyses. In the other abyssal plains area, cadmium is correlated positively with Ba, Cu, Mg, Mn, Mo, and Ni, and negatively with Al, Co, Fe, K, Na, and Pb. In the other seamounts area, cadmium is correlated positively with Ba, Ca, Cu, Ni, and Zn, and negatively with Co, Cr, Mn, and Pb.

Chromium

Chromium concentrations in Pacific nodules vary from 1 to 150 ppm, with a median value of 10 to 40 ppm and a weighted mean of 31 ppm based on 394 sample analyses. The median value for CC-Zone area nodules is 15 to 20 ppm with a mean value of 27 ppm. The CC-Zone and other abyssal plains areas contain the lower chromium values by about a factor of two compared with the two seamounts areas. The medians, however, show that all areas are similar with some increased chromium levels in the other seamounts area. Figure 34 provides histograms that show chromium distribution in each of the four areas.

Chromium occurs in Pacific nodules associated with the gangue minerals, possibly the silicates, because of its tendency to be positively correlated (table 19) with Si. Chromium content in nodules is considerably lower than in deep-sea clays or oceanic basalts and is generally associated in nodules with the entrapped sediment or other extraneous phases.

Chromium in CC-Zone area nodules is correlated positively with no elements and negatively with Zr. In the MPS area, chromium is correlated positively with Al, Cu, Mg, Ni, Si, and Ti, and negatively with Ca, Na, and Zr based on a very limited number of sample analyses. In the other abyssal plains area, chromium is correlated positively with Si and negatively with Na, Sr, and Zr. In the other seamounts area, chromium is correlated positively with Fe and K and negatively with Al, Cd, Na, and Ti based on a limited number of sample analyses.

Lead

Lead concentrations in Pacific nodules vary from 50 to 4,700 ppm, with a range of median values for the different areas in the Pacific of 400 to 1,800 ppm and a weighted mean of 742 ppm based on 2,417 sample analyses. The median value for CC-Zone area nodules is 400 to 500 ppm with a mean of 450 ppm. This area contains the lowest lead levels corresponding to the low iron levels in this area. The other areas have two to three times this level of lead as median and mean values. The highest values occur in the MPS area with a median value of 1,700 to 1,800 ppm and mean of 1,860 ppm. Figure 35 provides histograms that show lead distribution in each of the four areas.

Lead is closely associated with iron in Pacific nodules, based on high correlations (table 19) for these two elements, and probably occurs in the amorphous iron phase. Lead in CC-Zone area nodules is correlated positively with Co, Fe,

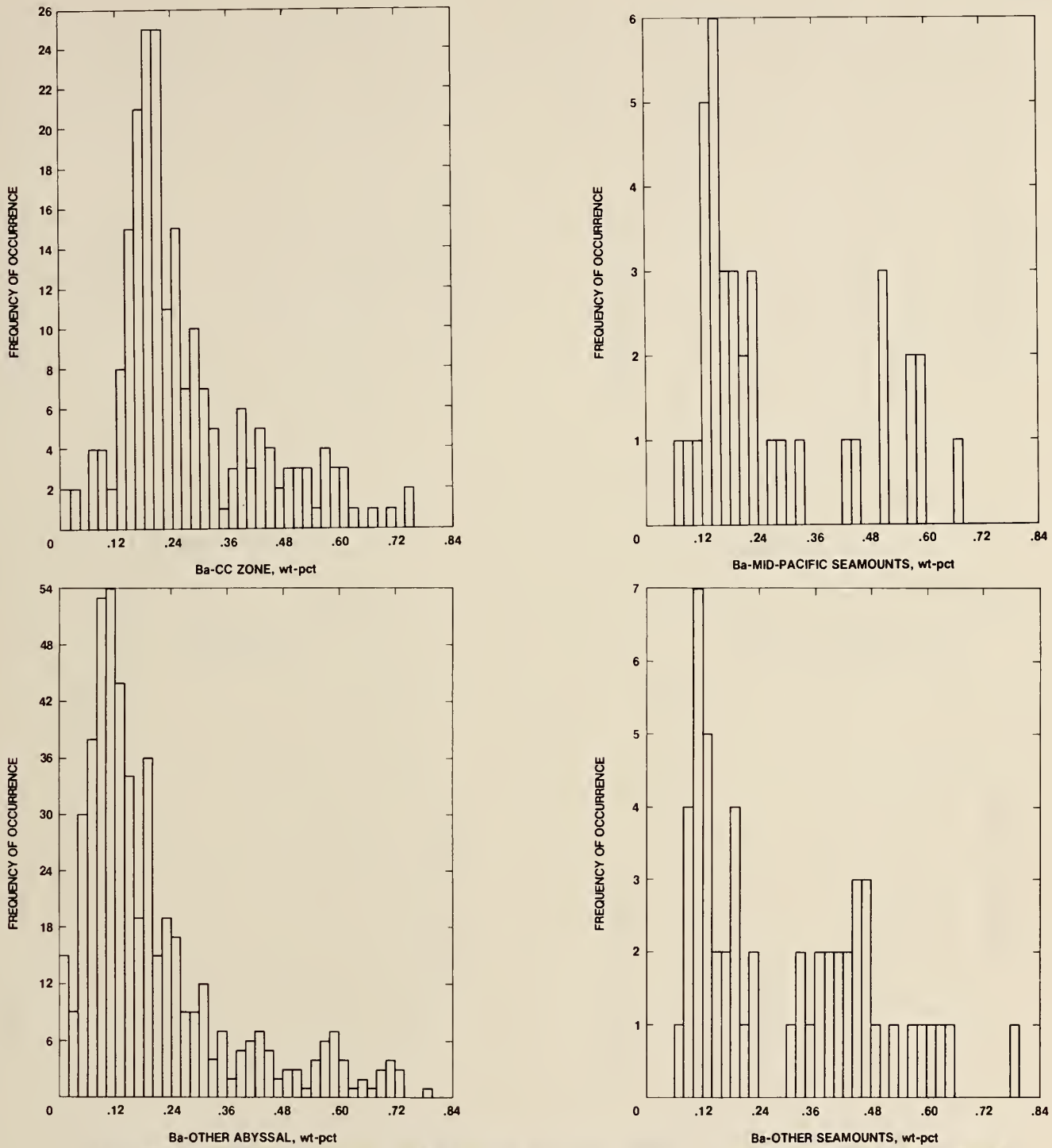

Figure 32.—Barium frequency distribution by environment for Pacific manganese nodules.

Figure 33.—Cadmium frequency distribution by environment for Pacific manganese nodules.

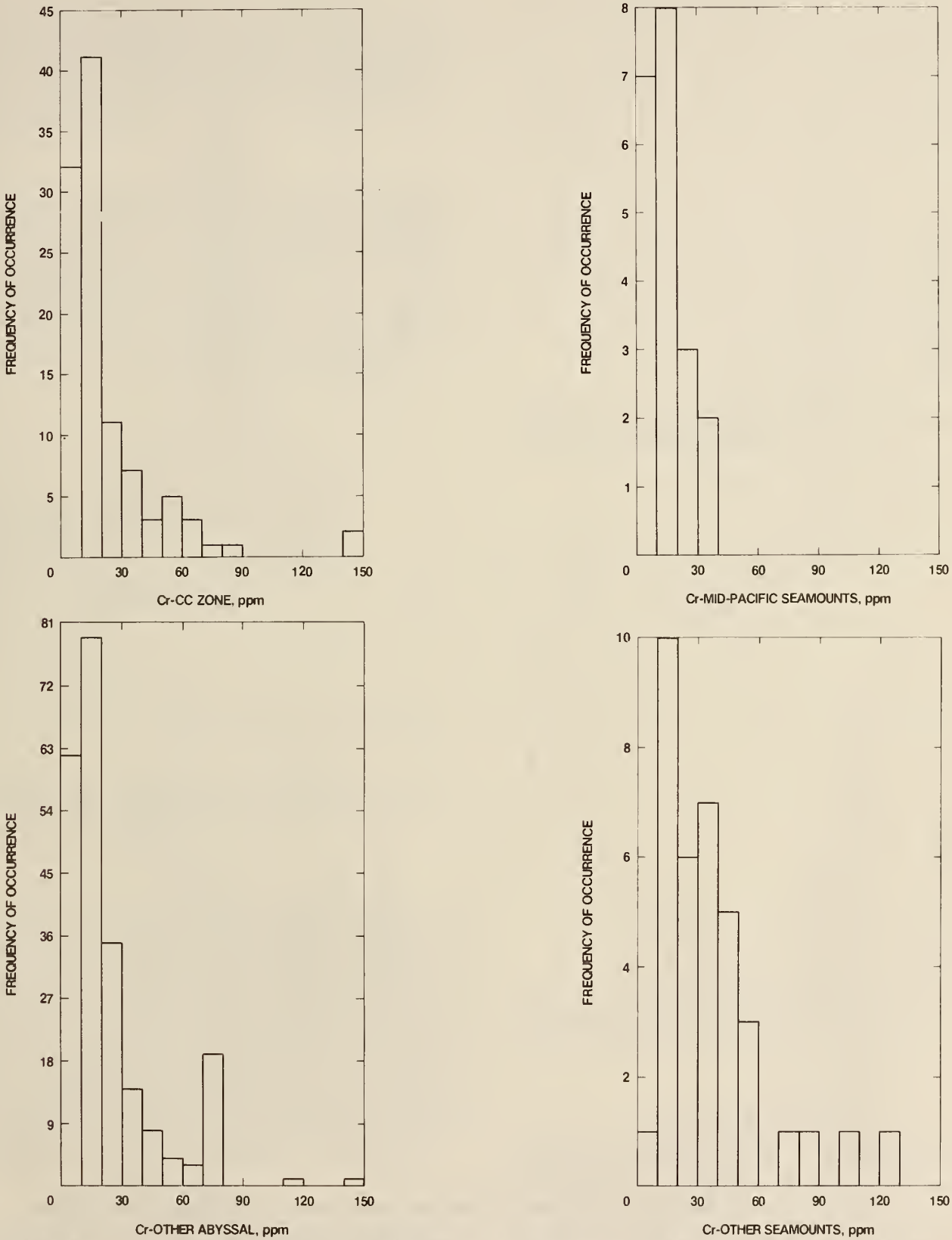

Figure 34.—Chromium frequency distribution by environment for Pacific manganese nodules.

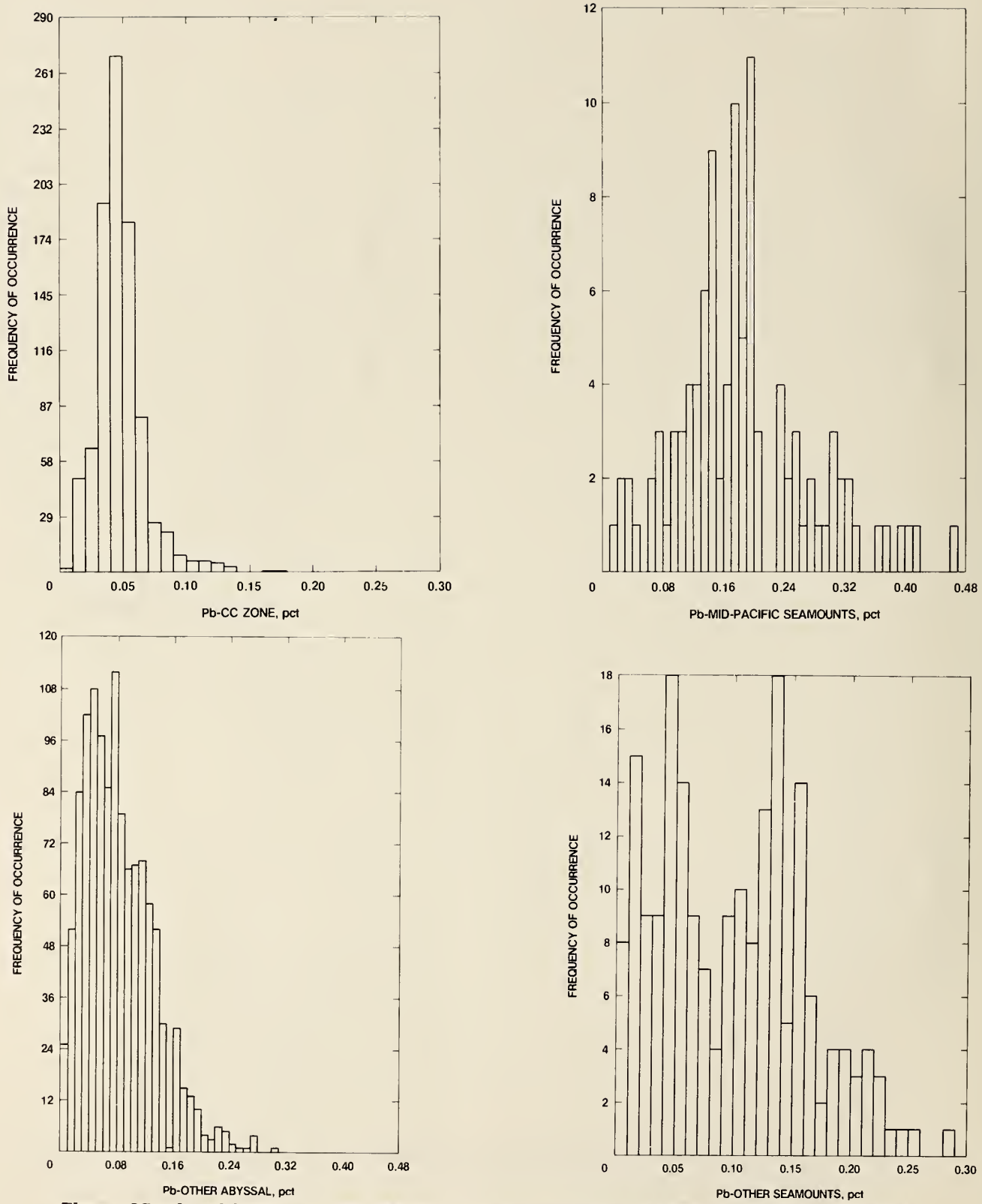

Figure 35.—Lead frequency distribution by environment for Pacific manganese nodules.

Sr, and Ti, and negatively with Cd, Cu, and Zn. In the MPS area, lead is correlated positively with Ba, Co, Mg, Mn, Sr, and Ti, and negatively with K, Na, Si, V, and Zr. In the other abyssal plains area, lead is correlated positively with Fe and Sr and negatively with Cd and Cu. In the other seamounts area, lead is correlated positively with Co, Mo, and Ti, and negatively with Cd.

Mercury

Mercury concentrations in Pacific nodules vary from 0.002 to 0.78 ppm, with a median value of 0.085 ppm and a mean of 0.15 ppm based on a limited 68 sample analyses. These very low levels are of little consequence with respect to environmental issues. Figure 36 is a histogram for Pacific nodules showing mercury distribution.

Mercury occurs at levels equal to or less than the surrounding sediments. It most likely is associated in the iron structure as mercury is significantly correlated only with iron based on the very limited amount of data available.

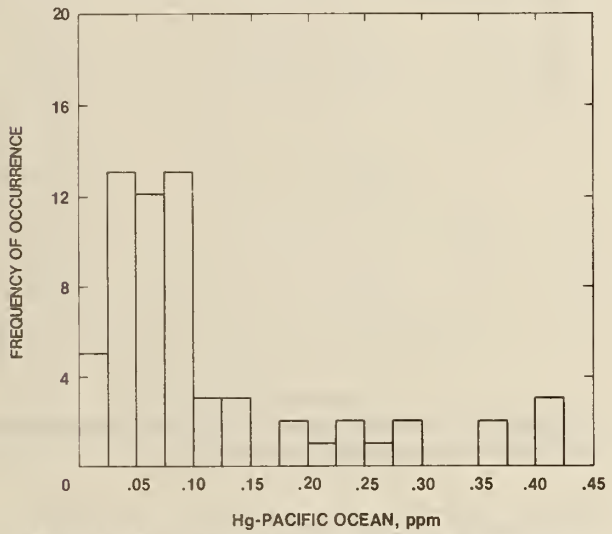

Figure 36.—Mercury frequency distribution for Pacific manganese nodules.

Selenium

Selenium concentrations in Pacific nodules vary from 30 to 77 ppm with a median value of 53 ppm and a mean of 52 ppm based on only 56 sample analyses obtained from Bureau of Mines analyses. Indications are that these values may be as much as a factor of 10 high based on limited information from other nodules that are under study. Therefore, these values may not be representative of the true levels in nodules and should be used with caution until more data become available. CC-Zone area nodules appear to have somewhat lower concentrations of selenium than other nodules. Further study is required to determine if these values are representative of all Pacific nodules. Figure 37 is a histogram for Pacific nodules showing selenium distribution. Selenium does not appear to be correlated with any major or minor element.

Silver

Silver concentrations in Pacific nodules vary from 0.001 to 0.68 ppm. with a median value of 0.039 ppm and a mean value of 0.10 ppm based on 56 sample analyses. Silver concentrations are equal to or less than silver concentrations of deep-sea clays. No interelement correlations are found for silver. Figure 38 is a histogram for Pacific nodules showing silver distribution.

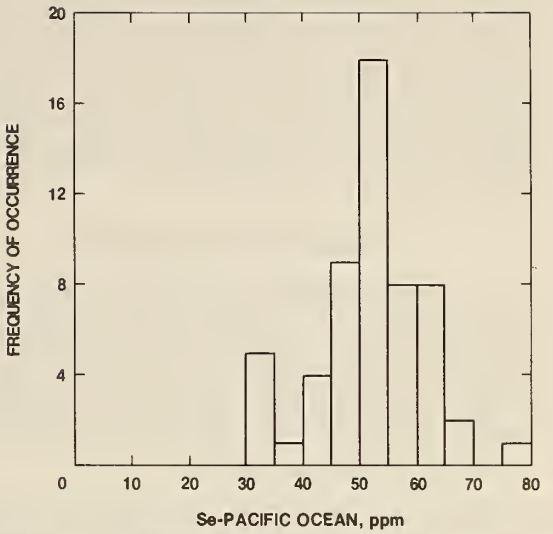

Figure 37.—Selenium frequency distribution for Pacific manganese nodules.

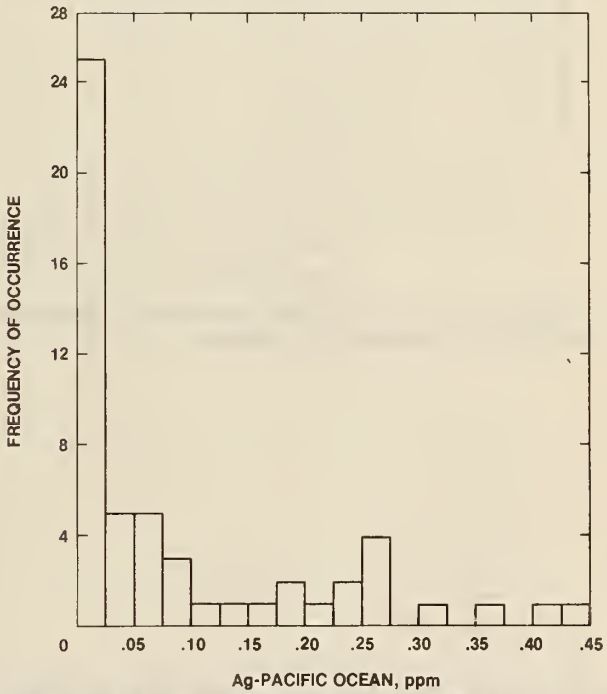

Figure 38.—Silver frequency distribution for Pacific manganese nodules.

General Observations

Nodules are enriched in As, Cd, Pb, and Se relative to their concentrations in deep-sea clays. The elements Ba, Cr, Hg, and Ag occur in Pacific nodules at levels similar to or less than corresponding levels of these elements reported for deep-sea clays.

In Pacific nodules, Ba and Cd are correlated with the Mn phases, and As, Pb, and Hg are correlated with the Fe phases. Barium may also occur as barite in the gangue minerals. Chromium appears to be correlated with silicon and may occur with entrapped sediments. No correlations for selenium and silver were noted.

The CC-Zone area and other abyssal plains areas contain

the lowest Cr, Pb, and Se levels and the highest levels of Ba and Cd. The highest lead values occur in the MPS area.

Data for As, Hg, Se, and Ag are very limited; most of these data were generated for this report from selected nodule samples. Data for Ba, Cd, Cr, and Pb are more prevalent, and interpretations of these data are made with greater confidence. Based on the available information, the concentrations of many of these elements are too low to warrant environmental interest.

RARE-EARTH ELEMENTS

The elements examined in this section are hafnium and all of the lanthanide series elements with the exception of promethium. For Pr, Dy, and Er, only limited sample analyses were available, and no histograms are provided. Figures 39 through 50 are histograms for those elements with greater than 40 sample analyses. Data for these elements are presented for the composite of the Pacific nodules as they are too limited to present by area. Table 11 lists the elements by atomic number with concentration range, median, mean, and total number of samples. A majority of the data available for these elements is from analysis of nodules taken from the CC-Zone area.

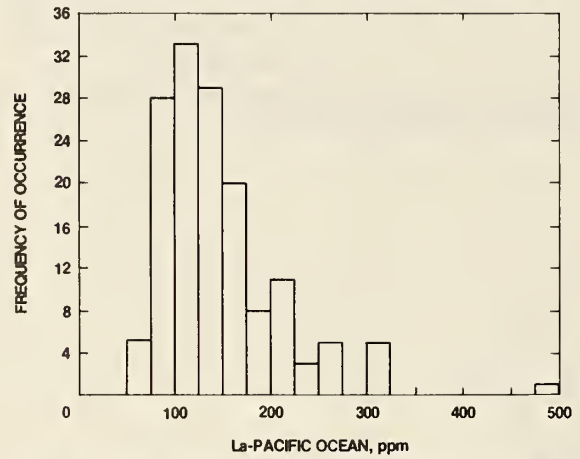

Figure 39.—Lanthanum frequency distribution for Pacific manganese nodules.

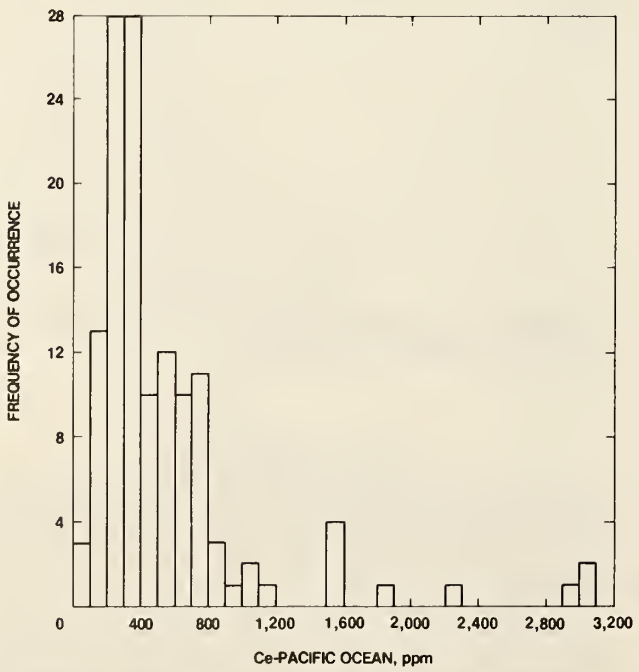

Figure 40.—Cerium frequency distribution for Pacific manganese nodules.

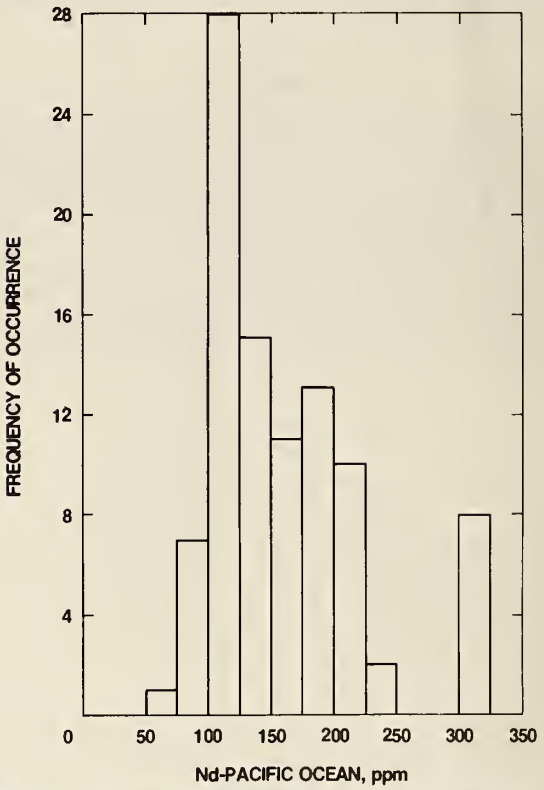

Figure 41.—Neodymium frequency distribution for Pacific manganese nodules.

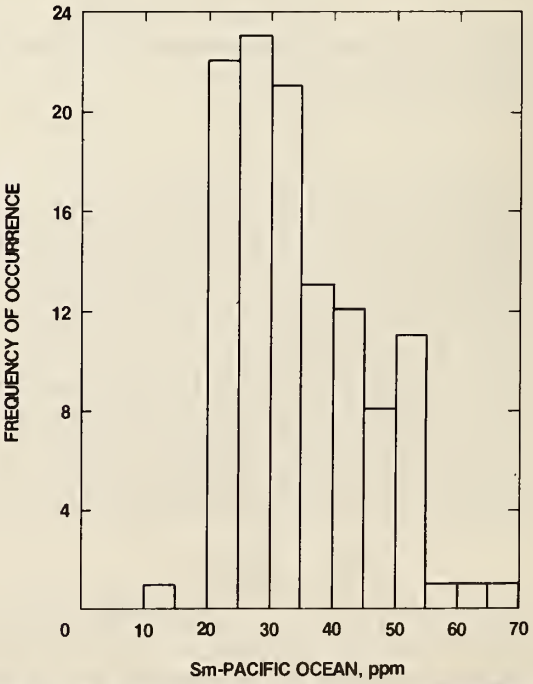

Figure 42.—Samarium frequency distribution for Pacific manganese nodules.

Table 11. — Rare-earth elements in Pacific manganese nodules, parts per million

Element	Range	Median	Mean	Number of samples
Lanthanum	66– 979	130	157	151
Cerium	74–3,000	345	530	131
Praseodymium	26– 46	34	36	8
Neodymium	60– 700	141	158	96
Samarium	14– 141	32	35	115
Europium	1– 27	7	9	115
Gadolinium	14– 53	33	32	57
Terbium	1– 11	5	5.4	104
Dysprosium	22– 42	32	31	18
Holmium	1– 8	4	4	66
Erbium	11– 27	19	18	18
Thulium	1– 9	2	2.3	41
Ytterbium	8– 100	17	20	171
Lutetium	1– 6	2	1.8	76
Hafnium	3– 14	5	6	96

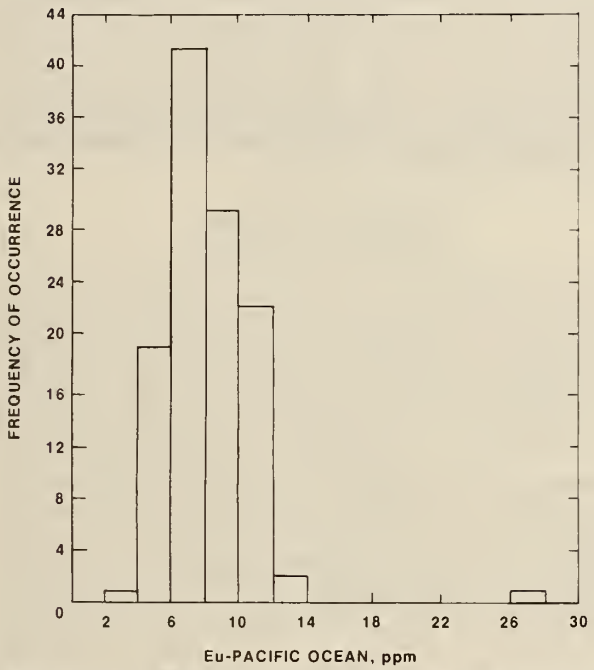

Figure 43.—Europium frequency distribution for Pacific manganese nodules.

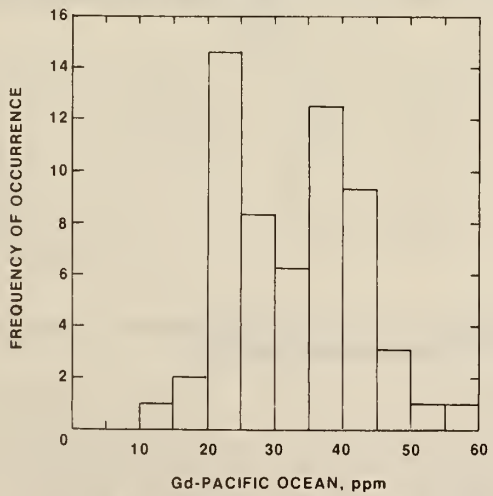

Figure 44.—Gadolinium frequency distribution for Pacific manganese nodules.

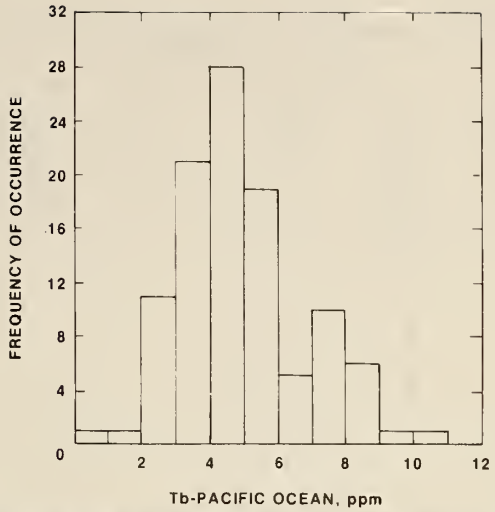

Figure 45.—Terbium frequency distribution for Pacific manganese nodules.

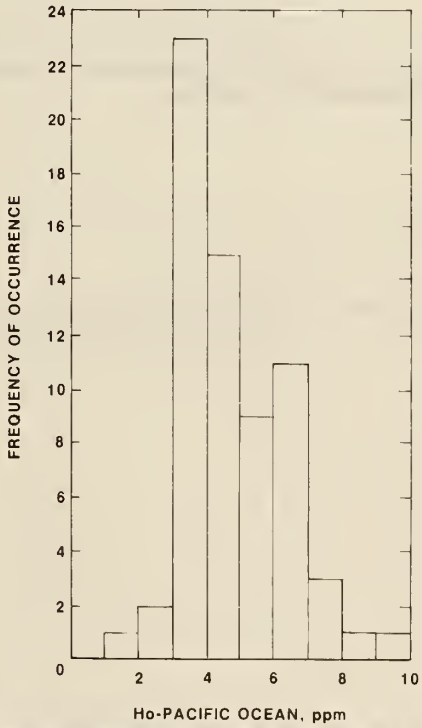

Figure 46.—Holmium frequency distribution for Pacific manganese nodules.

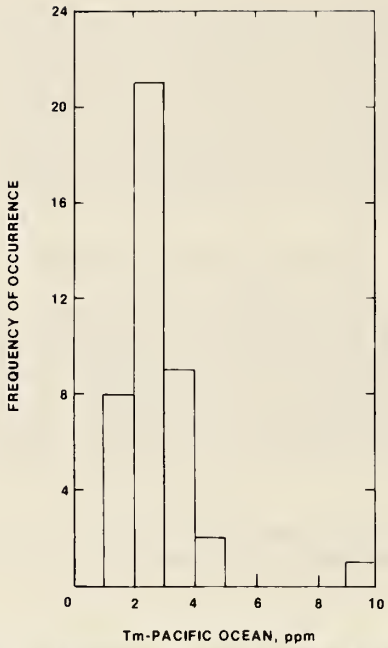

Figure 47.—Thulium frequency distribution for Pacific manganese nodules.

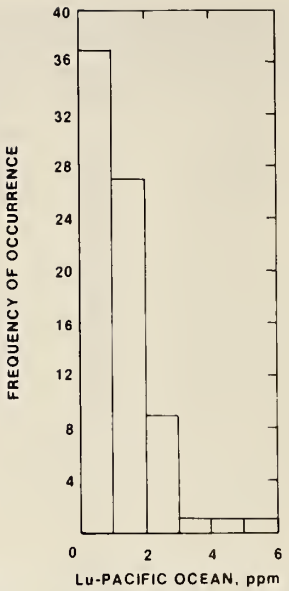

Figure 49.—Lutetium frequency distribution for Pacific manganese nodules.

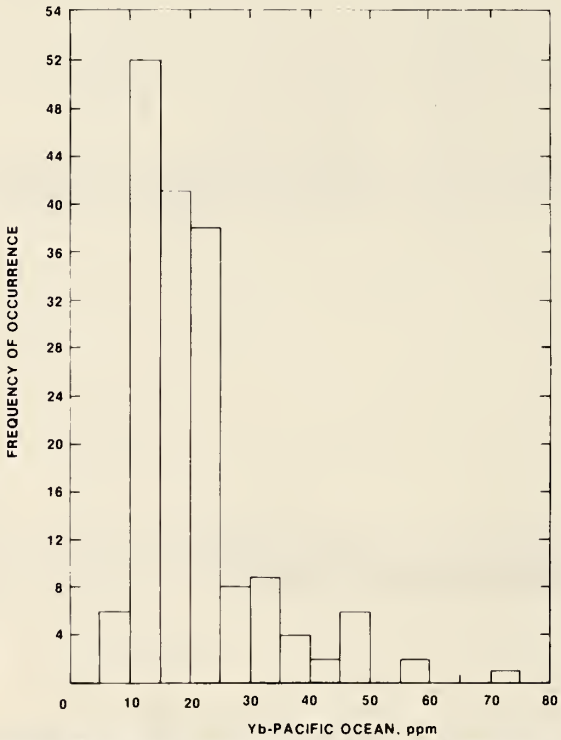

Figure 48.—Ytterbium frequency distribution for Pacific manganese nodules.

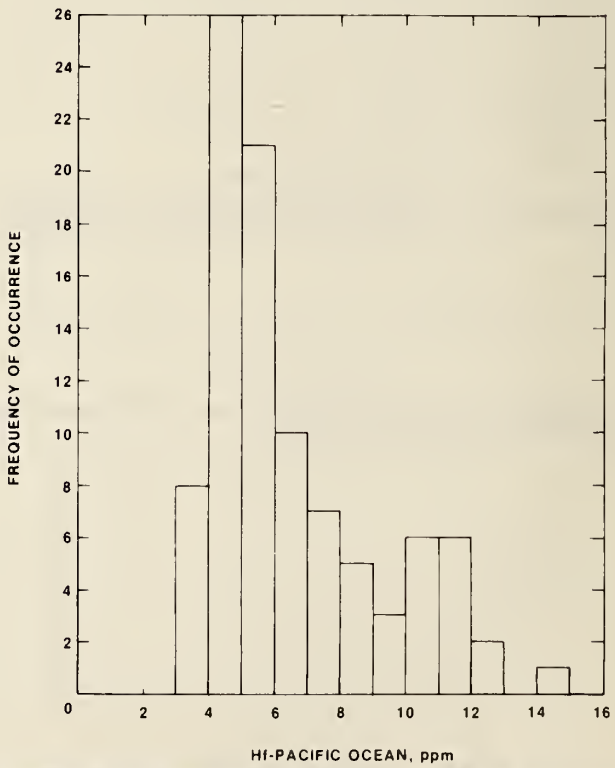

Figure 50.—Hafnium frequency distribution for Pacific manganese nodules.

The rare-earth values for Pacific nodules are primarily based on three publications, Glasby (*60*), Piper and Williamson (*107*), and Elderfield (*41*), plus data from the Sediment Data Bank (*48*). Rare-earth element content of nodules, with the exception of cerium, exhibits a decrease in rare-earth content relative to seawater content with increasing atomic number. Cerium shows a large enrichment relative to other rare-earth elements because of its oxidation to Ce^{4+} in nodules and is associated primarily with the iron phase. Other rare-earth elements occur as oxides in both the iron and gangue phosphate phases. It has been reported that total rare-earth element content of Pacific nodules increases with increasing distance from land and is correlated with both the iron and manganese contents of nodules (*127*). A negative correlation of rare earths to silica content has also been observed. Rare-earth elements are incorporated in nodules mainly from seawater. Most variations of rare-earth content of nodules can be explained by dilution of the iron and manganese phases by silicate minerals. The rare earths are preferentially incorporated into nodules due to hydrolysis under oxidizing conditions (*60*). The rare-earth elements (exclusive of cerium) occur in two phases, a phosphate phase composed of fish debris and/or recrystallized biogenic apatite, and the hydrous iron oxide phase with chemisorbed phosphate.

PRECIOUS-METAL-GROUP ELEMENTS

The elements in this section are those elements that are classified as precious metals and/or platinum-group metals. Very limited sample analyses are available for Au, Ir, Pd, Pt, Re, and Ru (*1, 45, 60, 112*); therefore, no histograms are presented. No data are available for Os and Rh, and Ag is discussed with the elements of environmental interest. A summary of the elemental composition of Pacific nodules for the six elements is given in table 12.

Gold values show a positive correlation with silica content, whereas iridium values show a negative correlation (*60*). Gold and palladium are depleted in Pacific nodules compared with deep sea sediments whereas iridium shows an enrichment in nodules relative to deep sea sediments. The ability for some of these elements to form stable anionic species (gold and rhenium) in seawater may explain their depletion in nodules.

Table 12. — Precious-metal-group elements in Pacific manganese nodules, nanograms per gram

Element	Range	Median	Mean	Number of samples
Gold	0.13– 3.9	1.92	1.93	10
Iridium	0.2 – 23.1	4.3	9.1	11
Palladium	2.9 – 9.2	6.3	6.2	10
Platinum	<5 –145	110	97	5
Rhenium	<.2	NAp	NAp	2
Ruthenium	18	NAp	NAp	1

NAp Not applicable.

RADIOACTIVE ELEMENTS

Only limited data are available on the radioactive elements, with only Ra, Th, and U being reported. Over 250 sample analyses are available for U and Th and nine values for Ra. Table 13 gives the Ra, Th and U data available for Pacific nodules. Figures 51 and 52 are histograms for thorium and uranium, respectively. Data for these elements were obtained from the Sediment Data Bank (*48*) and other sources (*12, 81, 83-88, 96, 102*).

Table 13. — Radioactive elements in Pacific manganese nodules

Element	Range	Median	Mean	Number of samples
Radium..pg/g	1.0– 35.7	5.1	8.5	9
Thorium..ppm	5 –154	21	28	283
Uranium..ppm	1 – 68	5	6.8	255

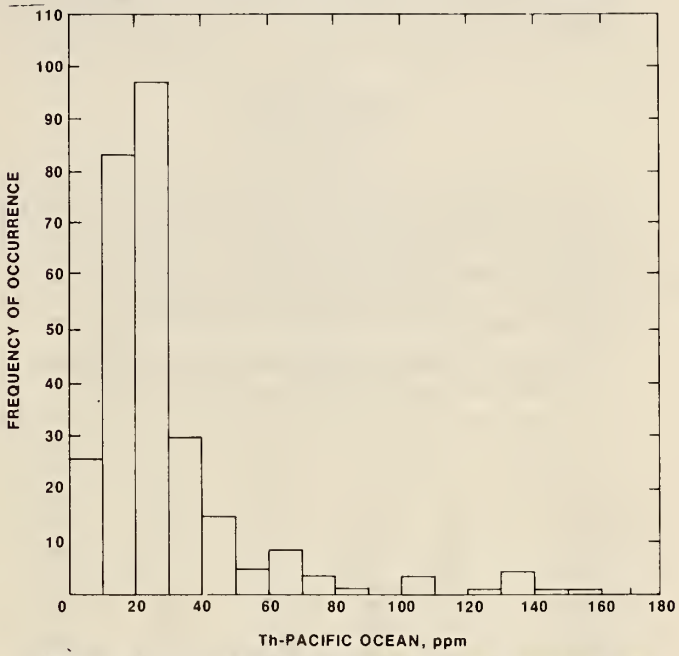

Figure 51.—Thorium frequency distribution for Pacific manganese nodules.

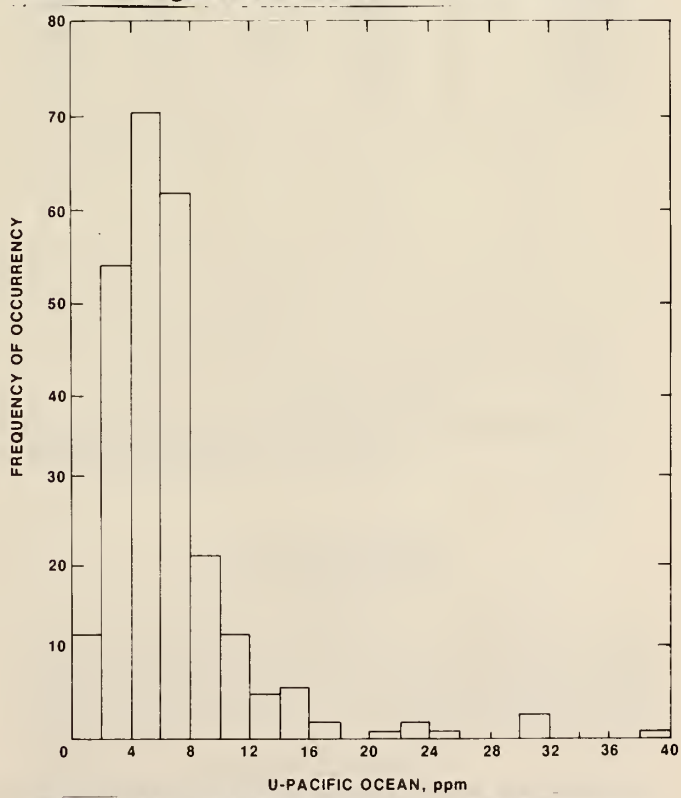

Figure 52.—Uranium frequency distribution for Pacific manganese nodules.

The uranium and thorium content of Pacific nodules (and other nodules) can be explained by coprecipitation from seawater with the iron phase. Uranium and thorium content of nodules is enriched over seawater and deep sea sediments. Their concentration is highest near the top surface interface with seawater and lowest at the bottom surface interface with the sediment. The interior of nodules has a concentration intermediate of the top and bottom surfaces.

Several authors (*81, 83, 85-87, 96*) have suggested that a relationship exists between the thorium and uranium content of nodules and the water depth from which they are taken.

OTHER TRACE ELEMENTS

The 17 elements in this section for which data are available are Sb, Be, Bi, B, Cs, Ga, Ge, Li, Nb, Rb, Sc, Ta, Te, Tl, Sn, W, and Y. Table 14 gives the available information on these elements for Pacific nodules. Figures 53 through 60 are histograms for those elements where greater than 40 sample analyses are available. Data for these elements come from the Sediment Data Bank (*48*) as well as other sources.

Table 14. — Other trace elements in Pacific manganese nodules, parts per million

Element	Range	Median	Mean	Number of samples
Antimony	14 – 72	36	37	103
Beryllium	2 – 15	2	4	29
Bismuth	6 – 31	23	21	13
Boron	17 –1,655	221	273	94
Cesium	<.50– 2.60	<.70	.75	7
Gallium	2 – 72	6	11	39
Germanium	3 – 90	37	42	4
Lithium	23 –1,055	100	160	25
Niobium	6 – 150	80	74	42
Rubidium	5 – 60	15	15	43
Scandium	1 – 29	10	10	159
Tantalum	2 – 20	11	11	4
Tellurium	172 – 272	214	216	17
Thallium	2 – 675	160	169	141
Tin	2 – 450	80	108	87
Tungsten	26 – 120	80	76	7
Yttrium	17 – 950	111	133	132

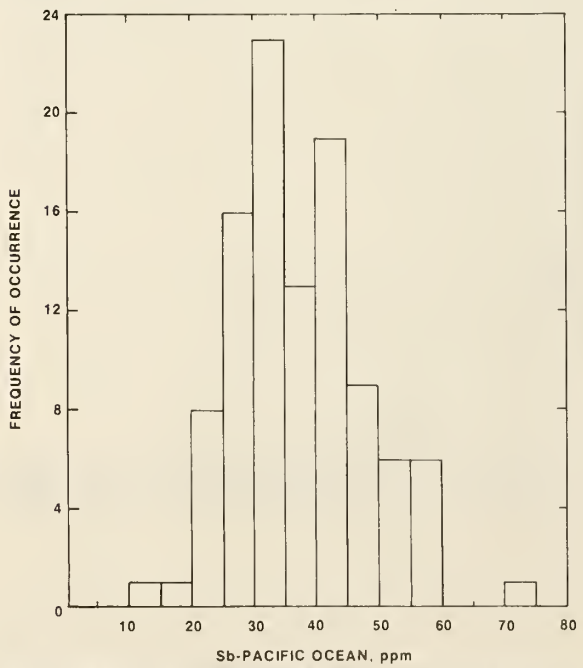

Figure 53.—Antimony frequency distribution for Pacific manganese nodules.

Of the 17 elements in this section, only eight have more than 40 sample analyses and only four have more than 100 sample analyses. Antimony is thought to be associated with the manganese phase. These trace elements may occur with any of the three phases and/or be present as a result of seawater residue incorporation.

Thallium merits special attention as the most enriched element in nodules when compared with deep sea sediments. An inverse correlation is observed between thallium and silica content of nodules. Thallium as Tl^{+} is stable in acid and alkaline environments whereas Tl^{3+} is stable only at low pH and forms thallic hydroxide precipitate when Tl^{3+} solutions are made basic. Thallium probably exists in nodules as thallic hydroxide, $Tl(OH)_3$. The nodule environment may oxidize the Tl^{+} in sediments and precipitate thallium as the hydroxide (*60*).

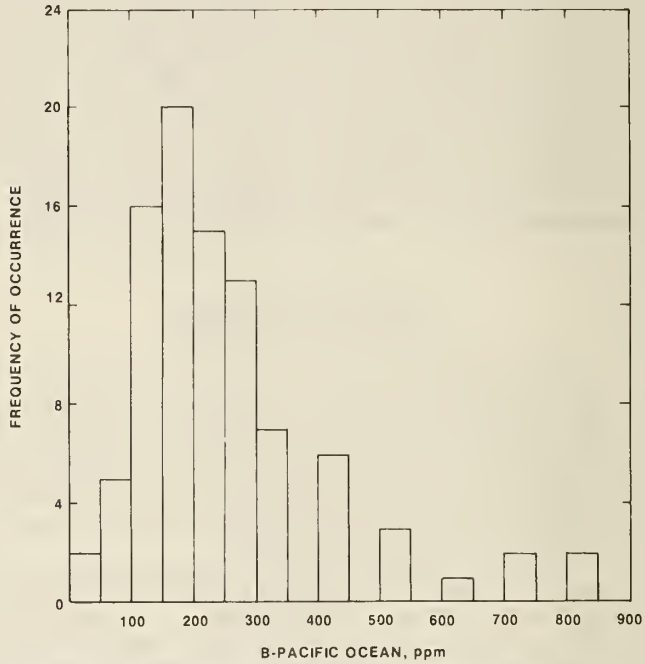

Figure 54.—Boron frequency distribution for Pacific manganese nodules.

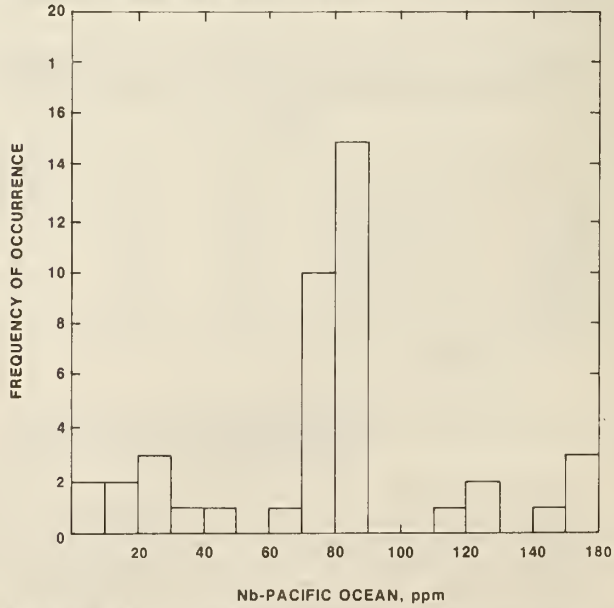

Figure 55.—Niobium frequency distribution for Pacific manganese nodules.

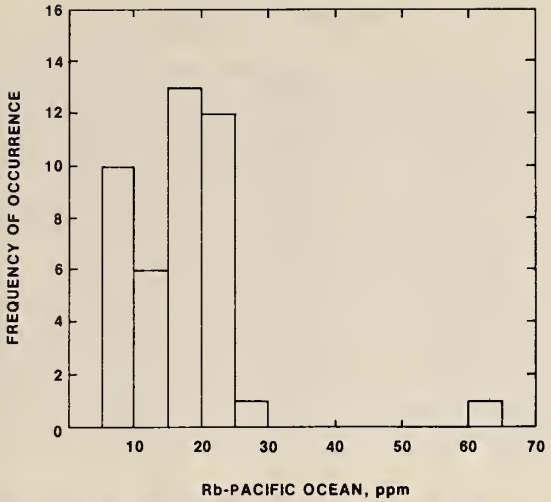

Figure 56.—Rubidium frequency distribution for Pacific manganese nodules.

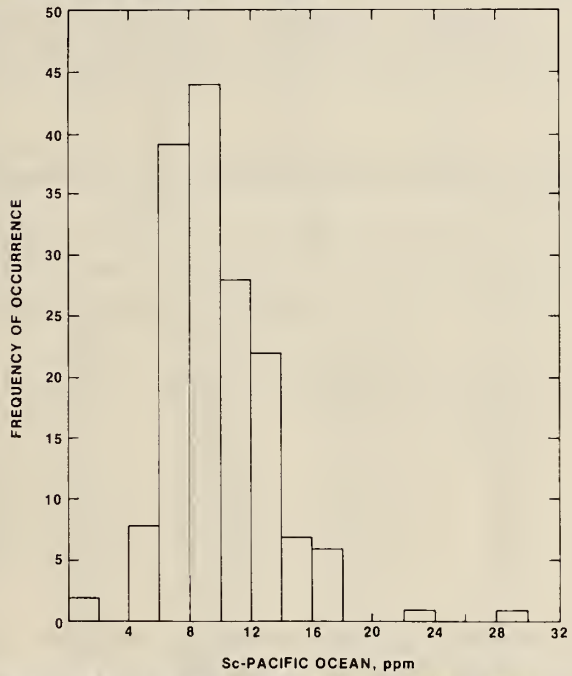

Figure 57.—Scandium frequency distribution for Pacific manganese nodules.

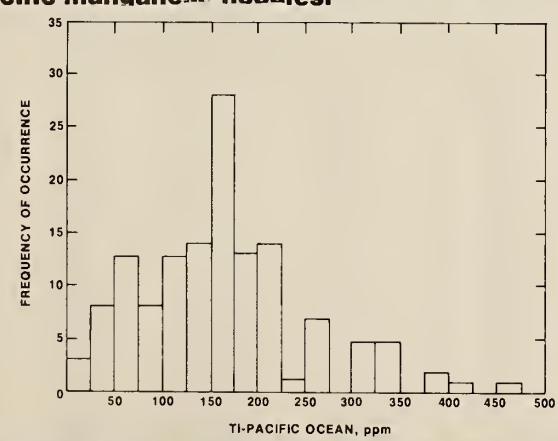

Figure 58.—Thallium frequency distribution for Pacific manganese nodules.

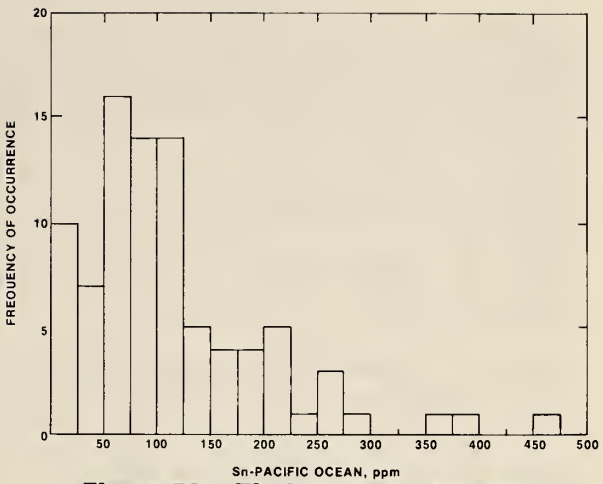

Figure 59.—Tin frequency distribution for Pacific manganese nodules.

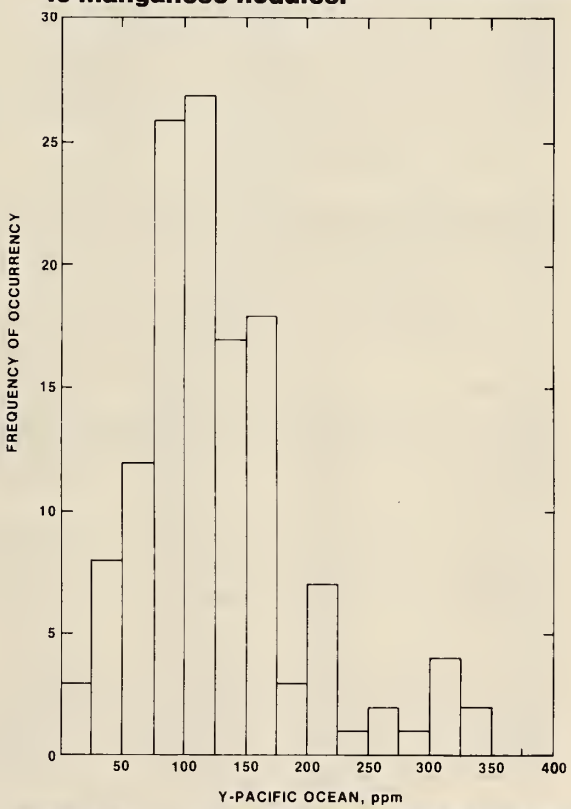

Figure 60.—Yttrium frequency distribution for Pacific manganese nodules.

ANION-FORMING ELEMENTS

The eight elements in this section occur almost exclusively as anions in the chemical structure of Pacific nodules. These elements are Br, C, Cl, F, I, N, P, and S occurring as bromide, carbonate, chloride, fluoride, iodide, nitrate, phosphate, and sulfate anions. The anions—chloride, fluoride, bromide, iodide—present in nodules are primarily the result of residues from evaporation of seawater.

Carbon occurs as carbonate in the form of gangue minerals such as calcite and other carbonate minerals and as entrapped organic matter.

Phosphorus is present as phosphate minerals such as apatite and calcium phosphate and is associated with the iron phases. Shark teeth inclusions in nodules increase the phosphate level substantially. Phosphorite pellets (apatite) have been observed as nucleii and inclusions in manganese nodules.

Sulfur as sulfate occurs in nodules in the form of barite ($BaSO_4$) and other sulfate minerals. The sulfide form is not very common in the oxidizing environment in which nodules are formed.

Data for nitrogen as nitrate are limited; nitrate is undoubtedly a residue from seawater. Table 15 is a summary of the data available for these elements.

Table 15. — Anion-forming elements in Pacific manganese nodules, weight-percent

Element	Form	Range	Number of samples
Bromine	Br^-	0.002–0.080	7
Carbon	$CO_3^=$	.30 –1.70	22
Chlorine	Cl^-	<.01 –1.10	10
Fluorine	F^-	<.01 – .05	6
Iodine	I^-	<.01 – .25	7
Nitrogen	NO_3^-	<.01 – .18	6
Phosphorus	P_2O_5	<.01 –2.20	158
Sulfur	$SO_4^=$	.07 –6.60	24

SUMMARY TABLES

This section of the report contains summary tables for the 21 major and minor elements for each of the four areas of the Pacific. Table 16 is the summary table for the CC-Zone area, the MPS area, the other abyssal plains area, and the other seamounts area. Table 17 gives the composite composition of all 74 elements discussed in this report. The mean values in table 17 for the 21 major and minor elements (including Ba, Cd, Cr, and Pb) are weighted averages based on the total number of analyses from each area. The median range for these elements is the lowest and highest median value for the four areas for each element. Table 18 is a list of those elements not included in this report owing to absence of data, exclusive of inert gases and transuranium elements. Table 19 lists interelement correlation coefficients found for the 21 major and minor elements from the CC-Zone area, the MPS area, the other abyssal plains area, and the other seamounts area.

CROSS SECTION ANALYSIS

The variation of elemental composition in a nodule cross section is shown in figures 61 through 65 and table 20. Figure 61 shows a cross section of a nodule and the analysis points.

Table 16. — Summary of major, minor, and some trace elements in Pacific manganese nodules, by area

Element	Range	Median	Mean	Number of samples	Range	Median	Mean	Number of samples
	Clarion-Clipperton zone				Other abyssal plains, >3,000 m			
Aluminum wt-pct	0.5–8.0	2.5–3.0	2.9	234	<0.5–10.0	2.5–3.0	3.0	570
Barium wt-pct	<0.01–0.76	0.20–0.22	0.28	213	<0.005–0.80	0.14–0.16	0.20	499
Cadmium ppm	1–35	10–15	12.3	127	1–35	5–10	10.7	133
Calcium wt-pct	<0.5–18.0	1.5–2.0	1.7	872	<0.5–13.0	1.5–2.0	1.8	914
Chromium ppm	1–150	15–20	27	107	1–150	15–20	25	227
Cobalt wt-pct	<0.1–0.9	0.20–0.30	0.24	1,925	<0.1–1.4	0.2–0.3	0.24	2,219
Copper wt-pct	0.1–2.0	1.0–1.1	1.02	2,236	<0.05–2.00	0.30–0.40	0.42	2,282
Iron wt-pct	1–25	6–7	6.9	2,215	1–25	12–13	12.7	2,325
Lead wt-pct	0.005–0.18	0.040–0.050	0.045	921	0.005–0.30	0.07–0.08	0.082	1,185
Magnesium wt-pct	<0.25–3.0	1.50–1.75	1.65	209	<0.25–5.00	1.25–1.50	1.43	361
Manganese wt-pct	1–39	26–27	25.4	2,227	1–40	18–19	18.5	2,354
Molybdenum wt-pct	<0.005–0.12	0.05–0.06	0.052	265	<0.005–0.13	0.03–0.04	0.036	746
Nickel wt-pct	0.1–2.0	1.3–1.4	1.28	2,237	0.1–2.0	0.50–0.60	0.63	2,334
Potassium wt-pct	0.20–3.0	0.80–0.90	1.01	123	0.10–3.0	0.70–0.80	0.93	335
Silicon wt-pct	1.0–25.0	6.0–6.5	7.6	339	0.5–25.0	7.0–8.0	8.8	460
Sodium wt-pct	0.50–6.75	2.00–2.25	2.79	106	<0.25–5.75	1.75–2.00	2.07	297
Strontium wt-pct	<0.005–0.16	0.040–0.050	0.045	78	<0.005–0.18	0.07–0.08	0.077	320
Titanium wt-pct	0.10–2.20	0.40–0.50	0.53	265	<0.05–2.50	0.60–0.70	0.78	854
Vanadium wt-pct	<.005–0.08	0.040–0.050	0.047	70	0.01–0.30	0.04–0.05	0.048	370
Zinc wt-pct	<0.05–0.95	0.10–0.15	0.14	1,539	<0.05–0.95	0.05–0.10	0.09	1,285
Zirconium wt-pct	0.010–0.09	0.030–0.040	0.035	33	<0.005–0.20	0.05–0.06	0.062	226
	Mid-Pacific seamounts				Other seamounts, <3,000 m			
Aluminum wt-pct	<0.25–6.00	0.25–0.75	1.20	48	<0.5–7.0	1.0–1.5	1.7	79
Barium wt-pct	0.04–0.68	0.18–0.20	0.30	39	0.06–0.80	0.32–0.34	0.37	59
Cadmium ppm	1–25	5–10	8.3	15	1–35	5–10	10.2	23
Calcium wt-pct	<0.5–25.0	2.0–2.5	4.2	91	<0.5–25.0	2.0–3.0	4.5	200
Chromium ppm	1–40	10–20	58	22	1–130	30–40	60	38
Cobalt wt-pct	<0.1–2.5	0.7–0.8	0.76	182	<0.05–1.40	0.20–0.30	0.31	293
Copper wt-pct	<0.01–1.00	<0.05	0.10	176	<0.05–1.20	<0.05	0.11	304
Iron wt-pct	2–25	14.5–15.5	14.7	185	1–25	16–17	15.6	312
Lead wt-pct	0.01–0.47	0.17–0.18	0.186	105	0.005–0.30	0.10–0.11	0.10	206
Magnesium wt-pct	0.50–3.50	0.75–1.25	1.41	35	<0.25–4.25	1.50–1.75	1.79	64
Manganese wt-pct	1–40	20–21	20.8	183	1–40	16–17	17.8	315
Molybdenum wt-pct	<0.005–0.11	0.05–0.06	0.05	56	<0.005–0.15	0.03–0.04	0.05	88
Nickel wt-pct	0.1–1.5	0.40–0.50	0.49	188	0.1–1.4	0.3–0.4	0.35	315
Potassium wt-pct	0.10–0.90	0.30–0.40	0.41	35	0.10–1.60	0.30–0.40	0.54	66
Silicon wt-pct	<0.5–15.0	2.0–3.0	3.6	45	<0.5–23.0	3.0–4.0	4.8	91
Sodium wt-pct	0.50–5.50	1.45–1.55	2.13	28	0.25–3.75	1.25–1.50	1.64	37
Strontium wt-pct	<0.005–0.30	0.14–0.15	0.13	27	<0.005–0.28	0.13–0.14	0.135	68
Titanium wt-pct	0.20–2.20	1.10–1.20	1.12	102	<0.05–1.60	0.40–0.50	0.47	89
Vanadium wt-pct	<0.005–0.30	0.07–0.08	0.086	29	<0.005–0.14	0.06–0.07	0.067	38
Zinc wt-pct	<0.05–0.25	0.05–0.10	0.07	82	<0.05–0.55	0.05–0.10	0.07	191
Zirconium wt-pct	<0.005–0.110	0.070–0.075	0.061	18	<0.005–0.20	0.04–0.05	0.054	27

Table 17. — Summary of elements in Pacific manganese nodules

Element and atomic number	Range	Median	Mean	Number of samples	Element and atomic number	Range	Median	Mean	Number of samples
Aluminum 13 wt-pct	<0.25–10.00	0.25–2.00	2.80	931	Molybdenum 42 wt-pct	<0.005–0.150	0.030–0.060	0.041	1,157
Antimony 51 ppm	14–72	36	37	103	Neodymium 60 ppm	60–700	141	158	96
Arsenic 33 ppm	20–450	164	159	122	Nickel 28 wt-pct	0.10–2.00	0.30–1.40	0.89	5,074
Barium 56 wt-pct	<0.005–0.800	0.140–0.340	0.239	810	Niobium 41 ppm	6–150	80	74	42
Beryllium 4 ppm	2–15	2	4	29	Nitrogen[2] 7 wt-pct	<0.01–0.18	0.04	0.056	6
Bismuth 83 ppm	6–31	23	21	13	Palladium 46 ng/g	2.9–9.2	6.3	6.2	10
Boron 5 ppm	17–1,655	221	273	94	Phosphorus[3] 15 wt-pct	<0.01–2.2	0.21	0.23	158
Bromine 35 wt-pct	0.002–0.080	0.05	0.05	7	Platinum 78 ng/g	5–145	110	97	5
Cadmium 48 ppm	1–35	5–15	11	298	Potassium 19 wt-pct	0.10–3.00	0.30–0.90	0.87	559
Calcium 20 wt-pct	<0.05–25.00	0.50–3.00	2.12	2,077	Praseodymium 59 ppm	26–46	34	36	8
Carbon[1] 6 wt-pct	0.30–1.70	0.19	0.18	22	Radium 88 pg/g	1.0–35.7	5.1	8.5	9
Cerium 58 ppm	74–3,000	345	530	131	Rhenium 75 ng/g	<0.2	NAp	NAp	2
Cesium 55 ppm	<0.5–2.6	<0.7	0.75	7	Rubidium 37 ppm	5–60	15	15	43
Chlorine 17 wt-pct	<0.01–1.10	0.86	0.07	10	Ruthenium 44 ng/g	18	NAp	NAp	1
Chromium 24 ppm	1–150	10–40	31	394	Samarium 62 ppm	14–141	32	35	115
Cobalt 27 wt-pct	<0.05–2.50	0.20–0.80	0.44	4,619	Scandium 21 ppm	1–29	10	10	159
Copper 29 wt-pct	<0.01–2.00	<0.05–1.10	0.66	4,998	Selenium 34 ppm	30–77	53	52	56
Dysprosium 66 ppm	22–42	32	31	18	Silicon 14 wt-pct	<0.5–25.0	2.0–8.0	7.8	935
Erbium 68 ppm	11–27	19	18	8	Silver 47 ng/g	2–680	39	101	56
Europium 63 ppm	1–27	7	9	115	Sodium 11 wt-pct	<0.25–6.75	1.25–2.25	2.20	468
Fluorine 9 wt-pct	<0.01–0.05	<0.01	0.013	6	Strontium 38 wt-pct	<0.005–0.300	0.040–0.150	0.083	493
Gadolinium 64 ppm	14–53	33	32	57	Sulfur[4] 16 wt-pct	0.07–6.6	0.4	1.84	24
Gallium 31 ppm	2–72	6	11	39	Tantalum 73 ppm	2–20	11	11	4
Germanium 32 ppm	3–90	37	42	4	Tellurium 52 ppm	172–272	214	216	17
Gold 79 ng/g	0.13–3.90	1.92	1.93	10	Terbium 65 ppm	1–11	5	5.4	104
Hafnium 72 ppm	3–14	5	6	96	Thallium 81 ppm	2–675	160	169	141
Holmium 67 ppm	1–8	4	4	66	Thorium 90 ppm	5–154	21	28	283
Iodine 53 wt-pct	0.01–0.25	0.023	0.051	7	Thulium 69 ppm	1–9	2	2.3	41
Iridium 77 ng/g	0.2–23.1	4.3	9.1	11	Tin 50 ppm	2–450	80	108	87
Iron 26 wt-pct	1–25	6–17	10.4	5,037	Titanium 22 wt-pct	<0.05–2.20	0.40–1.20	0.73	1,310
Lanthanum 57 ppm	66–979	130	157	151	Tungsten 74 ppm	26–120	80	76	7
Lead 82 wt-pct	0.005–0.470	0.040–0.180	0.072	2,417	Uranium 92 ppm	1–68	5	6.8	255
Lithium 3 ppm	23–1,055	100	160	25	Vanadium 23 wt-pct	<0.005–0.300	0.040–0.080	0.051	507
Lutetium 71 ppm	1–6	2	1.8	76	Ytterbium 70 ppm	8–100	17	20	171
Magnesium 12 wt-pct	<0.25–5.00	0.75–1.75	1.53	669	Yttrium 39 ppm	17–950	111	133	132
Manganese 25 wt-pct	1–40	16–27	21.6	5,079	Zinc 30 wt-pct	<0.05–1.00	0.05–0.15	0.11	3,097
Mercury 80 ng/g	2–775	85	152	68	Zirconium 40 wt-pct	<0.005–0.200	0.040–0.075	0.058	304

NAp Not applicable. [1]As $CO_3^=$. [2]As NO_3^-. [3]As P_2O_5. [4]As $SO_4^=$.

Table 18. — Elements for which no data were found for Pacific manganese nodules (exclusive of inert gases and transuranium elements)

	Atomic number		*Atomic number*
Actinium	89	Polonium	84
Astatine	85	Promethium	61
Francium	87	Protactinium	91
Indium	49	Rodium	45
Osmium	76	Technetium	43

Table 19. — Interelement correlation coefficients for Pacific manganese nodules, by area

Element	Al	Ba	Ca	Cd	Co	Cr	Cu	Fe	K	Mg	Mn	Mo	Na	Ni	Pb	Si	Sr	Ti	V	Zn	Zr
CLARION-CLIPPERTON ZONE																					
Al	1	0.34	*	–0.49	*	*	0.41	*	0.63	–0.50	–0.52	*	0.67	*	*	0.53	–0.50	*	–0.30	*	*
Ba	.34	1	–0.31	*	*	*	*	*	*	*	*	*	.40	*	*	*	*	*	*	*	*
Ca	*	–.31	1	.33	*	*	*	*	*	*	*	*	*	*	*	*	.56	*	.30	*	*
Cd	–.49	*	.33	1	–0.30	*	.42	–0.30	*	*	.31	0.45	–.32	0.57	–0.44	*	*	*	*	*	*
Co	*	*	*	–.30	1	*	*	.33	*	*	*	*	*	*	.40	*	*	0.36	*	*	*
Cr	*	*	*	*	*	1	*	*	*	*	*	*	*	*	*	*	*	*	*	*	–0.58
Cu	.41	*	*	.42	*	*	1	–.64	–.37	.63	.67	.39	–.48	.80	–.37	–.40	.66	–.59	.30	0.44	–.54
Fe	*	*	*	–.30	.33	*	–.64	1	*	–.41	–.42	–.30	*	–.59	.54	*	*	.57	*	–.49	.74
K	.63	*	*	*	*	*	–.37	*	1	–.51	–.59	*	.69	*	*	.40	–.44	*	*	*	*
Mg	–.50	*	*	*	*	*	.63	–.41	–.51	1	.69	*	–.62	.52	*	*	.63	–.34	*	*	*
Mn	–.52	*	*	.31	*	*	.67	–.42	–.59	.69	1	.71	–.43	.75	*	–.57	.50	–.49	.37	.51	*
Mo	*	*	*	.45	*	*	.39	–.30	*	*	.71	1	*	.63	*	*	*	*	*	*	*
Na	.67	.40	*	–.32	*	*	–.48	*	.69	–.62	–.43	*	1	*	*	.30	–.78	.36	–.36	*	*
Ni	*	*	*	.57	*	*	.80	–.59	*	.52	.75	.63	*	1	*	–.41	.30	–.54	.36	.47	*
Pb	*	*	*	–.44	.40	*	–.37	.54	*	*	*	*	*	*	1	*	.49	.44	*	–.30	*
Si	.53	*	*	*	*	*	–.40	*	.40	*	–.57	*	.30	–.41	*	1	–.37	*	*	*	*
Sr	–.50	*	.56	*	*	*	.66	*	–.44	.63	.50	*	–.78	.30	.49	–.37	1	–.30	*	*	*
Ti	*	*	*	*	.36	*	–.59	.57	*	–.34	–.49	*	.36	–.54	.44	*	–.30	1	*	–.30	.42
V	–.30	*	.30	*	*	*	.30	*	*	*	.37	*	–.36	.36	*	*	*	*	1	*	*
Zn	*	*	*	*	*	*	.44	–.49	*	*	.51	*	*	.47	–.30	*	*	–.30	*	1	–.43
Zr	*	*	*	*	*	–.58	–.54	.74	*	*	*	*	*	*	*	*	*	.42	*	–.43	1

* No significant correlation found. Coefficients < –0.3 or > 0.3 are considered significant

Table 19. — Interelement correlation coefficients for Pacific manganese nodules, by area — Con.

Element	Al	Ba	Ca	Cd	Co	Cr	Cu	Fe	K	Mg	Mn	Mo	Na	Ni	Pb	Si	Sr	Ti	V	Zn	Zr
MID-PACIFIC SEAMOUNTS																					
Al	1	*	*	*	−0.31	0.74	−0.31	*	*	0.44	−0.53	−0.34	−0.34	−0.35	*	*	*	0.31	*	*	0.68
Ba	*	1	*	*	.42	*	*	−0.45	*	*	*	*	.33	*	0.44	*	*	*	*	0.57	−.38
Ca	*	*	1	*	−.31	−.41	*	−.60	*	*	−.46	*	*	*	*	*	0.61	*	*	*	*
Cd	*	*	*	1	*	*	*	*	*	*	*	*	*	*	*	*	*	*	*	*	*
Co	−.31	.42	−.31	*	1	*	*	*	−0.41	.53	.47	*	−.34	.30	.74	−0.61	.61	.46	*	*	.42
Cr	.74	*	−.41	*	*	1	.31	*	*	.64	*	*	−.51	.33	*	.40	*	.59	*	*	−.41
Cu	−.31	*	*	*	*	.31	1	*	*	*	*	*	*	*	*	*	*	*	*	*	−.70
Fe	*	−.45	−.60	*	*	*	*	1	*	*	*	*	*	*	*	*	*	.46	*	*	.67
K	*	*	*	*	−.41	*	*	*	1	*	*	*	.52	*	−.32	.52	*	*	0.46	*	*
Mg	.44	*	*	*	.53	.64	*	*	*	1	*	*	*	.43	.67	*	.44	*	*	−.42	−.42
Mn	−.53	*	−.46	*	.47	*	*	*	*	*	1	.59	*	.70	.54	*	.39	*	*	.43	.39
Mo	−.34	*	*	*	*	*	*	*	*	*	.59	1	.33	.61	*	*	*	*	−.52	*	*
Na	−.34	.33	*	*	−.34	−.51	*	*	.52	*	*	.33	1	.54	−.33	.57	−.59	−.43	.38	.69	*
Ni	−.35	*	*	*	.30	.33	*	*	*	.43	.70	.61	.54	1	*	*	*	*	*	.64	*
Pb	*	.44	*	*	.74	*	*	*	−.32	.67	.54	*	−.33	*	1	−.40	.65	.31	−.31	*	−.38
Si	*	*	*	*	−.61	.40	*	*	.52	*	*	*	.57	*	−.40	1	−.66	*	*	*	.58
Sr	*	*	.61	*	.61	*	*	*	*	.44	.39	*	−.59	*	.65	−.66	1	.62	*	*	−.36
Ti	.31	*	*	*	.46	.59	*	.46	*	*	*	*	−.43	*	.31	*	.62	1	−.30	−.34	.59
V	*	*	*	*	*	*	*	*	.46	*	*	−.52	.38	*	−.31	*	*	−.30	1	.31	*
Zn	*	.57	*	*	*	*	*	*	*	−.42	.43	*	.69	.64	*	*	*	−.34	.31	1	−.59
Zr	.68	−.38	*	*	.42	−.41	−.70	.67	*	−.42	.39	*	*	*	−.38	.58	−.36	.59	*	−.59	1
OTHER ABYSSAL PLAINS, >3,000 m																					
Al	1	*	*	−0.52	−0.30	*	*	*	0.50	*	−0.56	−0.30	*	*	*	0.65	*	*	*	−0.32	*
Ba	*	1	*	.56	*	*	*	*	*	*	*	*	*	*	*	*	*	*	*	*	*
Ca	*	*	1	*	*	*	*	*	*	0.30	*	*	*	*	*	*	*	*	*	*	*
Cd	−.52	.56	*	1	−.48	*	0.84	−0.71	−.94	.99	.63	.31	−0.77	0.85	−0.36	*	*	*	*	*	*
Co	−.30	*	*	−.48	1	*	*	.36	*	*	*	*	*	*	*	−.44	0.48	*	*	*	*
Cr	*	*	*	*	*	1	*	*	*	*	*	*	−.34	*	*	.57	−.35	*	*	*	−0.33
Cu	*	*	*	.84	*	*	1	−.53	*	*	.58	*	*	.82	−.30	*	*	*	*	.32	*
Fe	*	*	*	−.71	.36	*	−.53	1	−.32	*	−.36	*	*	−.49	.37	*	.51	0.30	0.38	*	.42
K	.50	*	*	−.94	*	*	*	−.32	1	*	−.33	*	*	*	*	.55	−.31	*	*	*	*
Mg	*	*	.30	.99	*	*	*	*	*	1	*	*	*	*	*	*	*	*	*	*	*
Mn	−.56	*	*	.63	*	*	.58	−.36	−.33	*	1	.45	*	.66	*	−.62	*	*	*	.30	*
Mo	−.30	*	*	.31	*	*	*	*	*	*	.45	1	*	.36	*	−.34	*	*	.36	*	*
Na	*	*	*	−.77	*	−.34	*	*	*	*	*	*	1	*	*	*	*	*	*	*	*
Ni	*	*	*	.85	*	*	.82	−.49	*	*	.66	.36	*	1	*	−.30	*	*	*	.33	*
Pb	*	*	*	−.36	*	*	−.30	.37	*	*	*	*	*	*	1	*	.31	*	*	*	*
Si	.65	*	*	*	−.44	.57	*	*	.55	*	−.62	−.34	*	−.30	*	1	−.35	*	−.42	*	−.34
Sr	*	*	*	*	.48	−.35	*	.51	−.31	*	*	*	*	*	.31	−.35	1	.43	*	*	*
Ti	*	*	*	*	*	*	*	.30	*	*	*	*	*	*	*	*	.43	1	*	*	*
V	*	*	*	*	*	*	*	.38	*	*	*	.36	*	*	*	−.42	*	*	1	*	*
Zn	−.32	*	*	*	*	*	.32	*	*	*	.30	*	*	.33	*	*	*	*	*	1	*
Zr	*	*	*	*	*	−.33	*	.42	*	*	*	*	*	*	*	−.34	*	*	*	*	1
OTHER SEAMOUNTS, <3,000 m																					
Al	1	*	−0.39	*	*	−0.33	*	*	*	*	−0.30	*	*	*	*	0.59	−0.47	*	0.46	*	0.52
Ba	*	1	*	0.98	*	*	*	−0.52	*	0.42	.53	*	*	*	*	−.34	.31	−0.36	−.50	*	*
Ca	−.39	*	1	.74	*	*	*	−.40	−0.33	*	*	*	−0.46	*	*	−.46	.63	−.40	−.53	*	*
Cd	*	.98	.74	1	−0.37	−.99	0.54	*	*	*	−.44	*	*	0.49	−0.34	*	*	*	*	0.30	*
Co	*	*	*	−.37	1	*	*	*	*	*	*	*	*	.30	.67	−.35	*	.60	*	*	*
Cr	−.33	*	*	−.99	*	1	*	.54	.31	*	*	*	−.40	*	*	*	*	−.35	*	*	*
Cu	*	*	*	.54	*	*	1	*	*	.40	*	*	*	.44	*	*	*	*	.34	.40	*
Fe	*	−.52	−.40	*	*	.54	*	1	*	*	−.30	*	*	*	*	*	*	.39	.42	*	.30
K	*	*	−.33	*	*	.31	*	*	1	*	*	*	*	*	*	*	−.30	*	.32	*	*
Mg	*	.42	*	*	*	*	.40	*	*	1	*	*	−.45	.34	*	*	−.37	*	*	*	*
Mn	−.30	.53	*	−.44	*	*	*	−.30	*	*	1	*	.34	.38	*	*	*	*	*	*	*
Mo	*	*	*	*	*	*	*	*	*	*	*	1	.61	*	.31	*	*	*	*	*	*
Na	*	*	−.46	*	*	−.40	*	*	*	−.45	.34	.61	1	*	*	*	*	*	*	−.45	*
Ni	*	*	*	.49	.30	*	.44	*	*	.34	.38	*	*	1	*	*	*	*	*	.48	*
Pb	*	*	*	−.34	.67	*	*	*	*	*	*	0.31	*	*	1	*	*	.36	*	*	*
Si	.59	−.34	−.46	*	−.35	*	*	*	*	*	*	*	*	*	*	1	−.55	*	*	*	*
Sr	−.47	.31	.63	*	*	*	*	*	−.30	−.37	*	*	*	*	*	−.55	1	*	*	*	*
Ti	*	−.36	−.40	*	.60	−.35	*	.39	*	*	*	*	*	*	.36	*	*	1	.30	*	*
V	.46	−.50	−.53	*	*	*	.34	.42	.32	*	*	*	*	*	*	*	*	.30	1	*	*
Zn	*	*	*	.30	*	*	.40	*	*	*	*	*	−.45	.48	*	*	*	*	*	1	*
Zr	.52	*	*	*	*	*	*	.30	*	*	*	*	*	*	*	*	*	*	*	*	1

* No significant correlation found. Coefficients <−0.3 or >0.3 are considered significant.

Table 20 gives the elemental variation by sampling site for the nodule in figure 61. Figures 62 through 65 show spatial distribution with respect to discrete sample locations on the same nodule for the elements Cu and Ni, Co and Zn, Fe and Pb, and Ba and Ce. Analysis of the sample sites was performed by neutron activitation analysis and atomic absorption spectrophotometry using small samples from each site.

Figures 62 through 65 show that concentrations of Cu vary directly with Ni and Zn and inversely with Ce, Fe, and Pb. Barium does not appear to snow any relationship and could be considered as associated with the accessory mineral phase. These plots show the tendency of Cu, Ni, Zn, and possibly Co in this nodule section to be associated with the Mn phase and Ce and Pb to be associated with the Fe phase. Although not shown, Mn varies similarly with the Cu and Ni scans (see table 20). Figure 61 also shows the amount of layering that takes place during nodule growth and the differences in light and dark areas.

Figure 61.—Unpolished cross section of nodule DH 9-9 (location 21°45′ N., 113°10′W, 3,500-m water depth). Numbered circles indicate locations of 24 discrete sampling sites for analysis.

Table 20. — Nodule cross section sample locations and analysis, figure 61

Sample location	Weight-percent								Parts per million													I,[1] wt-pct
	Ba	Co	Cu	Fe	Mn	Ni	Pb	Zn	Ce	Cr	Cs	Eu	Hf	La	Lu	Sc	Sm	Ta	Tb	Th	Yb	
1	0.251	0.05	0.45	7.8	23.5	0.85	0.04	0.31	203	29.3	24.5	7.1	4.2	147	2.8	4.5	38.7	ND	5.2	24.8	18.8	16.0
2	.212	.02	.61	4.6	27.5	1.00	.02	.34	115	19.9	30.1	5.0	2.8	87.4	1.8	3.3	20.6	1.1	3.7	10.0	12.0	17.7
3	.232	.03	.55	5.3	25.5	.92	.02	.30	146	21.3	29.5	5.6	ND	96.1	1.9	3.1	23.3	1.6	4.1	13.2	13.4	12.7
4	.285	.06	.51	7.4	25.0	.82	.03	.27	199	22.2	29.3	7.1	ND	132	2.7	3.9	29.5	2.2	5.0	20.7	18.6	8.4
5	.335	.06	.56	7.7	24.5	.80	.02	.25	215	19.7	31.8	6.6	ND	136	2.7	4.5	28.2	1.4	4.6	27.0	18.3	14.2
6	.445	.04	.67	4.5	28.5	.80	.02	.36	126	16.9	40.8	5.2	2.9	104	2.1	2.1	24.3	.6	3.7	10.4	13.2	7.8
7	.504	.03	.70	3.4	29.5	.76	.01	.43	86.8	22.3	15.1	4.6	3.0	111	1.8	2.6	22.0	1.2	3.3	7.1	11.2	7.8
8 and 17	.637	.13	.51	9.6	24.0	.74	.03	.18	252	30.1	25.8	4.4	7.3	143	2.2	7.0	25.2	.8	3.4	29.5	14.7	13.0
9	ND	ND	.53	ND	25.0	.78	.04	.18	ND	ND	ND	ND	ND	ND	ND	ND	ND	ND	ND	ND	ND	11.7
10 and 15	.774	.18	.53	7.7	27.5	.98	.02	.18	215	32.5	23.7	4.4	2.9	115	1.7	5.8	20.2	3.1	2.0	38.1	13.7	8.0
11 and 12	ND	.16	.66	9.6	26.5	.93	.03	.20	ND	ND	20.2	5.6	9.2	ND	ND	7.3	ND	2.5	1.0	39.1	ND	15.0
13 and 14	1.270	.10	.67	5.6	28.5	1.09	.02	.21	216	14.9	21.4	3.8	ND	121	1.6	5.0	22.3	1.2	1.3	16.9	11.8	10.4
16	.583	.14	.50	12.1	21.5	.60	.02	.15	185	33.8	22.0	3.8	6.9	111	2.0	9.7	21.5	3.8	2.4	34.8	14.2	22.1
18	ND	.10	.58	6.4	26.0	.64	.02	.16	190	29.3	32.6	3.8	2.8	104	1.6	5.2	18.6	1.1	2.3	22.3	10.9	12.3
19	.511	.05	.73	4.8	27.5	.92	.02	.30	109	20.9	30.3	4.5	ND	105	1.9	4.5	22.9	ND	3.1	11.9	13.6	8.0
20	.317	.04	.74	5.3	27.5	1.04	.02	.33	144	24.9	35.0	4.5	4.8	101	1.9	5.2	21.5	.6	2.6	14.5	13.2	15.4
21	.303	.04	.65	5.9	26.5	.94	.02	.36	130	18.5	30.1	5.5	2.7	112	2.3	5.0	27.3	1.4	3.4	16.3	15.9	10.0
22	.282	.06	.63	6.1	26.0	.96	.04	.33	196	22.2	24.5	6.1	ND	126	2.6	5.4	33.5	ND	3.7	19.5	18.0	13.5
23	.292	.04	.49	5.8	26.5	.80	.02	.34	161	24.1	26.4	5.9	3.7	117	2.5	5.1	28.3	1.4	3.7	15.3	18.5	8.7
24	.265	.04	.40	6.2	26.5	.80	.02	.34	170	22.9	24.2	6.1	3.8	114	2.4	5.5	27.8	.9	4.1	19.1	16.5	14.4

ND Not detected. [1] Insoluble in HCl.

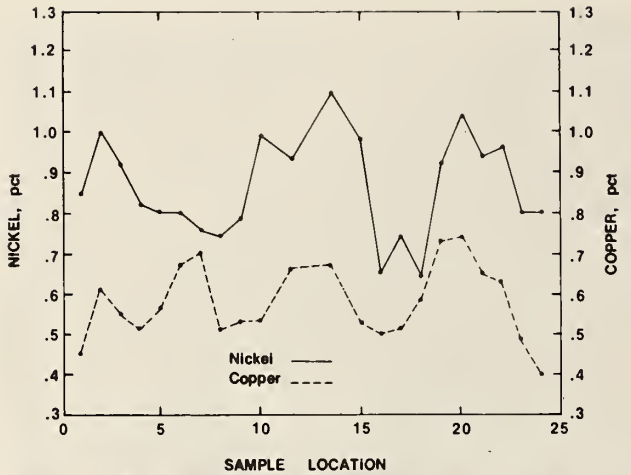

Figure 62.—Spatial distribution of nickel and copper concentrations with respect to discrete sample locations on nodule cross section DH 9-9, figure 61.

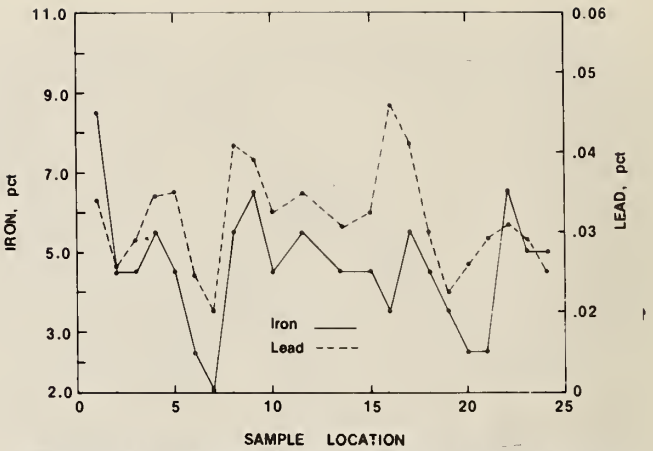

Figure 64.—Spatial distribution of iron and lead concentrations with respect to discrete sample locations on nodule cross section DH 9-9, figure 61.

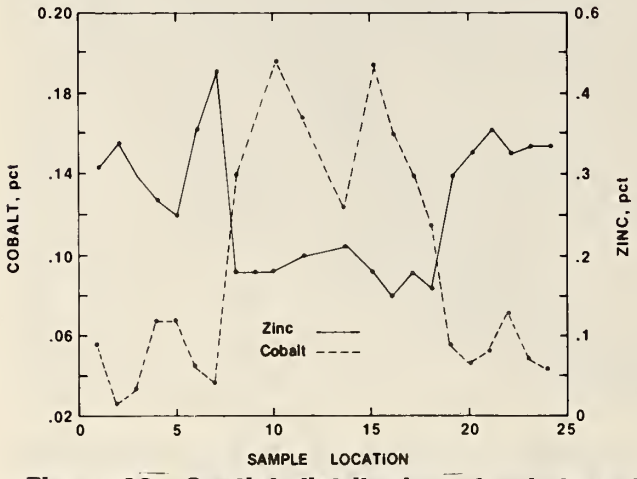

Figure 63.—Spatial distribution of cobalt and zinc concentrations with respect to discrete sample locations on nodule cross section DH 9-9, figure 61.

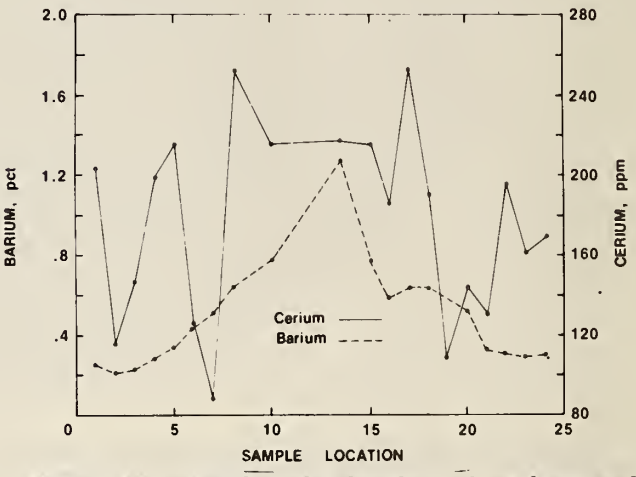

Figure 65.—Spatial distribution of barium and cerium concentrations with respect to discrete sample locations on nodule cross section DH 9-9, figure 61.

REFERENCES[5]

1. Agiorgitis, G., and H. Gundlach. Platin-Gehalte in Tiefsee-Mangenkrollen. Naturwissenschaften, v. 65, 1978, p. 534.

2. Ahrens, L. H., J. P. Willis, and C. C. Oosthuizen. Further Observations on the Composition of Manganese Nodules With Particular Reference to Some of the Rarer Elements. Geochim. Cosmochim. Acta, v. 31, 1967, pp. 2169-2180.

3. Andrushchenko, P. F., and N. S. Skornyakova. The Textures and Mineral Composition of Iron-Manganese Concretions From the Southern Part of the Pacific Ocean. Oceanology, v. 9, 1969, pp. 229-242.

4. _____. Composition, Structure, and Characteristic Features of Formation of Fe-Mn Nodules in the Pacific Ocean. Manganese Deposits of the Soviet Union, ed. by D. S. Sapuzhnika. Israel Program for Scientific Translations, Jerusalem, 1970, pp. 101-124.

5. Arrhenius, G. Pelagic Sediments. Ch. in The Sea, ed. by M. N. Hill. Interscience, New York, v. 3, 1963, pp. 655-727.

6. Aumento, F., D. E. Lawrence, and A. G. Plant. The Ferromanganese Pavement on San Pablo Seamount. Geol. Survey Canada, Paper 68-32,, 1968, 30 pp.

7. Barnes, S. S. The Formation of Oceanic Ferromanganese Nodules. Ph.D. Thesis, Univ. Calif., San Diego, Calif., 1967, 59 pp.

8. Bezrukov, P. L., and P. F. Andrushchenko. (Iron-Manganese Nodules From the Indian Ocean.) Izv. Akad. Nauk SSSR Ser. Geol., No. 7, 1972, pp. 3-20.

9. Bezrukov, P. L., and N. S. Skornyakova. Ferromanganese Nodules of the Pacific Ocean. Memoirs—Am. Assoc. Pet. Geol., v. 25, 1976, pp. 376-381.

10. Bischoff, J. L., and D. Z. Piper. Marine Geology and Oceanography of the Pacific Manganese Nodule Province. Plenum Press, New York, 1979, 842 pp.

11. Bonatti, E., and Y. R. Nayudu. The Origin of Manganese Nodules on the Ocean Floor. Am. J. Sci., v. 263, 1965, pp. 17-39.

12. Buchowiecki, J., and R. D. Cherry. Thorium, Radium and Potassium in Manganese Nodules. Chem. Geol., v. 3, 1968, pp. 111-117.

13. Burns, R. G. Uptake of Cobalt into Ferromanganese Nodules, Soils, and Synthetic Manganese (IV) Oxides. Geochim. Cosmochim. Acta, v. 40(1), 1976, pp. 95-102.

14. Burns, R. G., and V. M. Burns. Mineralogy. Ch. in Marine Manganese Deposits, ed. by G. P. Glasby. Elsevier Scientific Publishing Co., Amsterdam, Netherlands. Elsevier Oceanography Series, v. 15, 1977, pp. 185-248.

15. _____. The Mineralogy and Crystal Chemistry of Deep-Sea Manganese Nodules, A Polymetallic Resource of the Twenty-first Century. Phil. Trans. Royal Soc. (London), v. A286, 1977, pp. 283-301.

16. _____. Authigenic Oxides. The Sea, v. 7—The Oceanic Lithosphere, Ch. 22, ed. by C. Emiliani. John Wiley & Sons, Inc., New York, 1981, pp. 875-914.

17. _____. Manganese Oxides. Ch. in Marine Minerals, ed. by R. G. Burns. Litho Crafters, Inc., Chelsea, Mich., v. 6, 1979, pp. 1-46.

18. Burns, R. G., and D. W. Fuerstenau. Electron Probe Determination of Inter-Element Relationships in Manganese Nodules. Am. Miner., v. 51, 1966, pp. 895-902.

19. Burns, V. M., and R. G. Burns. Diagenetic Features Observed Inside Deep-Sea Manganese Nodules From the North Equatorial Pacific. Scanning Electron Microscopy, v. 1, 1978, pp. 245-252.

20. _____. Post-Depositional Metal Enrichment Processes Inside Manganese Nodules From the North Equatorial Pacific. Earth and Planetary Sci. Letters, v. 39, 1978, pp. 341-348.

21. Buser, W. The Nature of the Iron and Manganese Compounds in Manganese Nodules. Proc. Internat. Oceanography Cong., v. 1, 1959, pp. 962-963.

22. Buser, W., and A. Grutter. Uber die Natur der Manganknollen. Schweiz. Miner. Petrogr. Mitt., v. 36, 1956, pp. 49-62.

23. Calvert, S. E. Geochemistry of Oceanic Ferromanganese Deposits. Phil. Trans. Roy. Soc. (London), v. A290, 1978, pp. 43-73.

24. Calvert, S. E., and N. B. Price. Composition of Manganese Nodules and Manganese Carbonates From Loch Fyne, Scotland. Contributions, Miner. Petrol., v. 29, 1970, pp. 215-233.

25. _____. Geochemical Variation in Ferromanganese Nodules and Associated Sediments From the Pacific Ocean. Marine Chem., v. 5, 1977, pp. 43-74.

26. Calvert, S. E., N. B. Price, G. R. Heath, and T. C. Moore, Jr. Relationship Between Ferromanganese Nodule Composition and Sedimentation in a Small Survey Area of the Equatorial Pacific. J. Marine Res., v. 36, 1978, pp. 161-183.

27. Carpenter, R., H. P. Johnson, and E. S. Twiss. Thermomagnetic Behavior of Manganese Nodules. J. Geophys. Res., v. 77, 1972, pp. 7163-7174.

28. Carpenter, R., and S. Wakeham. Mossbauer Studies of Marine and Fresh Water Manganese Nodules. Chem. Geol., v. 11, 1973, pp. 109-116.

29. Chukhrov, F. V., A. I. Gorshkov, E. S. Rudnitskaya, V. V. Berezovskaya, and A. V. Sivtsov. (Vernadite.) Izvest. Akad. Nauk SSSR Ser. Geol., No. 6, 1978, pp. 5-19.

30. Chukhrov, F. V., A. I. Gorshkov, E. S. Rudnitskaya, and A. V. Sivtsov. (Characteristics of Birnessite.) Izvest. Akad. Nauk SSSR Ser. Geol., No. 9, 1978, pp. 67-76.

31. Chukhrov, F. V., A. I. Gorschkov, and A. V. Sivtsov. (New Structural Variety of Todorokite.) Izvest. Akad. Nauk SSSR Ser. Geol., No. 5, 1981, pp. 88-91.

32. Chukhrov, F. V., A. I. Gorshkov, A. V. Sivtsov, and V. V. Berezovskaya. (Structural Varieties of Todorokite.) Isvest. Akad. Nauk SSSR Ser. Geol., No. 12, 1978, pp. 86-95.

33. _____. New Data of Natural Todorokite. Nature, v. 278, 1979, pp. 631-632.

34. _____. (New Mineral Phases of Oceanic Manganese Microconcretions.) Izvest. Akad. Nauk SSSR Ser. Geol., No. 1, 1979, pp. 83-90.

35. Chukhrov, F. V., A. I. Gorshkov, B. B. Zvyagin, and L. P. Ermilova. Iron Oxides as Minerals of Sedimentary Environments and Chemogenic Eluvium. Proc. 2d Internat. Symp. on Geology and Geochemistry of Manganese, Sydney, Australia, Aug. 17-24, 1976, ed. by I. Varentsov. V. 1, 1980, pp. 231-257.

36. Chukhrov, F. V., B. B. Zvyagin, A. I. Gorshkov, L. P. Ermilova, V. V. Korovushkin, E. S. Rudnitskaya, and N. Yu. Yakubovskava. (Feroxyhyte, A New Modification of FeOOH.) Internat. Geol. Rev., v. 19, 1976, pp. 873-890.

37. Crerar, D. A., and H. L. Barnes. Deposition of Deep-Sea Manganese Nodules. Geochim. Cosmochim. Acta, v. 38, 1974, pp. 279-300.

38. Cronan, D. S. The Geochemistry of Some Manganese Nodules and Associated Pelagic Deposits. Ph.D. Thesis, Imperial College, Univ. of London, March 1967.

39. Cronan, D. S. Underwater Minerals. Academic Press, Inc., Ltd., London, England, 1980, 362 pp.

40. Cronan, D. S., and J. S. Tooms. The Geochemistry of Manganese Nodules and Associated Pelagic Deposits From the Pacific and Indian Oceans. Deep-Sea Res., v. 16, 1969, pp. 335-359.

41. Elderfield, H., C. J. Hawkesworth, M. J. Greaves, and S. E. Calvert. Rare Earth Element Geochemistry of Oceanic Ferromanganese Nodules and Associated Sediments. Geochim. Cosmochim. Acta, v. 45, 1981, pp. 513-528.

42. Fewkes, R. H., W. D. McFarland, W. R. Reinhart, and R. K. Sorem. Development of a Reliable Method for Evaluation of Deep Sea Manganese Nodule Deposits (Contract GO274013, Wash. State Univ.). BuMines OFR 64-80, Jan. 12, 1979, 94 pp.; NTIS PB 80-182116.

43. _____. Evaluation of Metal Resources at and Near Proposed Deep Sea Mine Sites (Contract GO284008, Wash. State Univ.). BuMines OFR 108-80, Feb. 15, 1980, 239 pp.; NTIS PB 80-228992.

44. Fisk, M. B., J. Z. Frazer, J. S. Elliot, and L. L. Wilson. Availability of Copper, Nickel, Cobalt, and Manganese From Ocean Ferromanganese Nodules (II) (Contract GO264024, Scripps Inst. Oceanography). BuMines OFR. 140(1)-80, Aug. 24, 1979, 63 pp.; NTIS PB 81-145963.

45. Flanagan, F. J., and D. Gottfried. USGS Rock Standards, III. Manganese-Nodule Reference Samples USGS Nod-A-1 and USGS-Nod-P-1. U.S. Geol. Survey Prof. Paper 1155, 1980, 39 pp.

46. Fleischer, M. Glossary of Mineral Species 1980. Mineralogical Record, Tucson, Ariz., 1980, 192 pp.

47. Frazer, F. W., and J. Ostwald. Chemical and Mineralogical Investigations on a Suite of Deep-Sea Manganese Nodules. Central Research Laboratories, CRL/TC/7/70, Broken Hill Proprietary Co., Ltd., and the Bureau of Mineral Resources, Shortland, Australia, 1970.

48. Frazer, J. Z., and M. B. Fisk. Availability of Copper, Nickel, Cobalt, and Manganese From Ocean Ferromanganese Nodules (III) (Contract GO264024, Scripps Inst. Oceanography). BuMines OFR 140(2)-80, Aug. 31, 1980, 112 pp.; NTIS PB 81-145971.

49. _____. Geological Factors Related to Characteristics of Seafloor Manganese Nodule Deposits (Contract GO264024, Scripps Inst. Oceanography). BuMines OFR 142-80, Apr. 30, 1980, 41 pp.; NTIS PB 81-145831.

50. Frazer, J. Z., M. B. Fisk, J. Elliot, M. White, and L. Wilson. Availability of Copper, Nickel, Cobalt, and Manganese From Ocean

[5] Titles enclosed in parentheses are translations from the language in which the item was published.

Ferromanganese Nodules (Contract GO264024, Scripps Inst. Oceanography). BuMines OFR 121-79, Sept. 10, 1978, 141 pp.; NTIS PB 300 #356.

51. Gager, H. M. Mossbauer Spectra of Deep-Sea Iron-Manganese Nodules. Nature, v. 220, 1968, pp. 1021-1023.

52. Gattow, G., and O. Glemser. Uber Manganoxyde VIII. Darstellung und Eigenschaften von Braunsteinen, III. Z. Anorg. Allg. Chem., v. 309, 1961, pp. 121-150.

53. Giovanoli, R. On Natural and Synthetic Manganese Nodules. Proc. 2d Internat. Symp. on Geology and Geochemistry of Manganese, Sidney, Australia, Aug. 17-24, 1976, ed. by I. Varentsov. V. 1, 1980, pp. 159-202.

54. Giovanoli, R., and P. Burki. Comparison of X-ray Evidence of Marine Manganese Nodules and Non-Marine Manganese Ore Deposits. Chimia, v. 29, 1975, pp. 266-269.

55. Giovanoli, R., P. Burki, M. Giuffredi, and W. Stumm. Layer Structured Manganese Oxide Hydroxides. IV: The Buserite Group. Chimia, v. 29, 1975, pp. 517-520.

56. Giovanoli, R., P. Burki, and P. Scheiss. Investigation of Manganese Nodules. Rept. No. 33A, Universitat Bern, Bern, Switzerland, 1973, 12 pp.

57. Giovanoli, R., W. Feitknecht, and F. Fischer. Uber Oxidhydroxide des vierwertigen Mangans mit Schichtengitter. Helv. Chim. Acta, v. 54, 1971, pp. 1112-1124.

58. Glasby, G. P. The Mineralogy of Manganese Nodules From a Range of Marine Environments. Mar. Geol., v. 13, 1972, pp. 57-72.

59. Glasby, G. P. (ed.). Marine Manganese Deposits. Elsevier Scientific Publishing Co., Amsterdam, Netherlands, Elsevier Oceanography Series, v. 15, 1977, 523 pp.

60. Glasby, G. P., R. R. Keays, and P. C. Rankin. The Distribution of Rare Earth, Precious Metal and Other Trace Elements in Recent and Fossil Deepsea Manganese Nodules. Geochem. J., v. 12, 1978, pp. 229-243.

61. Goncharov, G. N., A. V. Kalyamin, and B. G. Lur'e. Iron-Manganese Concretions From the Pacific Ocean Studied by a Nuclear, γ-Resonance Method. Dokl. Akad. Nauk SSSR, v. 212, 1973, pp. 720-723.

62. Goodell, H. G., M. A. Meylan, and B. Grant. Ferromanganese Deposits of the South Pacific Ocean, Drake Passage, and Scotia Sea. Antarc. Res. Ser., v. 15, 1971, pp. 27-92.

63. Goodier, J. How Manganese Nodules Develop. Oceanology Internat. Offshore Technol., v. 7, 1972, pp. 45-48.

64. Glover, E. D. Characterization of Marine Birnessite. Am. Miner., v. 62, 1977, pp. 278-285.

65. Grant, J. B. A Comparison of the Chemistry and Mineralogy With the Distribution and Physical Aspects of Marine Manganese Concretions of the Southern Oceans. Contributions, Sediment Res. Lab., Fla. State Univ., Tallahassee, Fla., v. 19, 1967, 99 pp.

66. Grill, E. V., J. W. Murray, and R. D. MacDonald. Todorokite in Manganese Nodules From a British Columbia Fjord. Nature, v. 219, 1968, pp. 358-359.

67. Harriss, R. C. Mercury Content of Deep-Sea Manganese Nodules. Nature, v. 219, 1968, pp. 54-55.

68. Harriss, R. C., J. H. Crocket, and M. Stainton. Palladium, Iridium and Gold in Deep-Sea Manganese Nodules. Geochim. Cosmochim. Acta, v. 32, 1968, pp. 1049-1056.

69. Hein, J. R., C. Gutmacher, and J. Miller. DOMES Area C: General Statement About Mineralogy, Diagenesis and Sediment Classification. DOMES, N.E. Pacific Nodule Province, Site C, Geology and Geochemistry. U.S. Geol. Survey OFR 76-548, 1976, 275 pp.

70. Hering, V. N. Metalle aus Tiefsee-Erzen. Stahl Eisen, v. 91, 1971, pp. 452-459.

71. Herzenberg, C. L., and D. L. Riley. Interpretation of the Mossbauer Spectra of Marine Iron-Manganese Nodules. Nature, v. 224, 1969, pp. 259-269.

72. Hewett, D. F., M. Fleischer, and N. Conklin. Deposits of the Manganese Oxides. Suppl. Econ. Geol., v. 58, 1968, pp. 1-51.

73. Hey, M. H., and P. G. Embrey. Twenty-eighth List of New Mineral Names. Miner. Mag., v. 39, 1974, pp. 903-932.

74. Hoffert, M. Les Argiles Rouges des Grands Fonds dans le Pacific Centre-Est: Authigenese, Transport, Diagenese. Ph.D. Dissertation, l'Universite Louis Pasteur, Strasbourg, France, 1980.

75. Hrynkiewicz, A. Z., A. J. Pustowka, B. D. Sawicka, and J. A. Sawicki. Mossbauer Study of Iron-Manganese Nodules at High Temperatures. Physica Status Solidi, v. 9, 1972, pp. K159-K163.

76. _____. Mossbauer Effect Analysis of Fe-Mn Nodules From Various Pacific Ocean Locations. Physica Status Solidi, v. 10, 1972, pp. 281-287.

77. Hrynkiewicz, A. Z., B. D. Sawicka, and J. A. Sawicki. The Mossbauer Effect in the Pacific Ocean Fe-Mn Nodules. Physica Status Solidi, v. 3, 1970, pp. 1039-1045.

78. Johnson, C. E., and G. P. Glasby. Mossbauer Determination of Particle Size in Microcrystalline Iron-Manganese Nodules. Nature, v. 222, 1968, pp. 376-377.

79. Kirchner, S. J., H. Oona, S. Perron, J. Q. Fernando, J. J. H. Lee, and H. Zeitlin. Proton-Induced X-Ray Emission Analysis of Deep-Sea Ferromanganese Nodules. Anal. Chem., v. 52, 1980, pp. 2195-2201.

80. Korkisch, J., H. Hubner, I. Steffan, G. Arrhenius, M. Fisk, and J. Frazer. Chemical Analysis of Manganese Nodules: Part I. Determination of Seven Main and Trace Constituents After Anion-Exchange Separation. Anal. Chim. Acta, v. 83, 1976, pp. 83-92.

81. Korkisch, J., I. Steffan, G. Arrhenius, M. Fisk, and J. Frazer. Chemical Analysis of Manganese Nodules: Part II. Determination of Uranium and Thorium After Anion-Exchange Separation. Anal. Chim. Acta, v. 90, 1977, pp. 151-158.

82. Krishnaswami, S. Authigenic Transition Elements in Pacific Pelagic Clays. Geochim. Cosmochim. Acta, v. 40, 1976, pp. 425-434.

83. Ku, T. L., and W. S. Broecker. Radiochemical Studies on Manganese Nodules of Deep-Sea Origin. Deep-Sea Res., v. 16, 1969, pp. 625-637.

84. _____. Uranium, Thorium, and Protactinium in Manganese Nodules. Earth and Planetary Sci. Letters, v. 2, 1967, pp. 317-320.

85. Kunzendorf, H., and G. H. W. Friedrich. Uranium and Thorium in Deep-Sea Manganese Nodules From the Central Pacific. Trans. Inst. Min. Met., Sect. B, v. 85, 1976, pp. B284-B288.

86. _____. The Distribution of U and Th in Growth Zones of Manganese Nodules. Geochim. Cosmochim. Acta, v. 40, 1976, pp. 849-852.

87. _____. Die Verteilung von Uran in Manganknollen in Abhangigkeit von der Knollenfazies und der Morphologie des Meeresbodens. Erzmetall, v. 30, 1977, pp. 590-592.

88. Kuroda, R., and S. Tatsuya. Anion-Exchange System in Magnesium Nitrate Media: Application to Chemical Analysis of Manganese Nodules for Thorium and Uranium. Fresenius Z. Anal. Chem., v. 300, 1980, pp. 107-111.

89. Landmesser, C. W., L. K. Kroenke, G. P. Glasby, G. H. Sawtell, S. Kingan, E. Utanga, A. Utanga, and G. Cowan. Manganese Nodules From the South Penrhyn Basin, Southwest Pacific. South Pacific Marine Geol. Notes, v. 1, 1976, pp. 17-39.

90. Manheim, F. T. Manganese-Iron Accumulations in the Shallow Marine Environment. Proc. Symp. on Marine Geochemistry, ed. by D. R. Schink and J. T. Corless. Occasional Pub., Narragansett Marine Lab., Univ. Rhode Island, Kingston, R.I., v. 3, 1965, pp. 217-276.

91. Maruyama, S., and H. Takeda. Ferromanganese Nodules. Ch. in Deep Sea Mineral Resources Investigations in Northwest Pacific, November-December 1972, ed. by H. Takeda. Geological Survey of Japan, Cruise Rept. No. 1, 1974, pp. 33-40.

92. McFarlin, P. F. Aragonite Vein Fillings in Marine Manganese Nodules. J. Sediment. Petrol., v. 37, 1967, pp. 68-72.

93. Mero, J. L. The Mineral Resources of the Sea. Elsevier Publishing Co., Amsterdam, Netherlands, 1965, 312 pp.

94. Meylan, M. A. The Mineralogy and Geochemistry of Manganese Nodules From the Southern Ocean. M.S. Thesis, Fla. State Univ., Tallahassee, Fla., 1968, 177 pp.

95. Meylan, M. A., and H. G. Goodell. Chemical Composition of Manganese Nodules From the Pacific-Antarctic Ocean, Drake Passage and Scotia Sea: Relation to Ferromanganese Oxide Mineralogy and Nucleus Type. Proc. IDOE Workshop, (pub. as Marine Geological Investigations in the Southwest Pacific and Adjacent Areas, ed. by G. P. Glasby and H. R. Katz), Suva, Fiji, Sept. 1-6, 1975, CCOP/SOPAC Tech. Bull. No. 2, 1976, pp. 99-117.

96. Mo, T., A. D. Suttle, and W. M. Sackett. Uranium Concentrations in Marine Sediments. Geochim. Cosmochim Acta, v. 37, 1973, pp. 33-57.

97. Monget, J. M., J. W. Murray, and J. Mascle. A World-Wide Compilation of Published Multicomponent/Analyses of Ferromanganese Concretions. Internat. Decade of Ocean Exploration (IDOE), Manganese Nodule Project Tech. Rept. No. 12, August 1976, 130 pp; NTIS PB-263389.

98. Murata, K. J., and R. C. Erd. Composition of Sediments From the Experimental Mohole Project. J. Sediment. Petrol., v. 34, 1964, pp. 633-655.

99. Murray, J. W. Iron Oxides. Ch. in Marine Minerals, ed. by R. G. Burns. Litho Crafters, Inc., Chelsea, Mich., v. 6, 1979, pp. 47-98.

100. Murray, J. W., and J. G. Dillard. The Oxidation of Cobalt (II) Adsorbed on Manganese Dioxide. Geochim. Cosmochim. Acta, v. 43, 1979, pp. 781-787.

101. Murray, J., and A. F. Renard. Deep-Sea Deposits. Rept. on the Scientific Results of the Voyage of HMS Challenger During the Years 1873-1876, Longmans and Co., London, England.

102. Nakanishi, T., M. Oohashi, M. Higashi, and M. Sakanove.

Radiochemical Studies of Deep-Sea Manganese Nodules. Sci. Rept. Kanazawa Univ., Kanazawa, Japan, v. 22, No. 1, June 1977, pp. 31-43.

103. Nohara, M. Manganese Minerals in Ferromanganese Nodules Dredged From the Sea Mounts in the Pacific Ocean. Chishitsugaku Zasshi, v. 78, 1972, pp. 699-701.

104. Okada, A., T. Minakuchi, and M. Shima. Study on the Manganese Nodule (V). Thermal Studies of the Iron-Manganese Phase. J. Oceanography Soc. of Japan, v. 28, 1972, pp. 39-47.

105. Okada, A., and M. Shima. Study on the Manganese Nodule. J. Oceanography Soc. of Japan, v. 26(3), 1970, pp. 151-158.

106. Ostwald, J., and F. W. Frazer. Chemical and Mineralogical Investigations on Deep Sea Manganese Nodules From the Southern Ocean. Miner. Deposita, v. 8, 1973, pp. 303-311.

107. Piper, D. Z., and M. Williamson. Composition of Pacific Ocean Ferromanganese Nodules. Marine Geol., v. 23, 1977, pp. 285-303.

108. Price, N. B., and S. E. Calvert. Compositional Vairation in Pacific Ocean Ferromanganese Nodules and Its Relationship to Sediment Accumulation Rates. Marine Geol., v. 9, 1970, pp. 145-171.

109. Rancitelli, L. A., and R. W. Perkins. Major and Minor Elemental Composition of Manganese Nodules. Inter-University Program of Research on Ferromanganese Deposits of the Ocean Floor, Phase I Report. Seabed assessment Program, IDOE, National Science Foundation, Washington, D.C., 1973, pp. 1-5.

110. Riley, J. P., and P. Sinhaseni. Chemical Composition of Three Manganese Concretions From the Indian and Pacific Ocean. J. Marine Res., v. 17, 1958, pp. 466-482.

111. Schweisfurth, R. Manganknollen im Meer. Naturwissenschaften, v. 58, 1971, pp. 344-347.

112. Shilo, N. A., L. V. Razin, G. A. Khomenko, and G. I. Agal'tov. The Mode of Occurrence of Gold and Platinum in Ferromanganese Nodules From the Ocean Floor. Doklady Akad. Nauk SSSR, v. 232(2), 1977, pp. 466-469.

113. Siegel, M. Studies of the Mineralogy, Chemical Composition, Textures, and Distribution of Manganese Nodules at a Site in the North Equatorial Pacific Ocean. Ph.D. Thesis, Harvard Univ., Cambridge, Mass., June 1981, 274 pp.

114. Skornyakova, N. S., and P. F. Andrushchenko. Zhelezo-Margantseviye Konkretsii v Tikhom Okeane (Ferro-Manganese Nodules in the Pacific Ocean). Ch. in Osadkocbrazovaniye v Tikhom Okeane (Sedimentation in the Pacific Ocean), ed. by P. L. Bezrukov. Akademiia Nauk SSSR, P. P. Shirshov Institute of Oceanology, Moscow, v. 6, Pt. 1-2, 1970, pp. 203-268.

115. Smith, R. E., J. D. Gassaway, and H. N. Giles. Iron-Manganese Nodules From Nares Abyssal Plain: Geochemistry and Mineralogy. Sci., v. 161, 1968, pp. 780-781.

116. Sorem, R. K. Manganese Nodules: Nature and Significance of Internal Structure. Econ. Geol., v. 62, 1967, pp. 141-147.

117. Sorem, R. K., and R. H. Fewkes. Manganese Nodules. IFI/Plenum Data Company, New York, 1979, 723 pp.

118. Sorem, R. K., R. H. Fewkes, W. D. McFarland, and W. R. Reinhart. Physical Aspects of the Growth Environment of Manganese Nodules in the "Horn Region," East Equatorial Pacific Ocean. Proc., La Genese des Nodules de Manganese, Paper 289, Colloques Internationaux du Centre National de la Recherche Scientifique, Paris, France, Sept. 25-30, 1978, pp. 61-76.

119. Sorem, R. K., and A. R. Foster. Internal Structure of Manganese Nodules and Implications in Beneficiation. Ch. in Ferromanganese Deposits on the Ocean Floor, ed. by D. R. Horn. National Science Foundation, Washington, D.C., 1972, pp. 167-181.

120. _____. Macroprobe X-Ray Analysis and Specimen Distance Effect. Norelco Rept., v. 19, 1972, pp. 21-26.

121. Stevenson, J. S., and L. S. Stevenson. Manganese Nodules From the Challenger Expedition at Redpath Museum. Can. Mineral., v. 10, 1970, pp. 599-615.

122. Summerhayes, C. P. Manganese Nodules From the Southwestern Pacific. NZOI J. Geol. and Geophys., v. 10, 1967, pp. 1372-1381.

123. Toth, J. R. Deposition of Submarine Crusts Rich in Manganese and Iron. Geol. Soc. of America Bull., pt. 1, v. 91, 1980, pp. 44-54.

124. Turner, S., and P. R. Buseck. Manganese Oxide Tunnel Structures and Their Intergrowths. Sci., v. 203, 1979, pp. 456-458.

125. _____. Todorokite: A New Family of Naturally Occurring Manganese Oxides. Sci., v. 212, 1981, pp. 1024-1027.

126. Turner, S., M. Siegel, and P. R. Buseck. Structural Features of Todorokite Intergrowths in Manganese Nodules. Nature, v. 296, 1982, pp. 841-842.

127. Volkov, I. I., and L. S. Fomina. New Data on the Geochemistry of the Rare Earths in the Ocean Sediments. Geochemistry Internat., v. 10, 1973, pp. 1178-1187.

128. Von Gumbel, A. Die Mineralogische-Geologische Beschaffenheit der auf der Forschungsreise S.M.S. "Gazelle" Gesammelten Meersgrund-Ablagerungen (The Geological Mineralogical Analysis of the Marine Sediments Collected on the Research Voyages of the SMS "Gazelle"). Die Forschungsreise S.M.S. "Gazelle" in den Jahren 1874 bis 1878. Hydrographischen Amt der Admiralitat, Berlin, 1888, pp. 69-116.

129. Von Heimendahl, M., G. L. Hubred, D. W. Fuerstenau, and G. Thomas. A Transmission Electron Microscope Study of Deep-Sea Manganese Nodules. Deep-Sea Res., v. 23, 1976, pp. 69-79.

130. Willis, J. P. Investigations on the Composition of Manganese Nodules With Particular Reference to Certain Trace Elements. M.S. Thesis, Univ. of Cape Town, Cape Town, Republic of South Africa, 1970.

131. Yabuki, H., and M. Shima. Uranium and Other Heavy Elements in Deep Sea Sediments Coexisting With Manganese Nodules. Sci. Papers, Inst. of Phys. Chem. Res. Japan, v. 67, 1973, pp. 155-156.

132. Zlatanova, R. Analyse Non Destructive d'Elements Traces: Etude d'un Nodule de Manganese. Rapport CEA-R-4413, Centre d'Etudes Nucleaires de Fontenay-aux-Roses, February 1973, 27 pp.

APPENDIX.—GLOSSARY OF MINERALOGICAL TERMS

Accrete.—The increase in size of an inorganic material by the external addition of fresh particles, as by adhesion.

Acicular.—A crystal that is needlelike in form.

Amorphous.—A mineral that lacks crystalline structure, or whose internal arrangement is so irregular that there is no characteristic external form.

Angstrom (Å).—A unit of length, used to express the length of light waves, equal to 10^{-4} micrometer or 10^{-8} centimeter.

Antiferromagnetic.—A type of magnetic order in which the moments of neighboring magnetic ions are alined antiparallel, so that there is no macroscopic spontaneous magnetization.

Antithetic.—Concentration of elements in rocks or minerals that vary inversely from one to the other.

Authigenic.—Rock constituents and minerals formed or generated in place, not having been transported but derived locally on the spot where they are now found.

Bathymetric.—Concerning the depth and topography of the ocean floor.

Benthic.—Pertaining to the ocean bottom, including marine life found there.

Botryoidal.—Having the form of a bunch of grapes.

Calcareous.—A material that contains a substantial amount of calcium carbonate.

Cell parameters.—The length of axes in the unit cell, given in angstroms.

Clastics.—Rocks or sediments composed principally of broken fragments that are derived from preexisting rocks or minerals and that have been transported individually for some distance from their places of origin.

Colloidal.—Fine-grained matter in suspension in seawater that does not occur in crystalline form. Smaller than clay particles.

Cryptocrystalline.—Crystalline substances of such fine-grained aggregates that their crystalline nature cannot be determined by an optical microscope, but can be determined by X-ray diffraction.

Crystal lattice.—The three-dimensional, regularly repeating atomic arrangement of a crystal, each point of which has identical surroundings. The lattice is built by the regular, parallel translation in space of the unit cell.

Detrital.—Loose rocks or minerals that are worn off or removed by mechanical means, as by disintegration or abrasion, later forming other rocks, minerals, or sediments.

Diagenesis.—The recombination or rearrangement of a mineral resulting in a new mineral.

d-spacing.—In refraction of X-rays by a crystal, the distance or separation between the successive and identical parallel planes in the crystal lattice.

Epitaxial.—An orientation of a crystal with that of the crystalline substrate on which it grew.

Euhedral.—A crystalline solid with well-formed faces.

Ferrimagnetic.—A type of magnetic order, magnetic ions at different crystal sites are opposed. However, there is a net magnetization because of inequality in the number or magnitude of atomic magnetic moments at the two sites.

Hexagonal.—One of the six crystal systems, having four crystallographic axes, three of which are of equal length, and are horizontal and intersect at angles of 120°. The fourth axis (vertical) is of different length and perpendicular to the plane of the other three.

Interstices.—Openings or spacings between objects.

Isometric.—One of the six crystal systems, having three mutually perpendicular axes of equal lengths.

Isostructural.—Minerals related to each other by analogous structures, generally having a common anion, and displaying extensive ionic substitution.

Isotropic.—A crystal whose physical properties do not vary according to crystallographic direction. Crystals that belong to the isometric system.

Mammillary.—An aggregate of crystals taking the form of rounded masses.

Metastable.—A phase that is stable with respect to small disturbances but that is capable of reaction with evolution of energy if sufficiently disturbed.

Monoclinic.—One of the six crystal systems, having three unequal axes, two of which are inclined to each other at an oblique angle and the third perpendicular to the plane of the other two.

Octahedra.—An atomic structure or arrangement in which an ion is surrounded by six ions of opposite charge, whose centers form the corners of an octahedron, which is an isometric crystal form of eight faces, and which are equilateral triangles.

Orthorhombic.—One of the six crystal systems, having three mutually perpendicular axes all of different lengths.

Polymorph.—A chemical substance that can crystallize in more than one form, such as rhombic and monoclinic sulfur.

Psilomelane.—A general term for mixtures of manganese minerals.

Rhombohedral.—A crystal form that is a parallelepiped whose six identical faces are rhombs; that is, oblique, equilateral parallelograms. Characteristic of the hexagonal system.

Siliceous.—An abundance of free silica.

Solid solution.—A single crystalline phase that may vary in composition within finite limits without the appearance of an additional phase.

Space group.—In a crystal structure, one of 230 different ways of arranging atoms in a homogeneous array.

Supergene.—A mineral deposit or enrichment formed by descending solutions.

Tetragonal.—One of the six crystal systems, having three mutually perpendicular axes, two of which (the horizontal axes) are of equal length, but the vertical axis is shorter or longer than the other two.

Triclinic.—One of the six crystal systems, having a onefold axis of symmetry and three axes of unequal lengths that all intersect at oblique angles.

Unit cell.—The fundamental parallelepiped that forms a crystal lattice by regular repetition in space.

Zeolite.—Signifies a group of hydrous aluminosilicates that are analogous in composition to the feldspars. They are characterized by their easy and reversible loss of water of hydration, and their swelling up on heating.

*U.S. GOVERNMENT PRINTING OFFICE : 1983 0-398-634/667

PD-203

THE LIBRARY OF CONGRESS

THE LIBRARY OF CONGRESS

DOBBS BROS. INC.
JUL 83
ST. AUGUSTINE
FLA.
32084

LIBRARY OF CONGRESS
0 002 959 844 7